# Evaluation of McWane Seismic Flex Coupling for Resistance to Earthquake-Induced Ground Deformation

Submitted to:
Stuart Liddell
National Manager - MASD
1201 Vanderbilt Road
Birmingham, Alabama 35234

(stuart.liddell@mcwaneductile.com)

By

C. Pariya-Ekkasut
B.A. Berger
H. E. Stewart
T.D. O'Rourke

Cornell University
School of Civil and Environmental Engineering
Hollister Hall
Ithaca, NY 14853

April, 2018

Principal Investigators

H. E. Stewart
T.D. O'Rourke

## ACKNOWLEDGEMENTS

The authors wish to recognize the excellent effort of Cornell graduate and undergraduate students and professional staff that made these experiments successful. Namely, the contributions of Corbin Atkins, Quinton Hubbell, Margaret Stack, Mia Stewart, James Strait, Benzhang Tang, Sarah Weinberg, and Dr. Brad Wham are gratefully acknowledged. The support from McWane Ductile is gratefully acknowledged, as are the welcomed discussions with and contributions of Hal Eddings, Stuart Liddell, Mark Niewodowski, Jerry Regula, and Charles Weaver from McWane Ductile.

## EXECUTIVE SUMMARY

McWane Ductile has developed a Seismic Flex Coupling (SFC) to connect to TR Flex® bell and spigot ductile iron (DI) pipes. Sections of 6-in. (150-mm)-diameter DI pipes with the McWane SFCs were tested at Cornell University to 1) evaluate the stress-strain-strength characteristics of the DI, 2) determine the capacity of the joint in direct tension and compression, 3) evaluate the bending resistance and moment vs. rotation relationship of McWane SFCs and one separated TR Flex® joint, and 4) evaluate the capacity of a 6-in. (150-mm) DI pipeline with McWane SFCs to accommodate fault rupture using the Cornell full-scale split-basin testing facility.

Test results are summarized for tensile stress-strain-strength characteristics, direct joint tension and compression, bending test results, pipeline response to fault rupture. The significance of test results is given under the headings that follow.

### Tensile Stress-Strain-Strength Characteristics

The uniaxial tension testing of ductile iron (DI) from McWane specimens was completed in accordance with ASTM – E8 2016 standards (ASTM, 2016). The yield stress and ultimate stress exceed the ANSI/AWWA C151/A21.51-17 60-42 specifications (AWWA, 2017) by 25% and 27%, respectively. The elastic modulus is E = 24,100 ksi (166 GPa), and Poisson's ratio is 0.27, consistent with typical DI.

### Bending Test Results

Four-point bending tests were performed on pressurized nominal 6-in. (150-mm)-sections of two McWane SFCs and one separated TR Flex® joint. The purpose of these tests was to develop moment vs. rotation relationships for these types of joints.

In the TR Flex® bending test, first leakage of approximately 10 drops/sec (25 ml/min) developed at a deflection of joint less than 12 degrees and an applied moment of 137 kip-in. (15.5 kN-m). The pipe leaked at a significant rate on the order of 10 gal/min (38 l/min) at 21.3 degrees of joint deflection. Significant leakage is defined as flow exceeding 10 gal/min (38 l/min).

Two tests were performed on SFCs. Specimen 1 showed stiffer rotational responses than Specimen 2, and first leaked at the X joint on the order of 10 drops/sec (25 ml/min) with an associated overall deflection of 17.7 degrees. Later in the test, Specimen 1 leaked at the B joint with a significant rate on the order of 10 gals/min (38 l/min) at 32.5 degrees of overall deflection.

Specimen 2 first leaked about 10 drops/sec (25 ml/min) at the X joint at the beginning of the test. The pipe failed and leaked at the B joint with a significant rate greater than 10 gals/min (38 l/min) at 36.0 degrees of overall deflection.

**Direct Joint Tension and Compression**

Three tension tests, two McWane SFCs and one separated TR Flex® joint, and one compression test were performed on the 6-in. (150-mm)-diameter DI specimens. All tests began at the fully inserted positions. In the TR Flex® joint tension test, the peak load of 96.5 kips (429 kN) was achieved at 0.73 in. (18.5 mm) of joint opening. Leakage was observed at 1.57 in. (39.8 mm) of displacement when the left-hand locking segment broke.

McWane SFC tension test specimens provided the average SFC total displacement of 11.0 in. (279 mm) under internal water pressure of 80 psi (550 kPa). The average maximum tensile force of 66.3 kips (295 kN) was measured at the average displacement of 12.0 in. (305 mm). Both SFC specimens were able to carry additional displacement until significant leakage was observed at the X joint at 13.2 in. (335 mm) of average total joint displacement.

The compressive testing showed that the McWane SFC had a maximum compressive load capacity at about the DI proportional limit of 204 kips (907 kN). Once the proportional limit was achieved, the pipe started to behave plastically and have irrecoverable deformation such that a significant rotation was observed at the B joint. However, no leakage was found during the compression test.

**Pipeline Response to Fault Rupture**

A 34-ft (10-m)-long, three-piece section of a ductile pipeline was tested at the Cornell Large-Scale Lifelines Facility. The pipeline had two McWane SFCs located 5 ft (1.5 m) north and south of the 50º fault. The pipe was pressurized to approximately 80 psi (550 kPa). The pipe was placed on a bed of compacted partially saturated sand, aligned, instruments checked, and then backfilled with compacted sand to a depth of cover of 33.5 in. (851 mm) above the pipe crown. The north section of the test basin was displaced along a 50º fault at a rate of 12 in. (300 mm) per minute. At a fault displacement of roughly 33.4 in. (848 mm), the pipe lost pressure. An additional 0.3 in. (76 mm) of test basin movement was applied to ensure a complete pressure loss in the system, and the test was then stopped. Following excavation, a spigot pullout was observed at the south B joint.

The test measurements confirm that the pipeline was able to accommodate fault rupture through

axial displacements and deflections at two SFCs. The data also provide a comprehensive and detailed understanding of how the movement was accommodated at each joint, the sequence of movements, and the combined axial pullout and rotation at each joint. The DI pipeline with two SFCs accommodated the total axial movement of 21.5 in. (546 mm). In the experiments, the X joint was installed at 1.5 in. (38 mm) from fully inserted position to accommodate joint instrumentation. Had the X joints been set at the fully inserted positions, the pipeline would have accommodated 24.5 in. (622 mm) of total axial displacement. On average, each SFC would have displaced on the order of 12.3 in. (274 mm). This displacement was nearly identical to the movement measured in the previous joint direct tension testing of the McWane SFC. The maximum deflection measured at the south SFC was about 10.5 degrees, thus demonstrating the ability of the joints to sustain significant levels of combined axial pullout and deflection. The maximum stresses sustained by the pipeline, corresponding to the largest pipeline deformation, were well within the elastic range of pipeline behavior.

The ductile iron pipeline equipped with McWane Seismic Flex Couplings (SFCs) was able to accommodate significant fault movement through axial pullout and joint deflection (rotation). Fault rupture simulated in the large-scale test was representative of the most severe ground deformation that occurs along the margins of liquefaction-induced lateral spreads and landslides.

**Significance of Test Results**

The amount of tensile strain that can be accommodated with the ductile iron pipeline will depend on the number and spacing of the McWane SFCs and the positioning of the spigot within the bell at the pipeline joints. The four-joint pipeline used in the large-scale split-basin test was able to accommodate at least 21.5 in. (461 mm) of axial extension, corresponding to an average tensile strain of 4.5% along the pipeline. Such extension is large enough to accommodate the great majority (over 99%) of liquefaction-induced lateral ground strains measured by high resolution LiDAR after each of four major earthquakes during the recent Canterbury Earthquake Sequence (CES) in Christchurch, NZ. These high resolution LiDAR measurements for the first time provide a comprehensive basis for quantifying the ground strains caused by liquefaction on a regional basis. To put the CES ground strains in perspective, the levels of liquefaction-induced ground deformation measured in Christchurch exceed those documented in San Francisco during the 1989 Loma Prieta earthquake and in the San Fernando Valley during the 1994 Northridge earthquake.

They are comparable to the levels of most severe liquefaction-induced ground deformation documented for the 1906 San Francisco earthquake, which caused extensive damage to the San Francisco water distribution system. The fault rupture test confirms that the DI pipes equipped with the McWane SFCs are able to sustain without leakage large levels of ground deformation through axial displacement and deflection under full-scale conditions of abrupt ground rupture.

## TABLE OF CONTENTS


Acknowledgements i
Executive Summary ii
Table of Contents vi
List of Figures viii
List of Tables xi

**Section** **Page**

1 Introduction and Organization 1
1.1. Report Organization 1
1.2. McWane SFC Description 1
2 Tensile Coupon Tests 3
2.1. Introduction 3
2.2. Tensile Coupon Testing and Procedure 3
2.3. Stress vs. Strain Relationships 3
2.4. Young's Modulus 3
2.5. Yield Strength, Proportional Limit, and Ultimate Strength and Strain 4
2.6. Poisson's Ratio 4
2.7. Comparison of Test Results to ANSI/AWWA C151/A21.51-17 7
3 Four-Point Bending Tests 8
3.1. Introduction 8
3.2. Locking Segment Locations 8
3.3. Test Procedures 9
3.4. Calculation Approach 10
3.5. TR Flex® Bending Test 11
3.5.1. Instrumentation 11
3.5.2. Pressure 11
3.5.3. Pipe Deflection (Rotation) 14
3.6. McWane SFC Bending Tests 18
3.6.1. Instrumentation 18
3.6.2. Test 1 (3-9) 18
3.6.2.1. Pressure 18
3.6.2.2. Pipe Deflection (Rotation) 18
3.6.3. Test 2 (12-6) 24
3.6.3.1. Pressure 24
3.6.3.2. Pipe Deflection (Rotation) 25
3.6.4. Comparisons of McWane SFC Bending Tests 31
3.7. Summary of Bending Tests 32

## TABLE OF CONTENTS (completed)


| Section | | Page |
|---|---|---|
| 4 | Joint Axial Tension and Compression Tests | 34 |
| 4.1. | Introduction | 34 |
| 4.2. | TR Flex® Tension Test | 34 |
| 4.2.1. | Instrumentation | 34 |
| 4.2.2. | Force vs. Displacement | 34 |
| 4.3. | McWane SFC Tension Tests | 39 |
| 4.3.1. | Instrumentation | 39 |
| 4.3.2. | Tension Test 1 Force vs. Displacement | 39 |
| 4.3.3. | Tension Test 1 and 2 Comparison | 42 |
| 4.4. | McWane SFC Compression Tests | 46 |
| 4.4.1. | Instrumentation and Test Procedures | 46 |
| 4.4.2. | Force vs. Displacement | 46 |
| 4.4.3. | Joint Rotation | 50 |
| 4.5. | Summary from Joint Tension and Compression Tests | 52 |
| 5 | Fault Rupture Test | 53 |
| 5.1. | Introduction | 53 |
| 5.2. | Experimental Setup | 53 |
| 5.2.1. | Test Procedure | 55 |
| 5.2.2. | Instrumentation | 55 |
| 5.2.3. | Soil Preparation | 60 |
| 5.3. | Experimental Results of Split Basin Test | 61 |
| 5.3.1. | Test Basin Movements | 61 |
| 5.3.2. | Internal Water Pressure | 61 |
| 5.3.3. | Survey Results | 62 |
| 5.3.4. | Joint Displacements | 63 |
| 5.3.5. | Joint Rotations (Deflections) | 66 |
| 5.3.6. | End Loads and Pipe Axial Forces | 68 |
| 5.3.7. | Bending Moments | 69 |
| 5.3.8. | Deformed Shape and Pipe Failure | 74 |
| 5.4. | Summary of Fault Rupture Test | 74 |
| 6 | Summary | 77 |
| References | | 81 |

## LIST OF FIGURES


| Figure | | Page |
|---|---|---|
| 1.1. | Overall Configuration of Seismic Flex Coupling (after McWane, 2016) | 2 |
| 2.1. | Schematic of Tensile Coupon Specimen | 4 |
| 2.2. | Tensile Coupon Test Setup | 5 |
| 2.3. | Average Young's Modulus and Yield Stress | 6 |
| 2.4. | Stress vs. Strain Curve to Failure | 6 |
| 2.5. | Transverse vs. Axial Strain in Elastic Range | 6 |
| 3.1. | Orientation of Locking Segments for Three Bending Tests | 9 |
| 3.2. | Fault Rupture Test Setup at 3 and 9 O'clock and Lateral Ground Motion | 9 |
| 3.3. | Cross-section of Instrumentation for TR Flex® Bending Test | 12 |
| 3.4. | Photo of TR Flex® Bending Specimen before Testing | 12 |
| 3.5. | Internal Pressure vs. Joint Rotation for TR Flex® Bending Test | 13 |
| 3.6. | Moment vs. Rotation for TR Flex® Bending Test | 15 |
| 3.7. | First Leakage of TR Flex® Bending Test Specimen | 15 |
| 3.8. | Invert Locking Segment Fell out of TR Flex® Joint | 16 |
| 3.9. | Significant Leakage of TR Flex® Bending Test Specimen | 16 |
| 3.10. | Photo of TR Flex® Bending Specimen after Testing | 17 |
| 3.11. | Damage at TR Flex® Plain End after TR Flex® Bending Test | 17 |
| 3.12. | Cross-section of Instrumentation for McWane SFC Bending Tests | 19 |
| 3.13. | Photo of McWane SFC Bending Specimen 1 (3-9) before Testing | 19 |
| 3.14. | Internal Pressure vs. Deflection for McWane SFC Bending Test 1 (3-9) | 20 |
| 3.15. | Moment vs. Deflection for McWane SFC Bending Test 1 (3-9) | 21 |
| 3.16. | Moment vs. Joint Rotations for McWane SFC Bending Test 1 (3-9) | 21 |
| 3.17. | First Leakage of McWane SFC Bending Test Specimen 1 (3-9) | 22 |
| 3.18. | Significant Leakage of McWane SFC Bending Test Specimen 1 (3-9) | 22 |
| 3.19. | Photo of McWane SFC Bending Specimen 1 (3-9) after Testing | 23 |
| 3.20. | Damage at TR Flex® Plain End after McWane SFC Bending Test 1 (3-9) | 24 |
| 3.21. | Internal Pressure vs. Deflection for McWane SFC Bending Test 2 (12-6) | 25 |
| 3.22. | Moment vs. Deflection for McWane SFC Bending Test 2 (12-6) | 26 |
| 3.23. | Moment vs. Joint Rotations for McWane SFC Bending Test 2 (12-6) | 26 |
| 3.24. | First Leakage of McWane SFC Bending Test Specimen 2 (12-6) | 27 |

## LIST OF FIGURES (continued)


| Figure | | Page |
|---|---|---|
| 3.25. | Invert Locking Segment Fell out of P Joint | 27 |
| 3.26. | Invert Locking Segment Fell out of B Joint | 28 |
| 3.27. | Significant Leakage of McWane SFC Bending Test Specimen 2 (12-6) | 29 |
| 3.28. | Photo of McWane SFC Bending Specimen 2 (12-6) after Testing | 29 |
| 3.29. | Damage at TR Flex® Plain End after McWane SFC Bending Test 2 (12-6) | 30 |
| 3.30. | Moment vs. Deflection Comparisons for McWane SFC Bending Tests | 30 |
| 4.1. | TR Flex® Tension Test Layout | 35 |
| 4.2. | Internal Pressure vs. Joint Opening for TR Flex® Tension Test | 35 |
| 4.3. | Tensile Force vs. Joint Opening for TR Flex® Tension Test | 35 |
| 4.4. | Successive Photos of TR Flex® Joint | 37 |
| 4.5. | Successive Photos of TR Flex® Looking at Left-Hand Locking Segment | 38 |
| 4.6. | TR Flex® Tension Test Layout | 40 |
| 4.7. | Internal Pressure vs. Total Joint Opening for McWane SFC Tension Test 1 | 40 |
| 4.8. | Tensile Force vs. B Joint Opening for SFC Tension Test 1 | 43 |
| 4.9. | Tensile Force vs. X Joint Opening for SFC Tension Test 1 | 43 |
| 4.10. | Tensile Force vs. P Joint Opening for SFC Tension Test 1 | 43 |
| 4.11. | Tensile Force vs. Total Joint Opening for SFC Tension Test 1 | 43 |
| 4.12. | Successive Photos of McWane SFC Tension Test 1 | 44 |
| 4.13. | Successive Photos of McWane SFC Tension Test 1 Looking at Left-Hand Locking Segment | 45 |
| 4.14. | Tensile Force vs. Total Joint Opening Comparison between McWane SFC Tension Tests 1 and 2 | 45 |
| 4.15. | Compression Test Layout | 48 |
| 4.16. | Test Specimen in Compression Frame | 48 |
| 4.17. | Internal Pressure vs. Joint Closure | 48 |
| 4.18. | Compressive Force vs. P Joint Closure for SFC Compression Test | 49 |
| 4.19. | Compressive Force vs. X Joint Closure for SFC Compression Test | 49 |
| 4.20. | Compressive Force vs. B Joint Closure for SFC Compression Test | 49 |
| 4.21. | Compressive Force vs. Total Joint Closure for SFC Compression Test | 49 |
| 4.22. | Irrecoverable Deformation at B Joint | 51 |

## LIST OF FIGURES (completed)


| Figure | | Page |
|---|---|---|
| 4.23. | Joint Vertical Rotations vs. Total Joint Displacement | 52 |
| 4.24. | Compressive Force and B Joint Vertical Rotation vs. Total Joint Displacement | 52 |
| 5.1. | Plan View of Pipe Centered McWane SFC Specimen in Test Basin | 54 |
| 5.2. | String Pot Setups | 58 |
| 5.3. | Pipe Joints with Protective Shielding | 58 |
| 5.4. | Particle Size Distribution of RMS Graded Sand | 61 |
| 5.5. | Fault Displacement vs. Time | 62 |
| 5.6. | Internal Water Pressure vs. Fault Displacement | 62 |
| 5.7. | Initial and Final Pipeline Positions from Surveying Measurements | 63 |
| 5.8. | South Joint Openings vs. Fault Displacement | 65 |
| 5.9. | North Joint Openings vs. Fault Displacement | 65 |
| 5.10. | Total SFC Displacement vs. Fault Displacement | 65 |
| 5.11. | South SFC Joint Rotations vs. Fault Displacement | 67 |
| 5.12. | North SFC Joint Rotations vs. Fault Displacement | 67 |
| 5.13. | Total SFC Deflections vs. Fault Displacement | 67 |
| 5.14. | Comparison of Average End Force from Load Cells and Strain Gages | 69 |
| 5.15. | Axial Forces in Pipe vs. Distance from Fault | 70 |
| 5.16. | Bending Moments in Pipe vs. Distance from Fault | 71 |
| 5.17. | Fault Rupture at Test End | 72 |
| 5.18. | Overhead View of Pipeline (a) before burial and (b) after excavation | 73 |
| 5.19. | B Joint Pullout at South SFC following Test without Protective Shield | 74 |

## LIST OF TABLES


| Table | | Page |
|---|---|---|
| 2.1. | Dimensions of Tensile Coupon Specimen | 4 |
| 2.2. | Summary of Material Properties for McWane DI | 7 |
| 2.3. | Comparison of McWane DI Material Properties to ANSI/AWWA C151/A21.51-17 | 7 |
| 3.1. | Instrumentation for TR Flex® Bending Test | 13 |
| 3.2. | Instrumentation for McWane SFC Bending Tests | 20 |
| 3.3. | Results of Four-Point Bending Tests | 33 |
| 4.1. | Instrumentation for TR Flex® Tension Test | 36 |
| 4.2. | Instrumentation for McWane SFC Tension Tests | 41 |
| 4.3. | Instrumentation for McWane SFC Compression Test | 47 |
| 5.1. | Strain Gage Locations and Coding System for SFC Fault Rupture Test | 56 |
| 5.2. | String Pot Locations and Labeling for McWane SFC Fault Rupture Test | 59 |
| 5.3. | Load Cell Locations and Labeling for McWane SFC Fault Rupture Test | 60 |
| 5.4. | Joint Openings of McWane SFCs | 66 |
| 5.5. | Joint Deflections of McWane SFCs | 68 |

# Section 1
# Introduction and Organization

This report is submitted to McWane Ductile (herein referred to as McWane), and presents the results of physical testing on the nominal 6-in. (150-mm)-diameter ductile iron pipes with McWane Seismic Flex Couplings (SFCs) and TR Flex® pipe The purpose of the testing is to demonstrate the ability of the SFCs to accommodate axial pullout and deflection, characterize the pipe mode of failure, and evaluate the ability of the SFCs to accommodate fault rupture. The work was undertaken in the Cornell Large Scale Lifelines Testing Facility, which is part of the Bovay Laboratory Complex at Cornell University.

## 1.1. Report Organization

The report is organized into six sections, the first of which provides introductory remarks and describes the report organization. Section 2 presents the results of tensile coupon tests to characterize the basic stress-strain-strength characteristics of the ductile iron. Section 3 presents test results from one direct tension test on two tension tests on SFCs, one separated TR Flex® joint, and one compression test on an SFC. Section 3 describes and reports on the results of four-point bending tests on two SFCs and also one separated TR Flex® joint. The tension and compression capacities of the joints are evaluated, and limit conditions of pipe leakage are provided in Section 4. A fault rupture test with two McWane SFCs is described in Section 5. Joint extensions, deflections, and pipe strains and forces from the full-scale test are given. Section 6 provides a summary of the testing and concluding remarks.

## 1.2. McWane SFC Description

The McWane Seismic Flex Coupling (SFC) consists of plain end and bell end adaptors that can be used at any location along a DI pipeline to connect to standard TR Flex® joints. Each joint is equipped with locking segments and a rubber gasket to prevent leakage. Each spigot has a weld bead that bears against the locking segments to resist pullout of the spigot from the bell. Figure 1.1 shows the overall 6-in. (150 mm) coupling with the Seismic Flex Coupling (SFC) with the plain end and bell end adaptors, and the TR Flex® bell and spigot ends. In Figure 1.1, the “B, X, and P” portions of the SFC are shown.

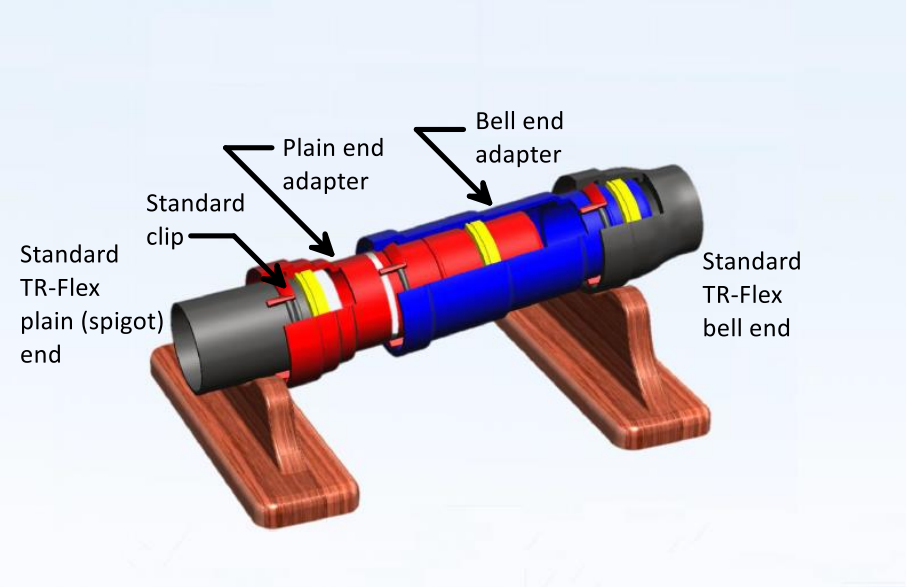


a)

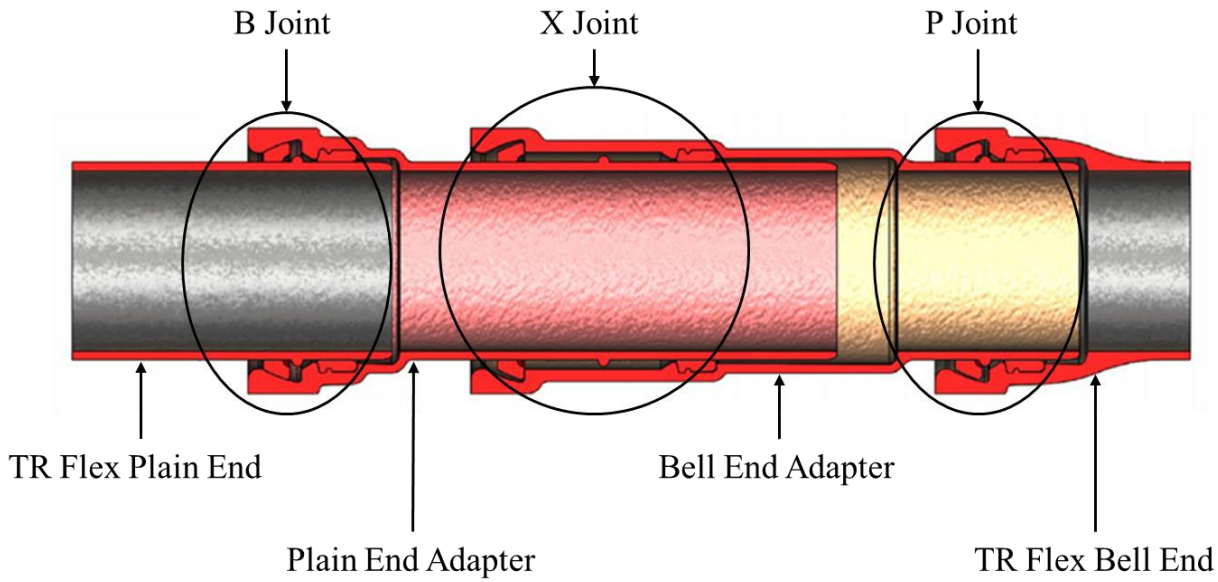


b)

Figure 1.1. Overall Configuration of Seismic Flex Coupling (after McWane, 2016)

## Section 2
## Tensile Coupon Tests

### 2.1. Introduction

This section of the report describes the uniaxial tension testing of ductile iron (DI) specimens provided by McWane. The test results are used to determine the strength and ductility of the material. Tensile coupons were machined from a DI pipe specimen and tested in tension to determine the yield strength, ultimate strength, and ultimate strain of the material. All testing was completed in accordance with ASTM – E8 2016 standards (ASTM, 2016).

### 2.2. Tensile Coupon Testing and Procedure

The tensile coupons were machined from the pipe to obtain the nominal dimensions shown in Figure 2.1 and Table 2.1. These dimensions comply with ASTM - E8 2016 (ASTM, 2016) for large diameter tubes. A Baldwin Hamilton 60 BTE Universal Testing Machine was used to apply tensile loads. Three tensile coupon specimens were tested. Bondable axial and transverse strain gages were used at the center of the reduced area of all three specimens. A laser extensometer also was used to measure axial strains. A photo of the test setup is provided in Figure 2.2.

### 2.3. Stress vs. Strain Relationships

The stress applied throughout the uniaxial tension test was computed by dividing the measured force by the original cross-sectional area of the specimen, referred as engineering stress. The uniaxial stresses vs. axial strains for all three specimens are shown in Figures 2.3 and 2.4. In the figures, the axial strains measured with the bondable strain gages and the laser extensometer were virtually identical, and provided nearly identical data until the specimen failed.

### 2.4. Young's Modulus

Young's modulus was computed using the elastic region of the stress vs. strain curve. These data are shown to a strain of 0.5% in Figure 2.3. Young's Modulus was determined by performing a linear regression for stress vs. strain from 2 ksi to 30 ksi (14 to 207 MPa). The average Young's Modulus is 24,100 ksi (166 GPa) with a standard deviation of 755 ksi (5.21GPa).

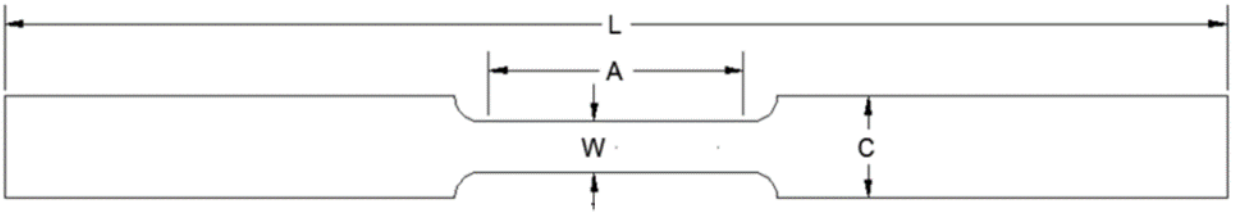


Figure 2.1. Schematic of Tensile Coupon Specimen

Table 2.1. Dimensions of Tensile Coupon Specimen

| Dimensions | Length (in.) |
|---|---|
| W – Width | 0.50 |
| R – Radius | 0.50 |
| L – Overall Length | 8.00 |
| A – Length of Reduced Section | 2.25 |
| C – Width of Grip Section | 1.00 |

## 2.5. Yield Strength, Proportional Limit, and Ultimate Strength and Strain

The yield strength, $\sigma_y$, was computed using the offset method, in which a line parallel to the linear part of the stress vs. strain plot is projected from 0.2% strain. The intersection of this line and the stress vs. strain curve provides an estimate of the yield stress for each specimen. The average yield stress is 52.7 ksi (363 MPa) with a standard deviation of 3.0 ksi (20.7 MPa). The 0.14% strain is taken as a proportional limit, beyond which the relationship between stresses and the strains is no longer linear. The average proportional stress is 32.8 ksi (226 MPa) with a standard deviation of 2.3 ksi (15 MPa). Figure 2.4 shows the full range of the stress vs. strain relationship. The average ultimate tensile stress and strain were 76.0 ksi (524 MPa) and 4.1% with a standard deviation of 3.1 ksi (212 MPa) and 0.7%, respectively.

## 2.6. Poisson's Ratio

Poisson's ratio, $\nu$, is the negative ratio of transverse strain to axial strain for uniaxial loading. Poisson's ratio for all specimens was approximately 0.27 with a very small standard deviation of 0.01.

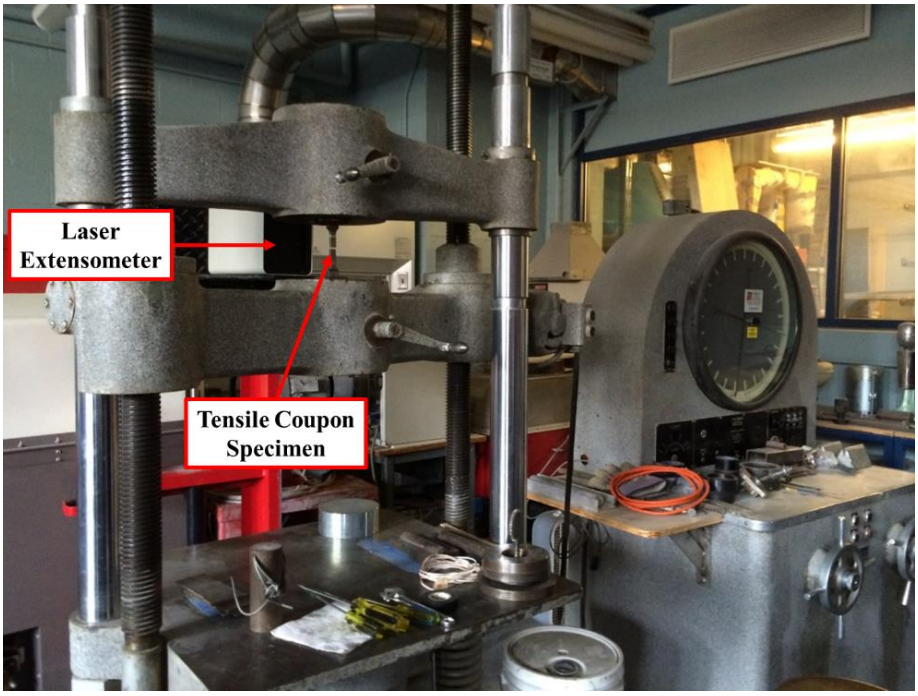


a) Baldwin Testing Apparatus

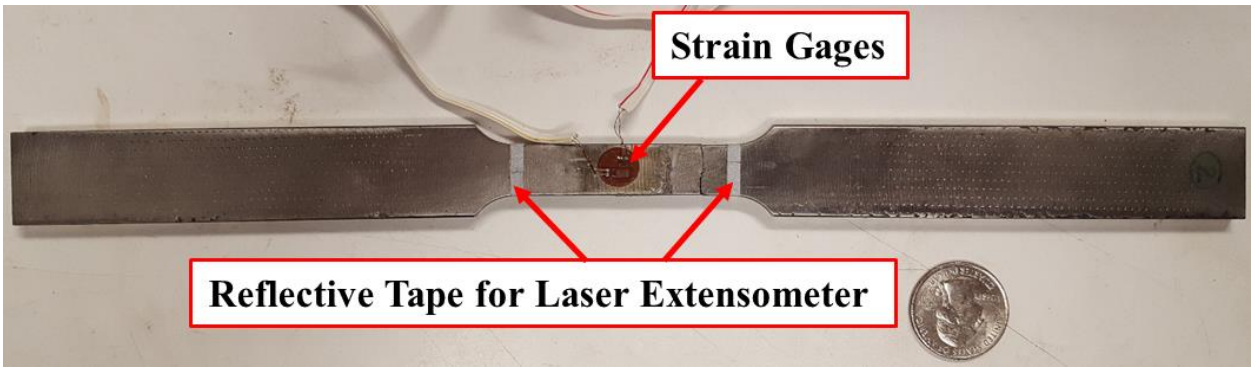


b) Tensile Coupon Instrumentations

Figure 2.2. Tensile Coupon Test Setup

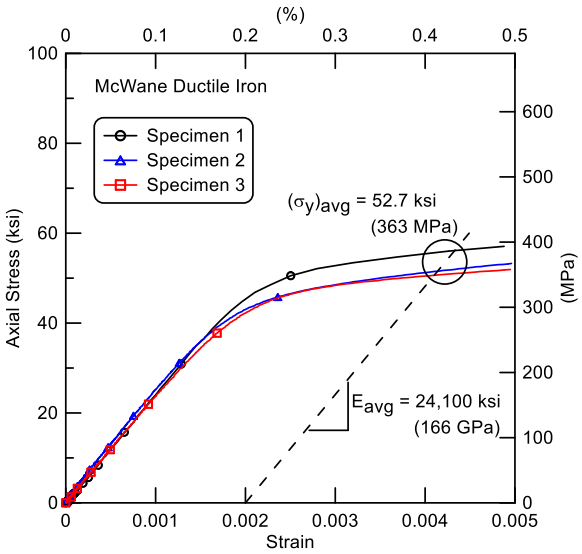


Figure 2.3. Average Young's Modulus and Yield Stress

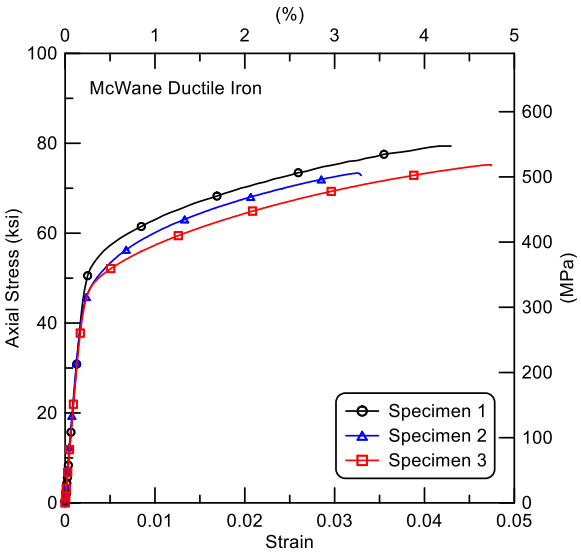


Figure 2.4. Stress vs. Strain Curve to Failure

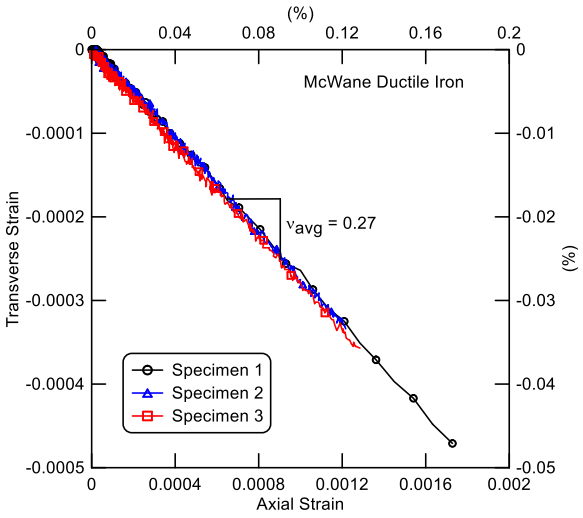


Figure 2.5. Transverse vs. Axial Strain in Elastic Range

Table 2.2. Summary of Material Properties for McWane DI

| Specimen | Young's Modulus, E (ksi) | Yield Stress, $\sigma_y$ (ksi) | Proportional Stress, $\sigma_{prop}$ (ksi) | Ultimate Stress, $\sigma_{ult}$ (ksi) | Elongation (%) | Poisson's Ratio, $\nu$ |
|---|---|---|---|---|---|---|
| 1 | 24,000 | 56.1 | 35.3 | 79.4 | 4.3 | 0.27 |
| 2 | 24,900 | 51.5 | 31.9 | 73.4 | 3.3 | 0.28 |
| 3 | 23,400 | 50.6 | 31.3 | 75.2 | 4.7 | 0.27 |
| Average | 24,100 | 52.7 | 32.8 | 76.0 | 4.1 | 0.27 |
| Standard Deviation | 755 | 3.0 | 2.2 | 3.1 | 0.7 | 0.01 |

1 ksi = 6.89 MPa

Table 2.3. Comparison of McWane DI Material Properties to ANSI/AWWA C151/A21.51-17

| Parameter | McWane DI | ANSI/AWWA specifications |
|---|---|---|
| Yield Stress (ksi) | 52.7 | 42 |
| Ultimate Stress (ksi) | 76.0 | 60 |
| Elongation (%) | 4.1 | 10 |

1 ksi = 6.89 MPa

## 2.7. Comparison of Test Results to ANSI/AWWA C151/A21.51-17

The uniaxial tension testing of DI from McWane specimens was completed in accordance with ASTM – E8 2016 standards (ASTM, 2016). Table 2.2 summarizes the material properties of McWane DI. The moduli, yield stress, ultimate stress, and strain at failure are tabulated in Table 2.3 to compare the material properties with ANSI/AWWA C151/A21.51-17 60-42-10 specifications (AWWA, 2017). The yield and ultimate stresses are 25% and 27% greater than the specifications, respectively. However, the strain at failure of McWane DI reported here is lower than the standard.

# Section 3
# Four-Point Bending Tests

## 3.1. Introduction

This section describes three pressurized four-point bending tests of nominal 6-in. (150-mm)-sections of two McWane Seismic Flex Couplings (SFCs) and one separated TR Flex® joint provided by McWane Ductile. The test results are used to determine the moment vs. rotation responses of McWane SFCs and TR Flex®. Of particular interest was the effect that the location of the locking segments had on the rotational response of SFCs. It should be noted that the term "rotation" in this report is equivalent to "deflection" as used commonly in the field and commercial pipeline information.

## 3.2. Locking Segment Locations

During the four-point bending tests the load is applied vertically. The TR Flex® joint and the second SFC bending tests had the slots positioned at the springlines of the pipe, and the locking segments were inserted such that they were located near the crown and invert of the pipe (the 12 [blue] and 6 o´clock [red] positions), as shown in Figure 3.1 a). When the slots are at the top during pipe installation, the vertical load applied to the pipe is representative of horizontal soil displacement, which is typically associated with the most severe conditions of soil-pipe interaction during earthquake-induced ground deformation.

The orientation of the first SFC was rotated 90 degrees such that its slots were located at the crown. The locking segments were inserted into the slot and pushed to the springlines such that they were at approximate 3 (red) and 9 (blue) o´clock positions as seen in Figure 3.1 b). This locking segment configuration produces somewhat larger rotations because of the lack of material at the slots at crown and invert. In the fault rupture test, the pipeline is installed with the slots at the crown and locking segments at the 3 and 9 o´clock positions as shown in Figure 3.2. Therefore, the second SFC four-point bending test is representative of the SFC deflection response in the fault rupture test.

a) 12 and 6 O´Clock (TR Flex® and SFC Test 2)

b) 3 and 9 O´Clock (SFC Test 1)

Figure 3.1. Orientation of Locking Segments for Three Bending Tests

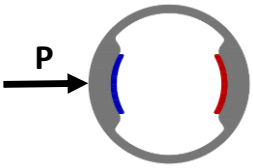


Figure 3.2. Fault Rupture Test Setup at 3 and 9 O'clock and Lateral Ground Motion

### 3.3. Test Procedures

The three four-point bending tests were performed as follows:

1) Install the pipe joint at a fully inserted position and level the pipe in the loading frame.
2) Check all instrumentation and data acquisitions systems.
3) Start data acquisition.
4) Fill the pipe with water and pressurize slowly, providing axial force sufficient to expand the joint.
5) Once the joint was fully opened, bleed air from the system and pressurize the pipe to approximately 80 psi (550 kPa).
6) Remove the temporary supports and lower the spreader beam onto the pipe.
7) Apply hydraulic actuator force to develop moment and rotation.
8) If the actuator reached the limit of its stroke without indication of pipe failure, unload the pipe, and readjust the actuator and crosshead.
9) Apply hydraulic actuator force onto the pipe again until pipe failure.

### 3.4. Calculation Approach

The test set-ups for the McWane SFCs and TR Flex® four-point bending tests are presented in Figures 3.3 and 3.12, respectively. For each set up the initial moment due to the self-weight of the pipe and water is calculated using a simply-supported beam approach, as follows

$$M_{distrib} = \frac{w l_t^{\,2}}{8} \tag{3.1}$$

where:

w = uniform load due to weight of the pipe and water, and

$l_t$ = the total pipe length between the outer supports.

The additional moment applied to the central portion of the specimen, $M_{central}$, was calculated as

$$M_{central} = \frac{PL}{2} \tag{3.2}$$

where:

P = the applied load due to the weight of the spreader beam plus the load applied by the hydraulic actuator in the load frame, and

L = the distance between the load and support points.

The moments due to the pipe, water, and spreader beam weights are included in the moment vs. rotation calculations.

The joint rotation can be calculated by taking the difference between two vertical string pot measurements (VSPs) along each section of a pipe, and dividing the difference by the pot separation distance. The arctangent of this result is the rotation of each section of the pipe. The overall deflection is the sum of the bell and spigot angles, as follows

$$\theta_{Bell}\,(°) = \tan^{-1}\left(\frac{\text{difference between two bell VSPs disp.}}{\text{distance between centers of two bell VSPs}}\frac{180^{\circ}}{\pi}\right) \tag{3.4a}$$

$$\theta_{Spigot}\,(°) = \tan^{-1}\left(\frac{\text{difference between two spigot VSPs disp.}}{\text{distance between centers of two spigot VSPs}}\frac{180^{\circ}}{\pi}\right) \tag{3.4b}$$

$$\theta_{Overall}\,(°) = \theta_{Bell}\,(°) + \theta_{Spigot}\,(°) \tag{3.5}$$

In the SFC bending tests, each individual joint rotation can be calculated as

$$\theta_{BA}\,(°) = \tan^{-1}\left(\frac{\text{difference between two VSPs disp. on bell adapter}}{\text{distance between centers of two VSPs on bell adapter}}\frac{180^{\circ}}{\pi}\right) \tag{3.6a}$$

$$\theta_{PA}\,(^\circ) = \tan^{-1}\left(\frac{\text{difference between two VSPs disp. on plain adapter}}{\text{distance between centers of two VSPs on plain adapter}}\frac{180^\circ}{\pi}\right) \quad (3.6b)$$

$$\theta_{P\ Flex\ Joint}\,(^\circ) = \theta_{Bell}\,(^\circ) + \theta_{BA}\,(^\circ) \quad (3.7)$$

$$\theta_{X\ Joint}\,(^\circ) = \theta_{BA}\,(^\circ) + \theta_{PA}(^\circ) \quad (3.8)$$

$$\theta_{B\ Joint}\,(^\circ) = \theta_{PA}\,(^\circ) + \theta_{Spigot}\,(^\circ) \quad (3.9)$$

## 3.5. TR Flex® Bending Test

### 3.5.1. Instrumentation

A cross-section of a nominal 6-in. (150-mm) TR Flex® bending test setup and instrumentation is shown in Figure 3.3. There were two temporary supports beneath the central loading points. The supports were used to level the test specimen and to support the self-weight of the pipe (including water for pressurized pipe) before vertical loading. Figure 3.4 is a photograph of the bending specimen before the test.

Table 3.1 lists the location, instrument type, and designation for the TR Flex® bending test. The primary instrumentation consisted of string potentiometers (string pots) to measure horizontal displacements at the crown and invert of the joint, referred as HSPs. Vertical displacements along the length of the specimen were measured using seven vertical string pots (VSPs). The VSPs were used to determine the vertical deformation of the test specimen and to calculate the rotation at various locations along the pipe. Strain gages were installed as a backup system to measure axial and bending strains in the DI pipe.

### 3.5.2. Pressure

The specimen was initially set up at a fully inserted position and had locking segments located at 12 and 6 o'clock [Figure 3.1a]. It was then pressurized with water to about 80 psi (550 kPa) while allowing the joint to extend fully in response to axial forces on the end caps. Figure 3.5 shows internal pressure vs. joint rotation from the bending test. The water pressure line remained open to maintain a nearly constant pressure.

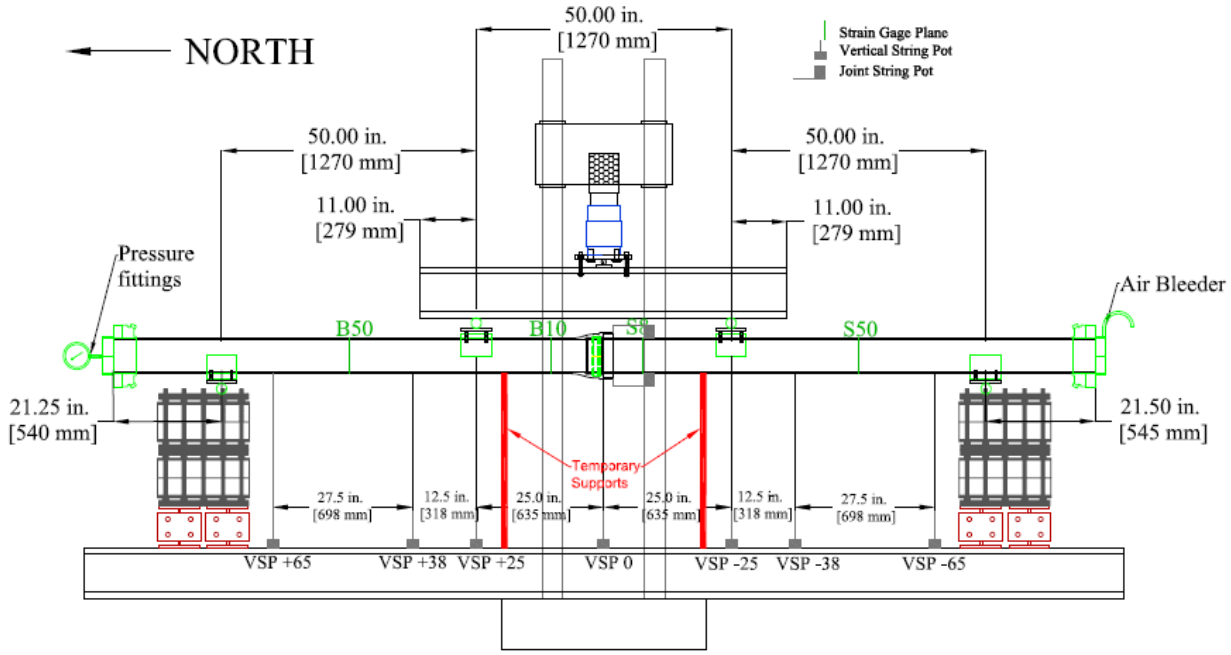


Figure 3.3. Cross-section of Instrumentation for TR Flex® Bending Test

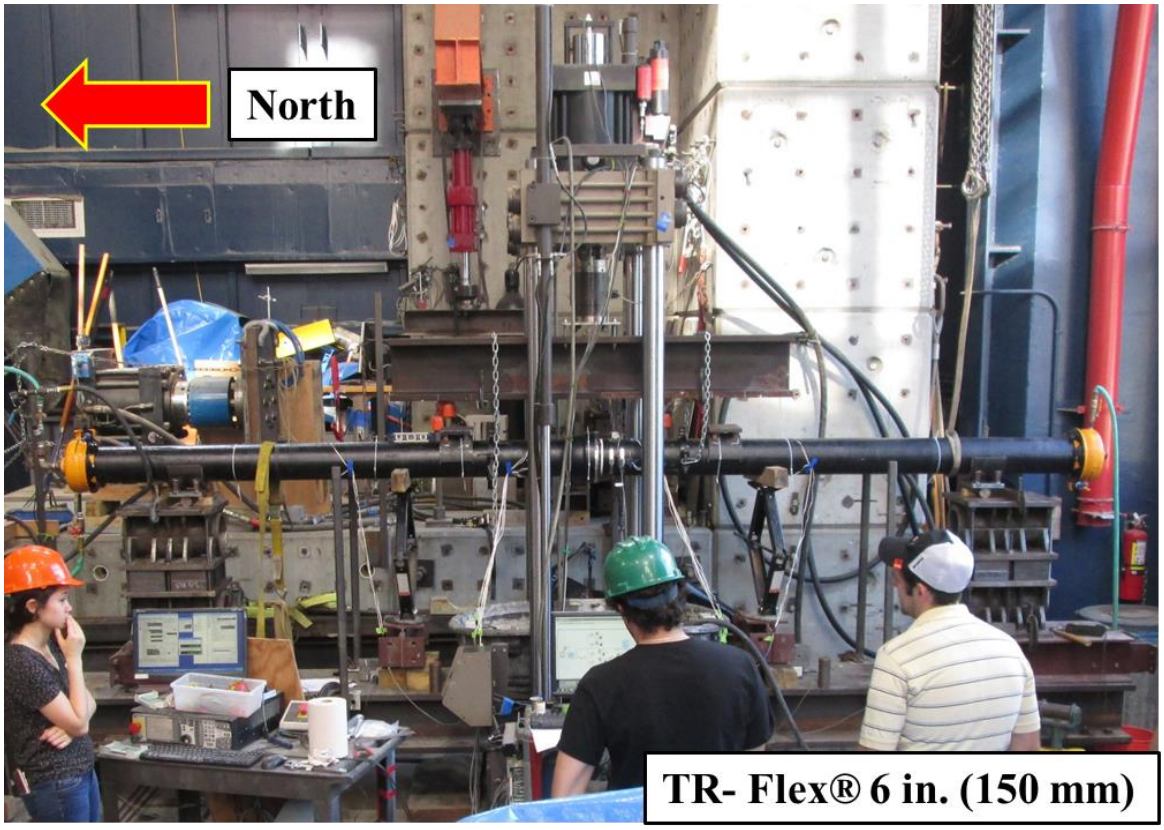


Figure 3.4. Photo of TR Flex® Bending Specimen before Testing

Table 3.1. Instrumentation for TR Flex® Bending Test

| Location | Instrument Description | Instrument Designation |
|---|---|---|
| -65 in. from Centerline | Vertical String Pot on Bell End | VSP -65 |
| -37.5 in. from Centerline | Vertical String Pot on Bell End | VSP -38 |
| -25 in. from Centerline | Vertical String Pot on Bell End | VSP -25 |
| 0 in. from Centerline | Vertical String Pot on Bell End | VSP 0 |
| 25 in. from Centerline | Vertical String Pot on Spigot End | VSP +25 |
| 37.5 in. from Centerline | Vertical String Pot on Spigot End | VSP +38 |
| 65 in. from Centerline | Vertical String Pot on Spigot End | VSP +65 |
| 4 in. from Centerline | Horizontal String Pot at Crown | HSP_C |
| 4 in. from Centerline | Horizontal String Pot at Invert | HSP_I |
| Top Center | Load Cell | Load |
| North End Cap | Pressure Gage | Pressure |

1 in. = 25.4 mm

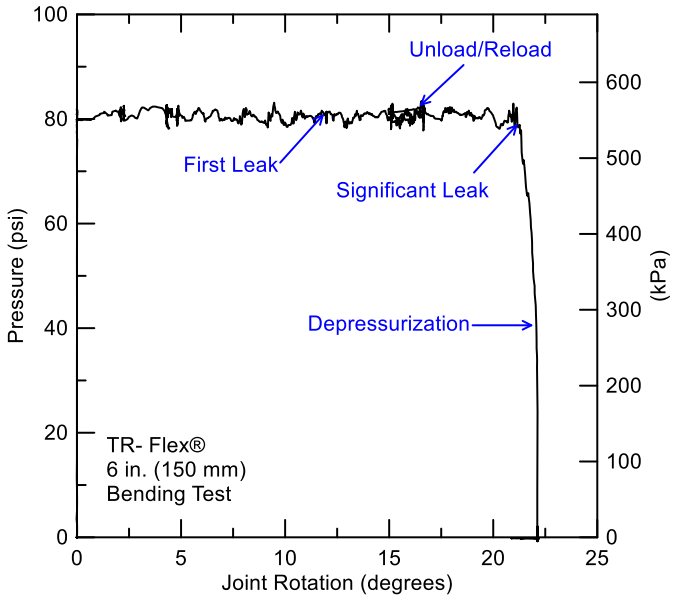


Figure 3.5. Internal Pressure vs. Joint Rotation for TR Flex® Bending Test

First leakage of approximately 10 drops/sec (25 ml/min) was observed at 11.9 degrees of pipe deflection. Due to safety concerns, direct measurements of leakage by collection of outflowing water at leakage locations around the joint were not performed. Estimates of leakage rates, however, were made by visual examination. Significant leakage is defined as flow exceeding 10 gals/min (38 l/min). The leakage observed was relatively constant during the test. The pipe reached 16.6 degrees of deflection at the end of actuator stroke. As the pipe was unloaded to reset the actuator, it rebounded to 15.1 degrees of rotation. During subsequent loading the pipe had significant leakage at 21.3 degrees of deflection. The pipe was then depressurized.

### 3.5.3. Pipe Deflection (Rotation)

The moment vs. rotation relationship is shown in Figure 3.6. After the temporary supports had been removed, the self-weight of the pipe and water caused a rotation of 4.8 degrees. First leakage of approximately 10 drops/sec (25 ml/min) developed at a rotation of 11.9 degrees and an applied moment of 137 kip-in. (15.5 kN-m) as shown in Figure 3.7. The leakage was relatively constant during the test. The test was continued until the deflection reached 16.6 degrees of joint rotation when the actuator reached the limit of its stroke.

As the pipe was unloaded to reset the actuator, it rebounded to 15.1 degrees of joint rotation. The actuator and crosshead were readjusted. The pipe was then reloaded. At 17.5 degrees of joint deflection, the invert locking segment fell out of the joint as illustrated in Figure 3.8. The pipe achieved a maximum moment of 387 kip-in. (44.0 kN-m) at 19.4 degrees of joint rotation. The pipe leaked at a significant rate at 21.3 degrees of joint rotation as shown in Figure 3.9. The test was then stopped, and the pipe was unloaded. There was a residual joint rotation of 20.9 degrees after unloading. Figure 3.10 shows a photograph of the TR Flex® bending specimen after the test. Further investigation after taking the joint apart shows that the pipe broke at the invert of the TR Flex® plain end. Figure 3.11 shows the spigot damage after the test.

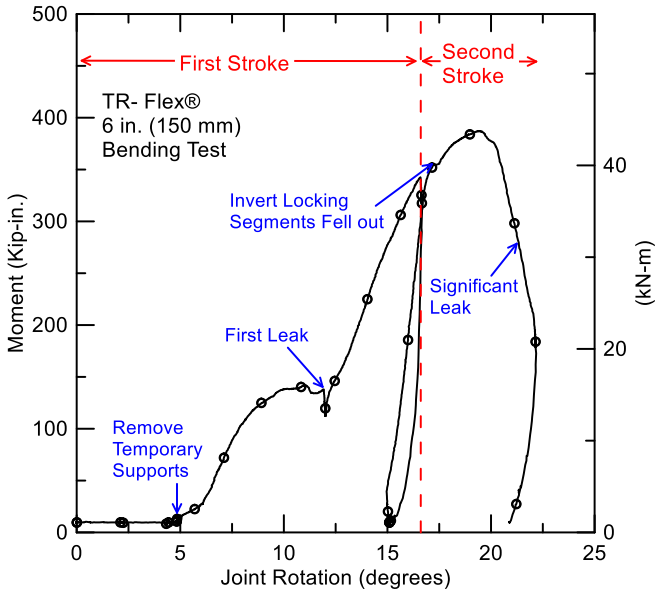


Figure 3.6. Moment vs. Rotation for TR Flex® Bending Test

Figure 3.7. First Leakage of TR Flex® Bending Test Specimen

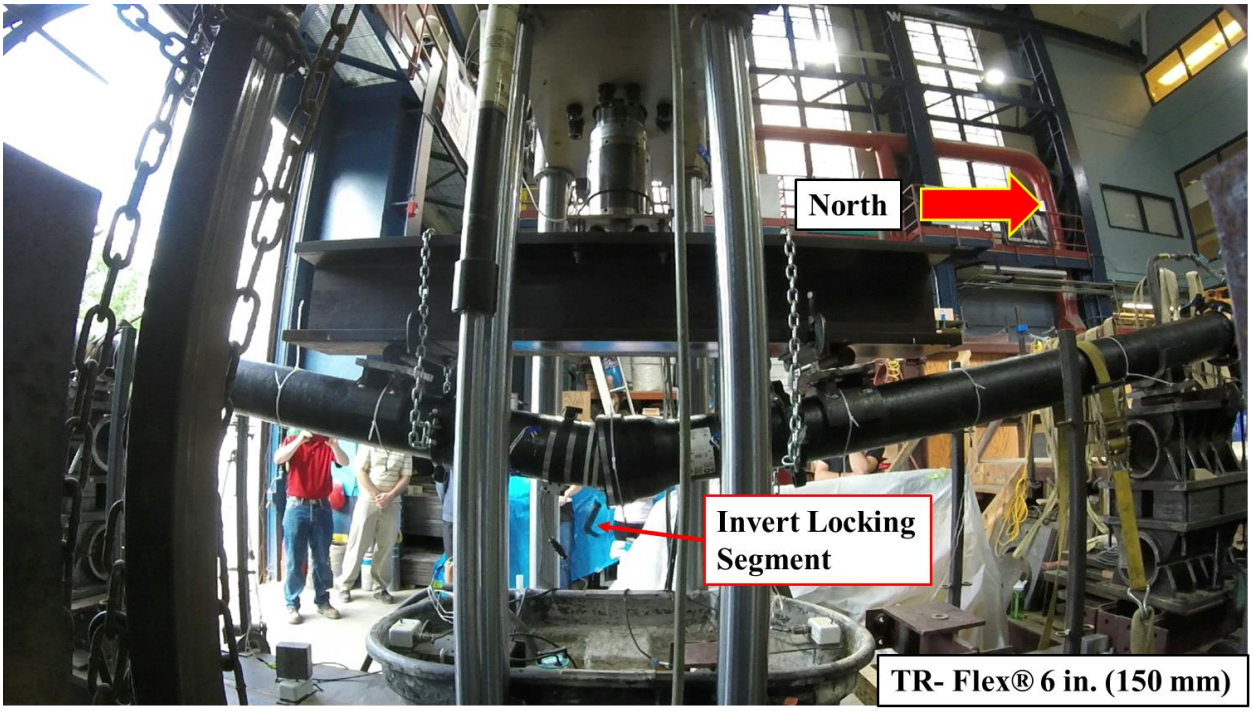


Figure 3.8. Invert Locking Segment Fell out of TR Flex® Joint

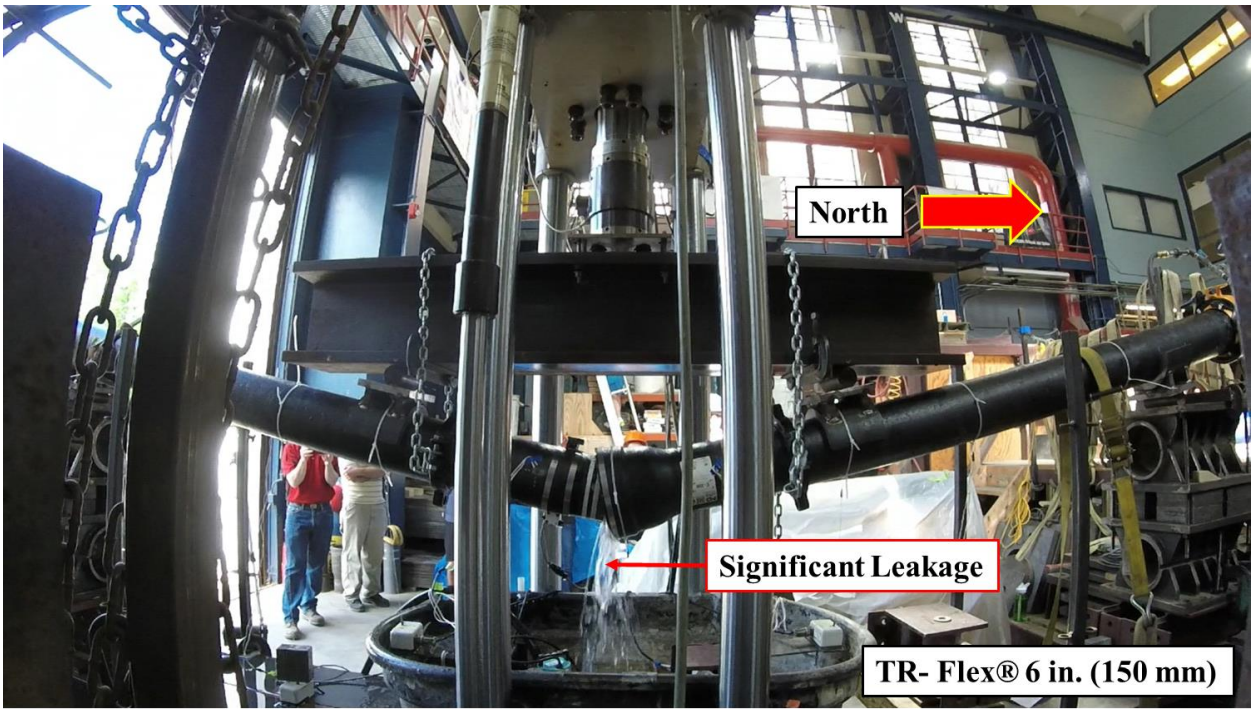


Figure 3.9. Significant Leakage of TR Flex® Bending Test Specimen

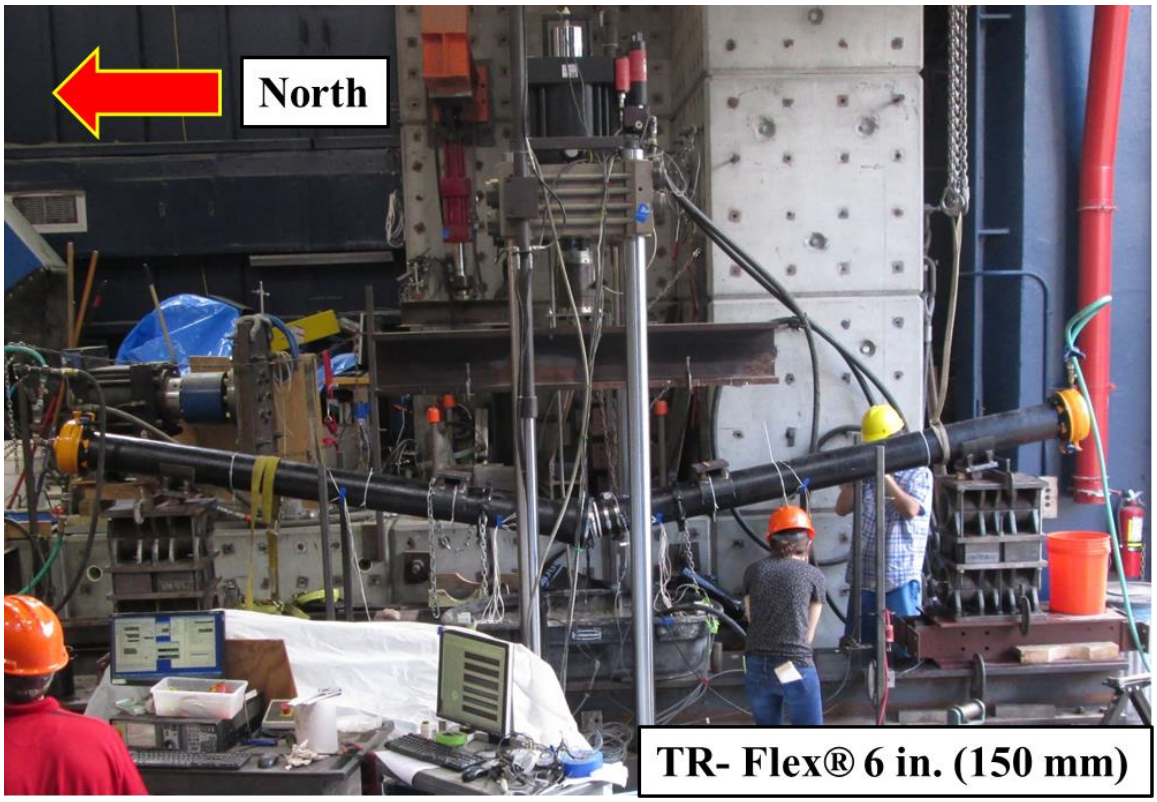


Figure 3.10. Photo of TR Flex® Bending Specimen after Testing

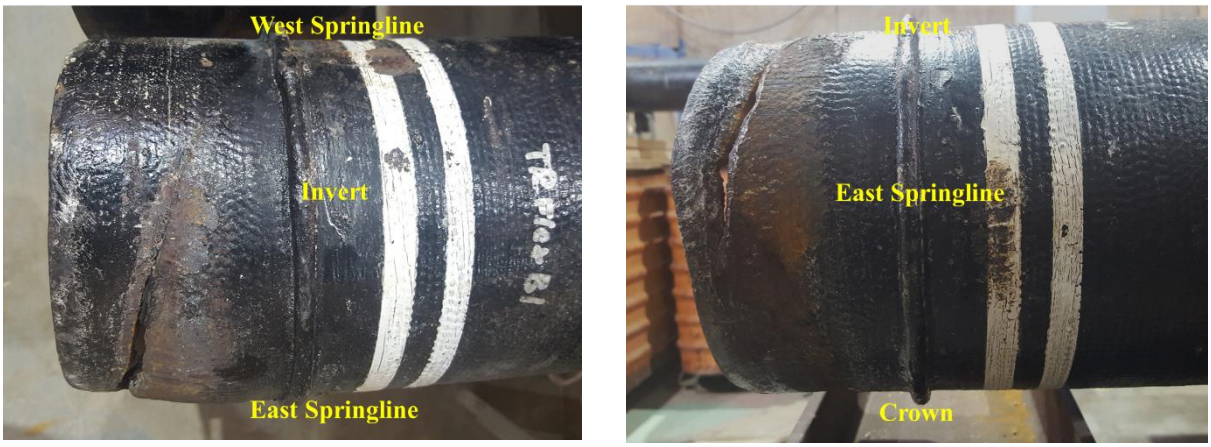


a) View from Invert b) View from East Springline

Figure 3.11. Damage at TR Flex® Plain End after TR Flex® Bending Test

### 3.6. McWane SFC Bending Tests

#### 3.6.1. Instrumentation

Figure 3.12 shows a cross-section of the McWane SFC bending tests. The test setup was similar to that for the TR Flex® bending test. The differences are that the spreader beam was replaced with a longer one, and an additional string pot was used. Figure 3.13 provides a photo of the test setup. Table 3.2 lists location, instrument type, and instrument designation.

#### 3.6.2. Test 1 (3-9)

##### 3.6.2.1.Pressure

The specimen was initially set up at a fully inserted position and had locking segments located at 3 and 9 o'clock (3-9) [Figure 3.1b]. The pipe was then pressurized with water to about 80 psi (550 kPa) while allowing the joint to extend fully in response to axial forces on the end caps. Figure 3.14 shows internal pressure vs. overall deflection. The water pressure line remained open to maintain a nearly constant pressure.

There was a slight drop of pressure to about 78 psi (540 kPa) at 17.7 degrees of overall deflection. The drop of pressure corresponds to first leakage on the order of 10 drops/sec (25 ml/min) at the X joint. This leakage at the X joint continued throughout the test. The pipe reached 28.8 degrees of deflection at the end of the first actuator stroke. As the pipe was unloaded to reset the actuator, there was a fluctuation in the internal pressure, and the pipe rebounded to 22.7 degrees of deflection. The pipe was then reloaded. At 32.5 degrees of overall deflection, the pipe had a significant leakage at a rate of about 10 gals/min (38 l/min), and the pipe was then depressurized.

##### 3.6.2.2.Pipe Deflection (Rotation)

The moment vs. overall deflection and individual rotation relationships are shown in Figures 3.15 and 3.16, respectively. After the temporary supports had been removed, the self-weight of the pipe and water caused a deflection of 8.2 degrees. Figure 3.17 shows first leakage that was observed at the X joint with 1.8 and 17.7 degrees of X joint rotation and overall deflection, respectively, with an associated applied moment of 219 kip-in. (24.7 kN-m). The leakage at the X joint was relatively constant during the test. The test was continued until the deflection reached 28.8 degrees and the actuator reached the end of its stroke.

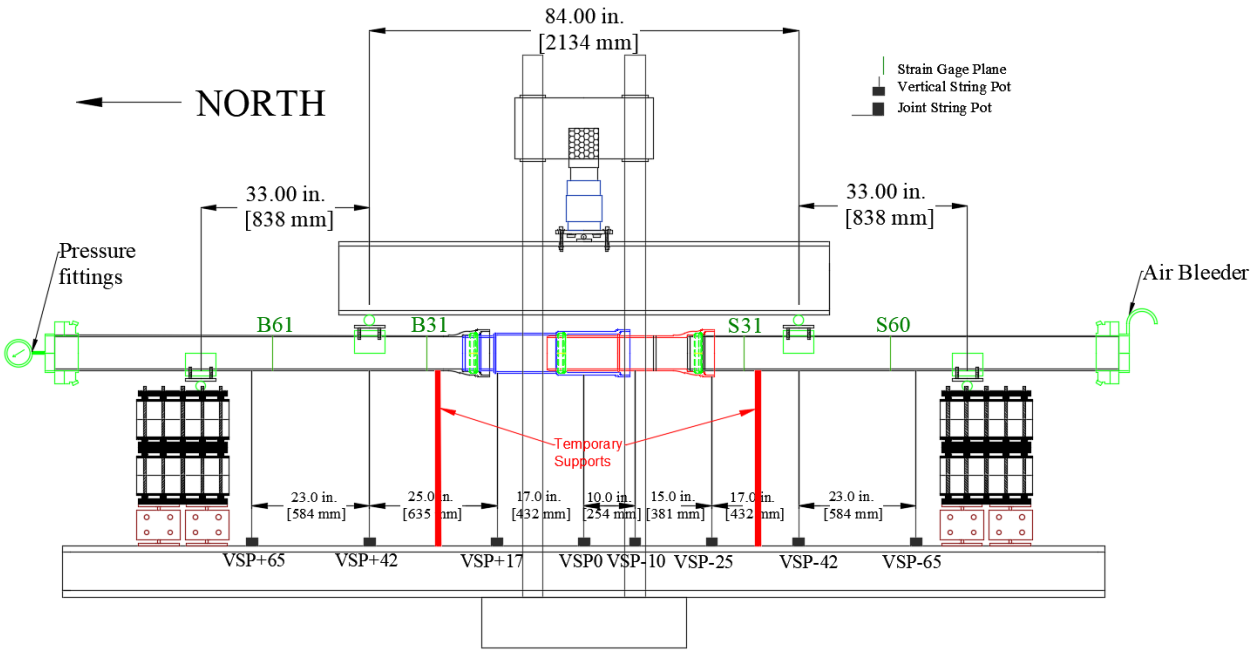


Figure 3.12. Cross-section of Instrumentation for McWane SFC Bending Tests

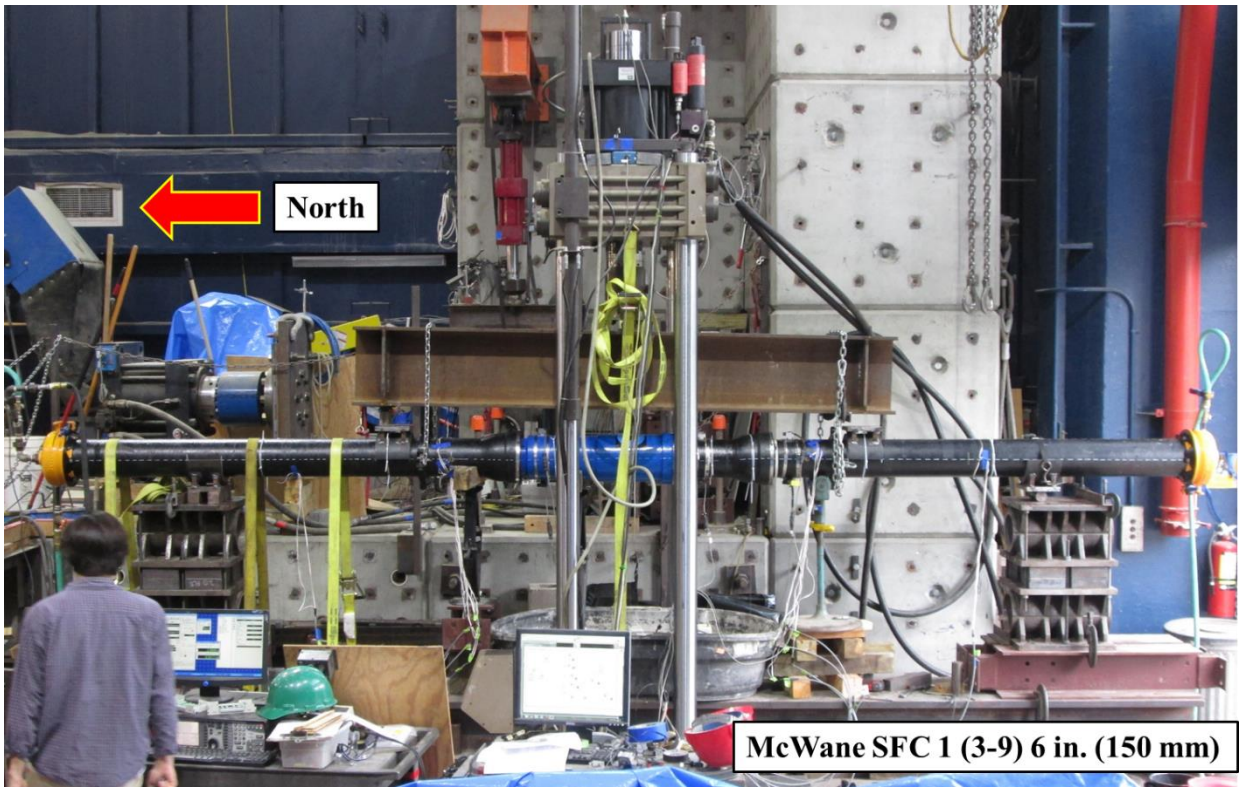


Figure 3.13. Photo of McWane SFC Bending Specimen 1 (3-9) before Testing

Table 3.2. Instrumentation for McWane SFC Bending Tests

| Location | Instrument Description | Instrument Designation |
|---|---|---|
| -65 in. from Centerline | Vertical String Pot on Bell End | VSP -65 |
| -42 in. from Centerline | Vertical String Pot on Bell End | VSP -42 |
| -25 in. from Centerline | Vertical String Pot on Bell End | VSP -25 |
| -10 in. from Centerline | Vertical String Pot on Bell End | VSP -10 |
| 0 in. from Centerline | Vertical String Pot on Bell End | VSP 0 |
| 17 in. from Centerline | Vertical String Pot on Spigot End | VSP +17 |
| 42 in. from Centerline | Vertical String Pot on Spigot End | VSP +42 |
| 65 in. from Centerline | Vertical String Pot on Spigot End | VSP +65 |
| 4 in. from Centerline | Horizontal String Pot at Crown | HSP_C |
| 4 in. from Centerline | Horizontal String Pot at Invert | HSP_I |
| Top Center | Load Cell | Load |
| North End Cap | Pressure Gage | Pressure |

1 in. = 25.4 mm

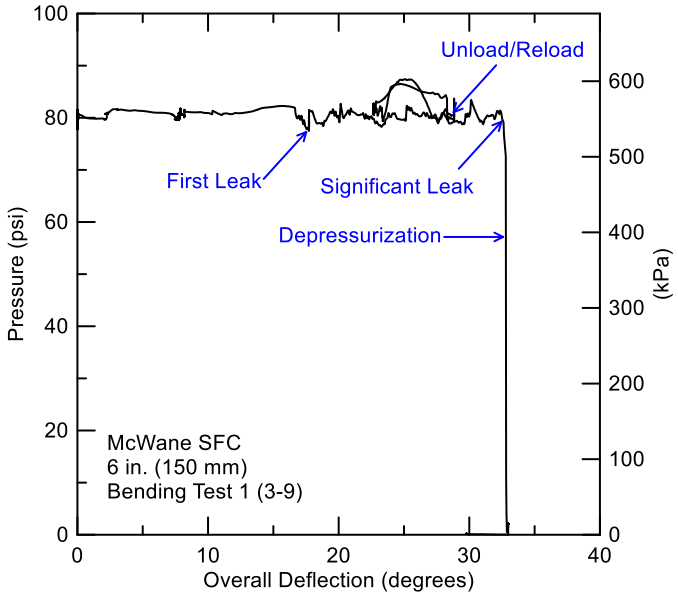


Figure 3.14. Internal Pressure vs. Deflection for McWane SFC Bending Test 1 (3-9)

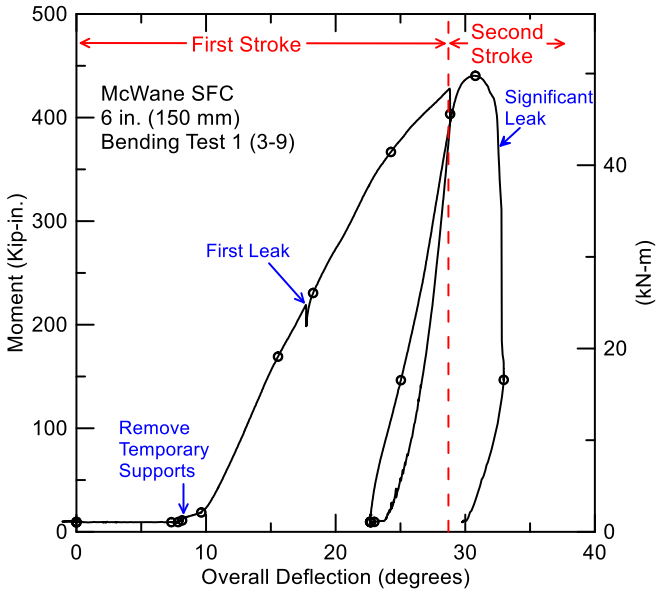


Figure 3.15. Moment vs. Deflection for McWane SFC Bending Test 1 (3-9)

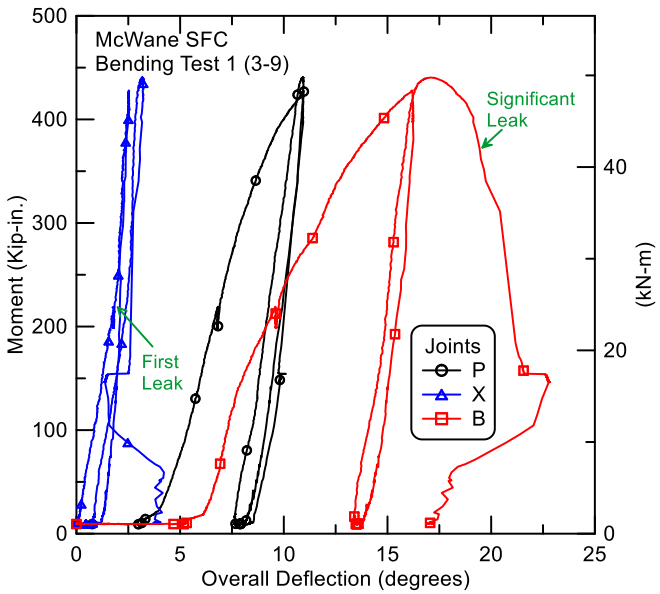


Figure 3.16. Moment vs. Joint Rotations for McWane SFC Bending Test 1 (3-9)

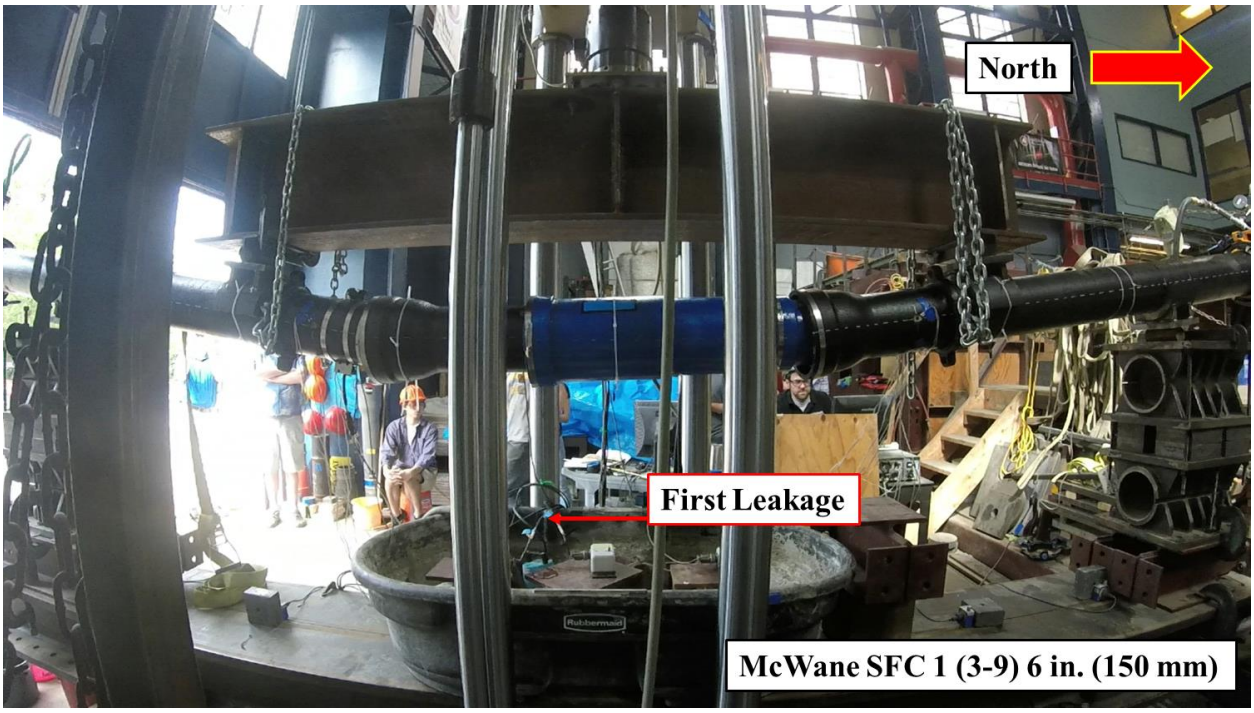


Figure 3.17. First Leakage of McWane SFC Bending Test Specimen 1 (3-9)

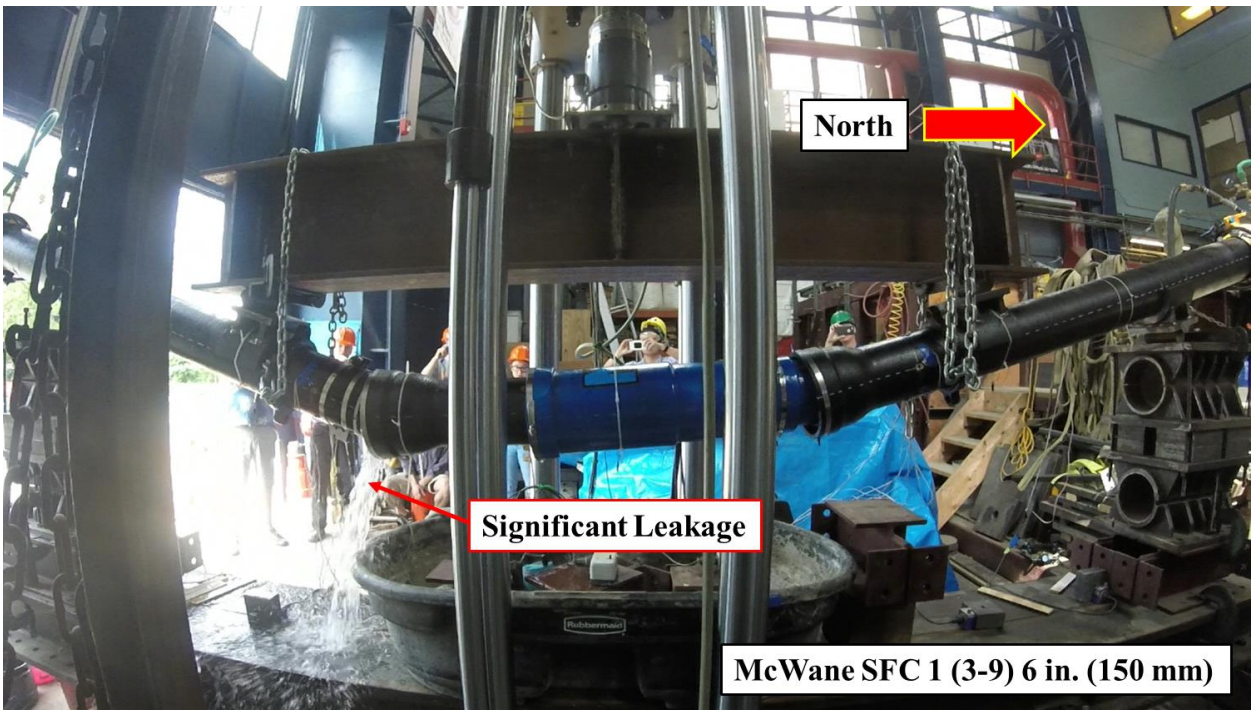


Figure 3.18. Significant Leakage of McWane SFC Bending Test Specimen 1 (3-9)

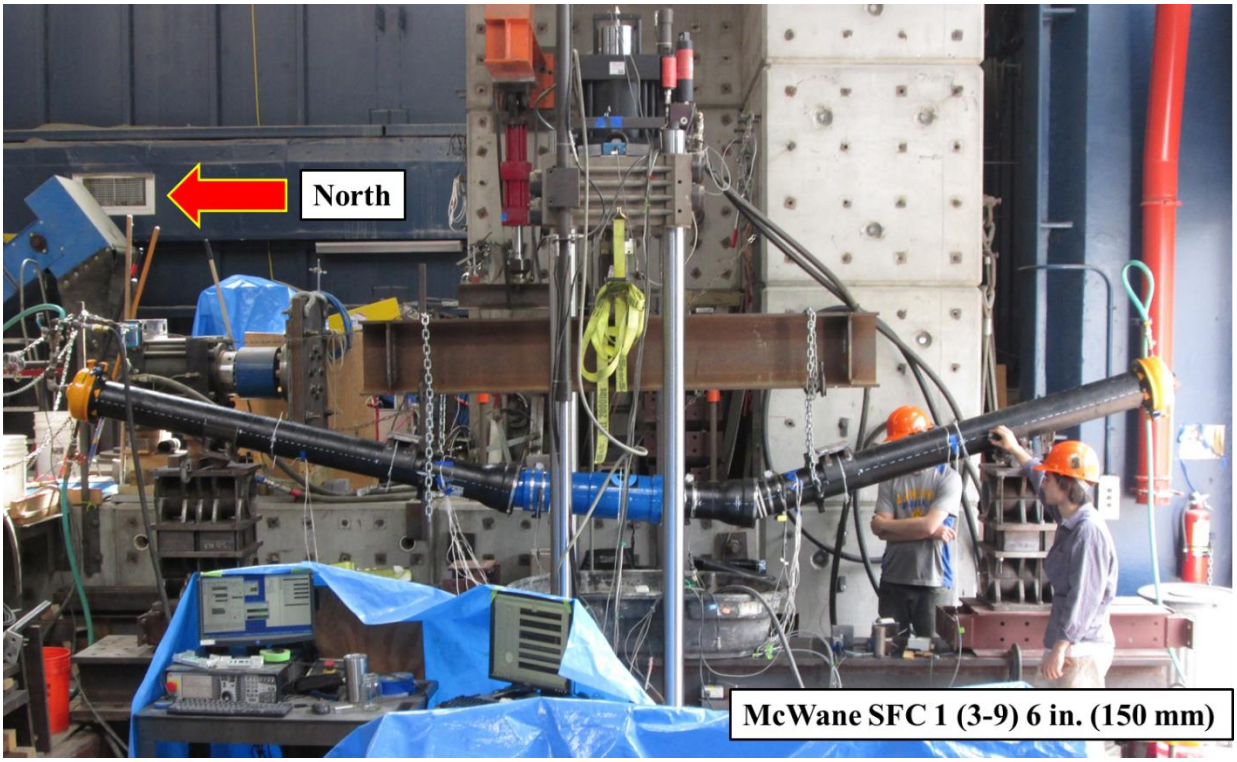


Figure 3.19. Photo of McWane SFC Bending Specimen 1 (3-9) after Testing

As the pipe was unloaded to reset the actuator, it rebounded to 22.7 degrees of overall deflection. The actuator and crosshead were readjusted. The pipe was then reloaded. The pipe achieved a maximum moment of 440 kip-in. (49.7 kN-m) at 30.6 degrees of deflection. The pipe leaked at the B joint with a significant rate at 19.4 and 32.5 degrees of B joint rotation and overall deflection, respectively. Figure 3.18 shows the significant leakage at the B joint. Shortly after the significant leakage, the test was stopped, and the pipe was unloaded. There was a residual deflection of 29.8 degrees after unloading. Figure 3.19 shows a photograph of the McWane SFC bending specimen 1 (3-9) after the test. Further investigation after taking the joints apart shows that the pipe has similar damage as the TR Flex® bending specimen such that the pipe broke at the invert of the TR Flex® plain end. Figure 3.20 shows the spigot damage after the test.

Figure 3.20. Damage at TR Flex® Plain End after McWane SFC Bending Test 1 (3-9)

### 3.6.3. Test 2 (12-6)

#### 3.6.3.1.Pressure

The specimen was initially set up at a fully inserted position and had locking segments located at 12 and 6 o'clock [Figure 3.1a]. The pipe was then pressurized with water to about 80 psi (550 kPa) while allowing the joint to extend fully in response to axial forces on the end caps. Figure 3.21 shows internal pressure vs. overall deflection. The water pressure line remained open to maintain a nearly constant pressure.

First leakage was observed at the X joint at the beginning of the test. The leakage stopped at a pipe deflection of 20.5 degrees. The pipe reached 26.1 degrees of deflection at the end of the first actuator stroke. As the pipe was unloaded to reset the actuator, it rebounded to 24.1 degrees of deflection. The pipe was then reloaded. At 34.9 degrees of overall deflection, there was another leak on the order of 2.4 fl. oz./min (75 ml/min) at the P joint. The pipe failed and had a significant leakage at a rate of greater than 10 gals/min (38 l/min) and lost internal pressure at 36.0 degrees of overall deflection.

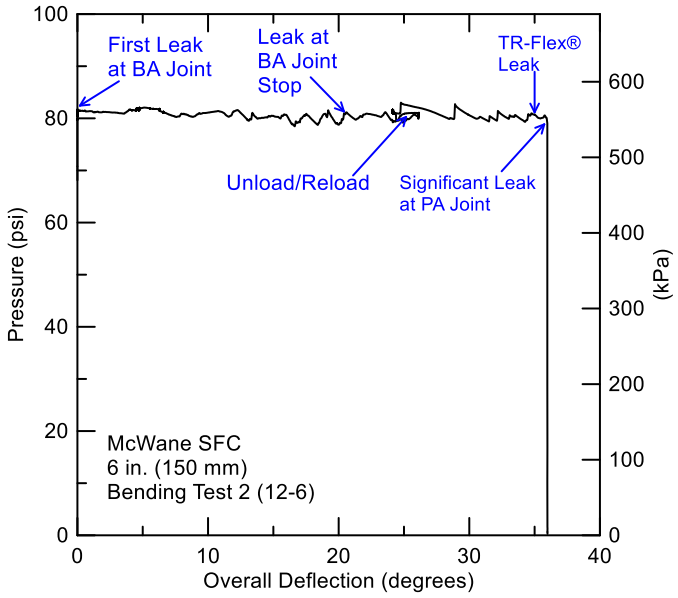


Figure 3.21. Internal Pressure vs. Deflection for McWane SFC Bending Test 2 (12-6)

### 3.6.3.2.Pipe Deflection (Rotation)

The moment vs. overall deflection and individual rotation relationships are shown in Figures 3.22 and 3.23, respectively. First leakage of approximately 10 drops/sec (25 ml/min) was observed at the X joint at the beginning of the test, as shown in Figure 3.24. After the temporary supports had been removed, the self-weight of the pipe and water caused a deflection of 4.5 degrees. The leakage at the X joint stopped when moment reached 202 kip-in. (22.8 kN-m) at 1.1 and 20.5 degrees of X joint rotation and pipe deflection, respectively. The pipe deflection continued to increase until the pipe reached a deflection of 23.5 degrees when the moment began to decline. When the moment dropped to 203 kip-in. (22.9 kN-m), the invert locking segment of the P joint fell out, as illustrated in Figure 3.25, at 11.3 and 25.6 degrees of P joint rotation and overall deflection, respectively. The test was continued until the rotation reached 26.1 degrees of deflection when the actuator reached the end of its stroke.

As the pipe was unloaded to reset the actuator, it rebounded to 24.1 degrees of overall deflection. The actuator and crosshead were readjusted. The pipe was then reloaded. Another invert locking segment fell out of the B joint, as shown in Figure 3.26, at B joint rotation and pipe deflection of 16.1 degrees and 32.2 degrees, respectively.

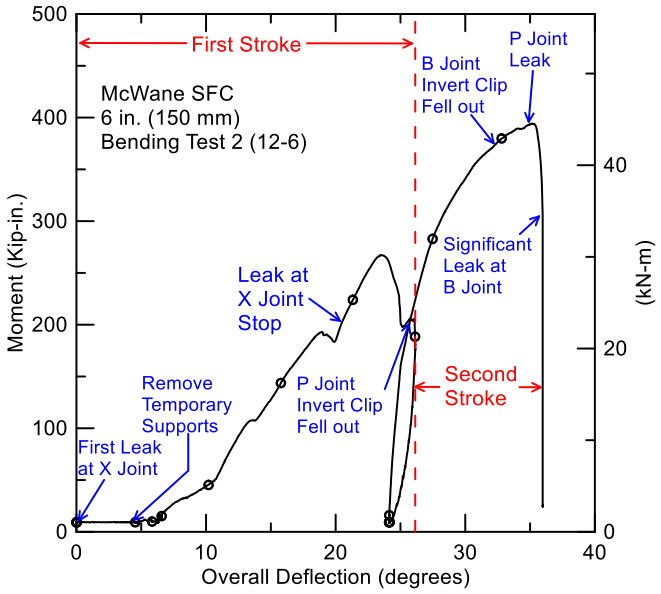


Figure 3.22. Moment vs. Deflection for McWane SFC Bending Test 2 (12-6)

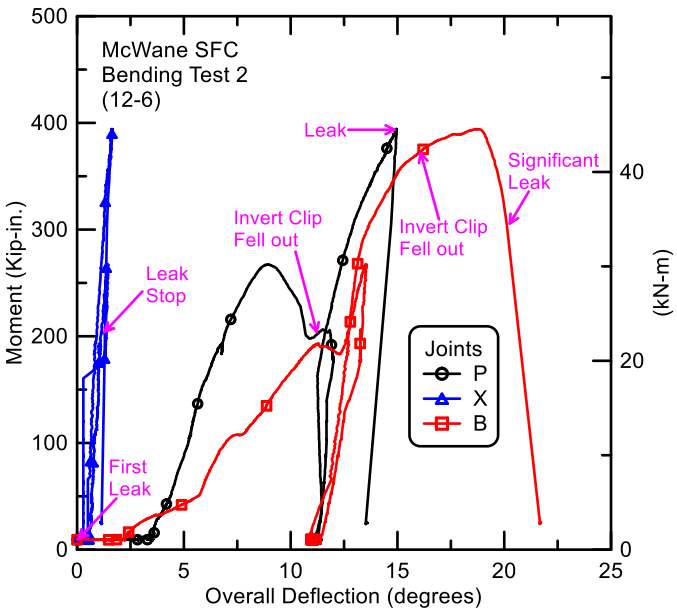


Figure 3.23. Moment vs. Joint Rotations for McWane SFC Bending Test 2 (12-6)

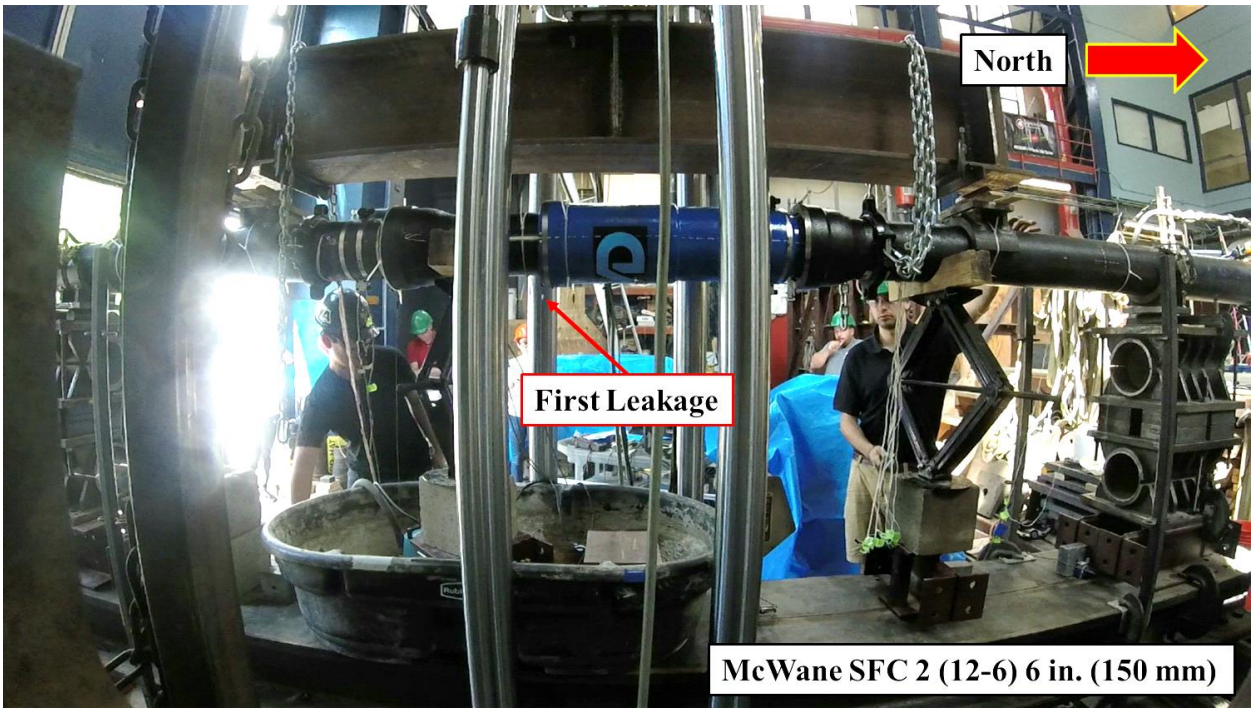


Figure 3.24. First Leakage of McWane SFC Bending Test Specimen 2 (12-6)

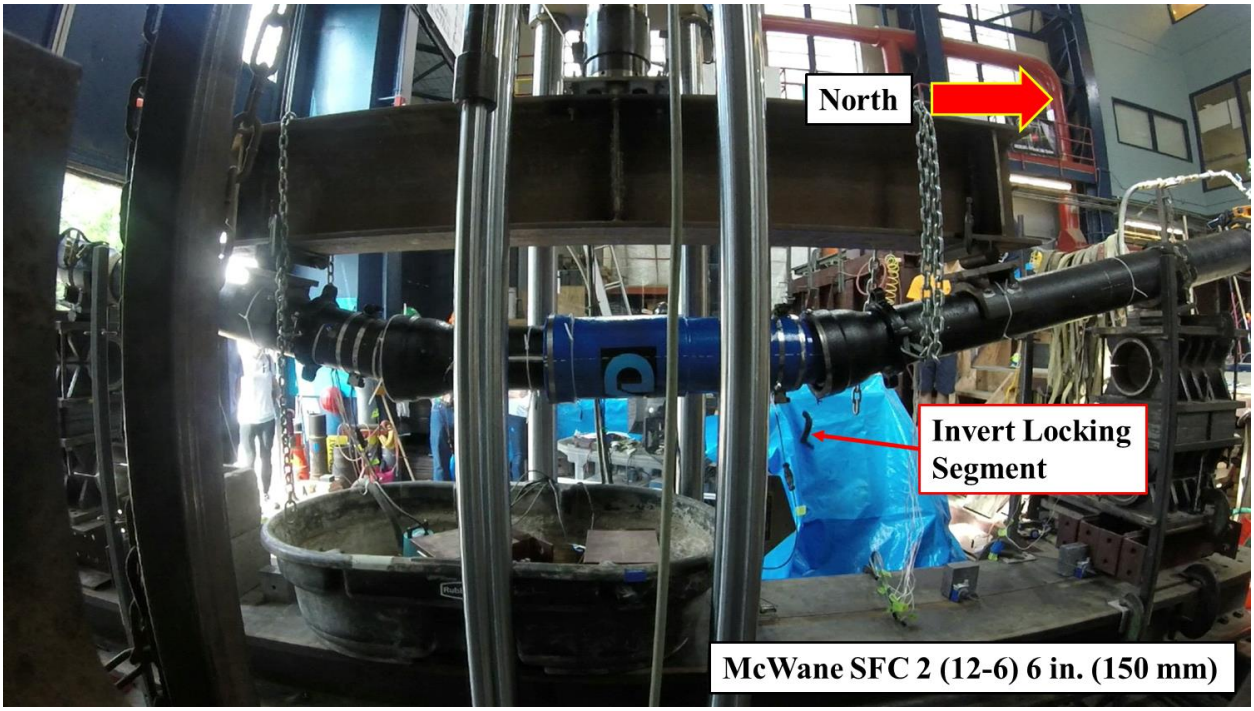


Figure 3.25. Invert Locking Segment Fell out of P Joint

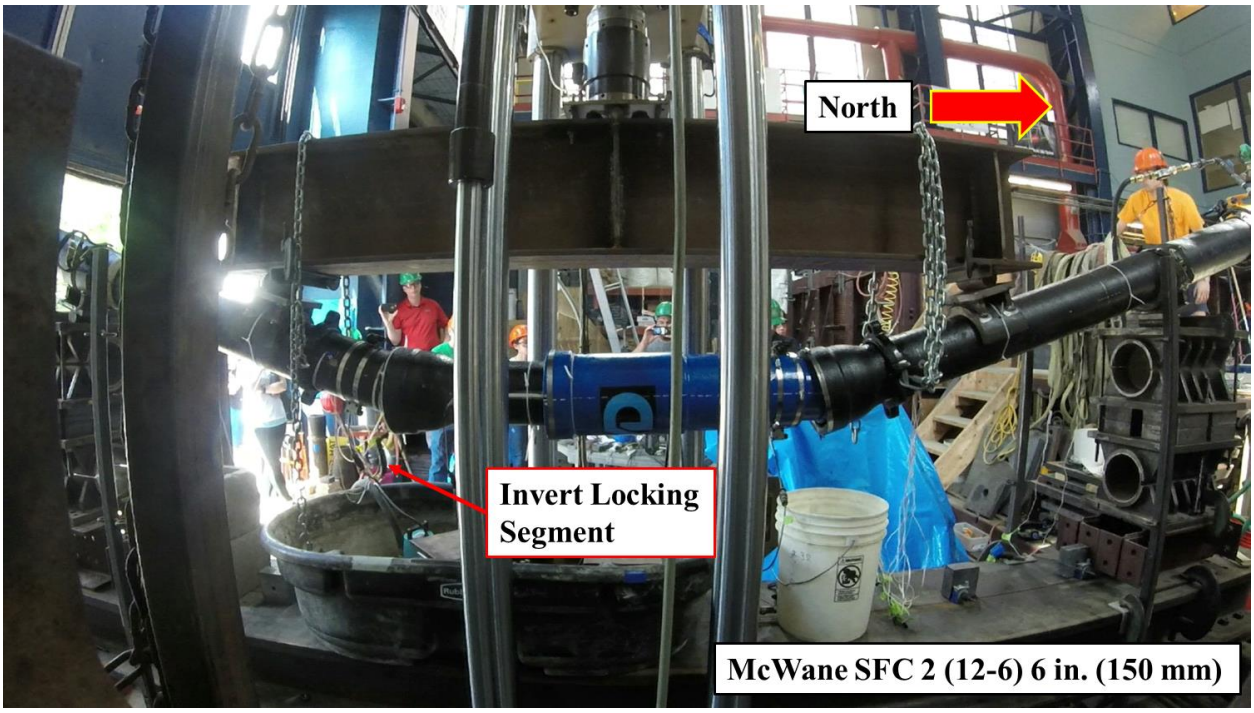


Figure 3.26. Invert Locking Segment Fell out of B Joint

When the pipe achieved a maximum moment of 393 kip-in. (44.4 kN-m), leakage of approximately 2.4 fl. oz./min (75 ml/min) was detected at the P joint at 14.9 and 34.9 degrees of P joint rotation and overall deflection, respectively. The applied moment then rapidly decreased, and the pipe failed and leaked at the B joint with a significant rate at 21.7 and 36.0 degrees of B joint rotation and overall deflection, respectively. Figure 3.27 shows the significant leakage at the B joint. Figure 3.28 shows a photograph of the McWane SFC bending specimen 2 (12-6) after the test. Further investigation after taking the joints apart shows that the pipe has similar damage as the previous bending tests such that the pipe broke at the invert of the TR Flex® Plain End. Figure 3.29 shows the damage at the TR Flex® plain end after the test.

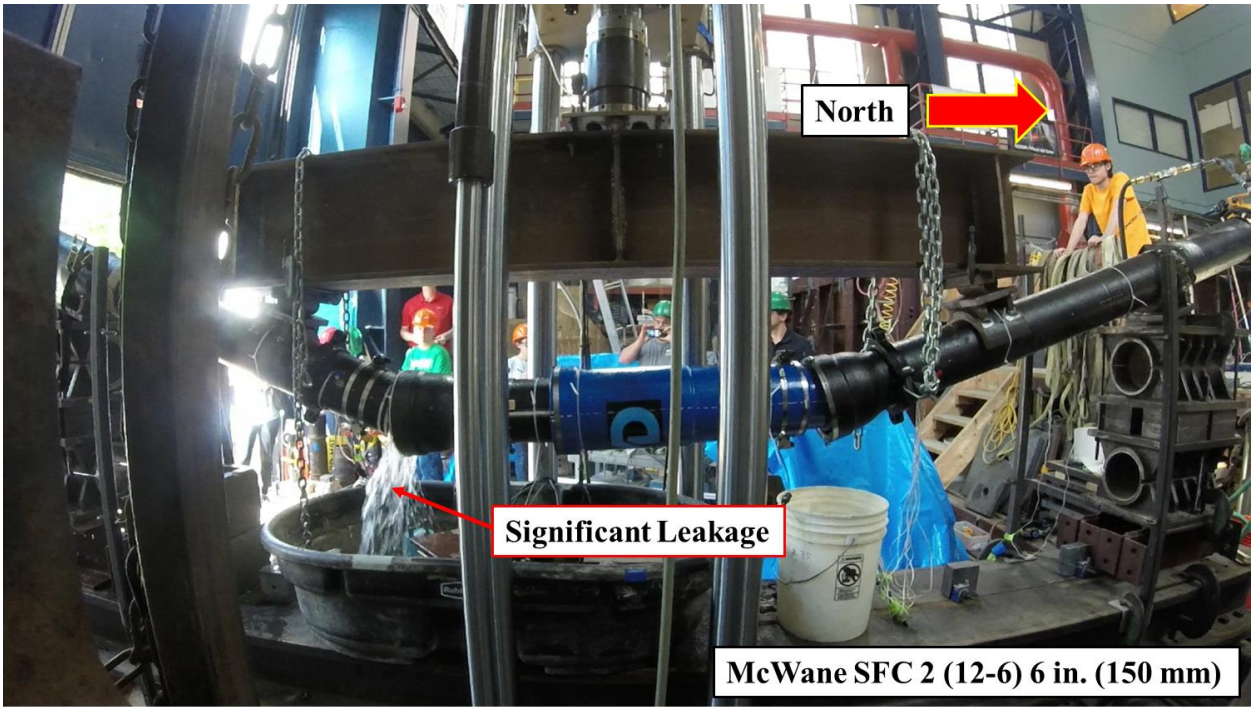


Figure 3.27. Significant Leakage of McWane SFC Bending Test Specimen 2 (12-6)

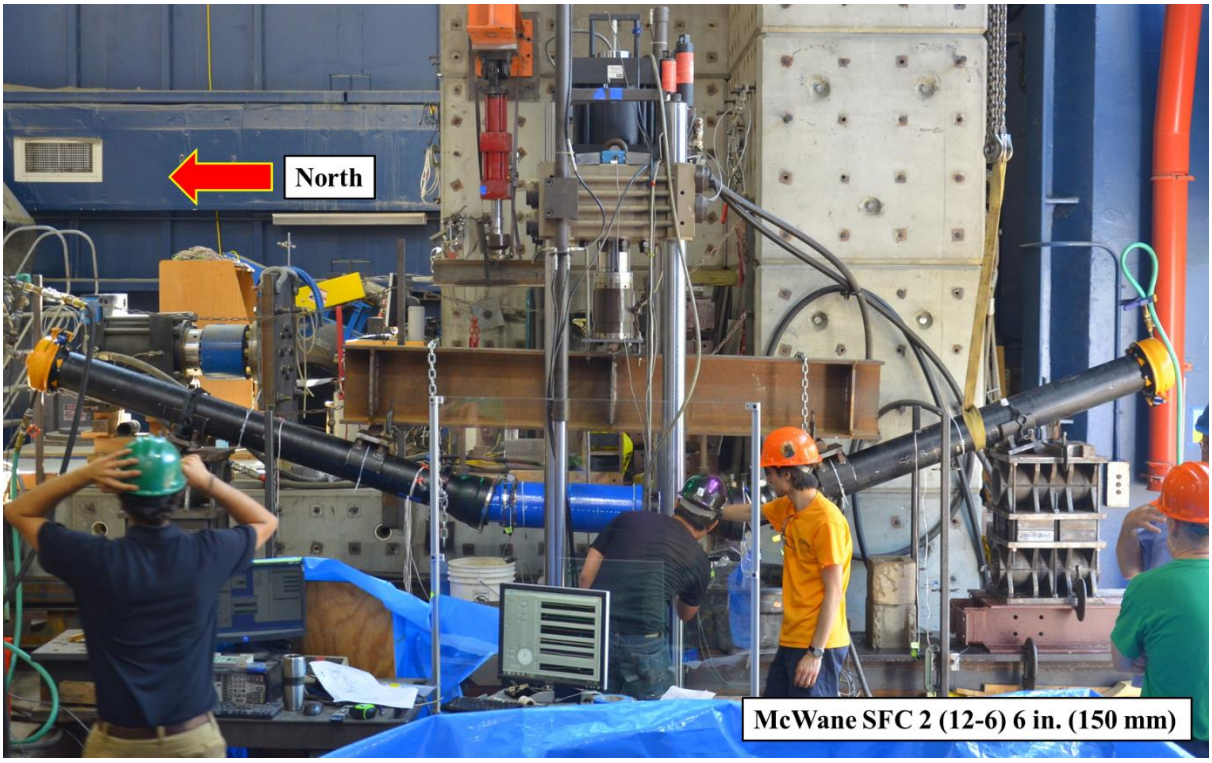


Figure 3.28. Photo of McWane SFC Bending Specimen 2 (12-6) after Testing

a) View from Invert

b) View from West Springline

Figure 3.29. Damage at TR Flex® Plain End after McWane SFC Bending Test 2 (12-6)

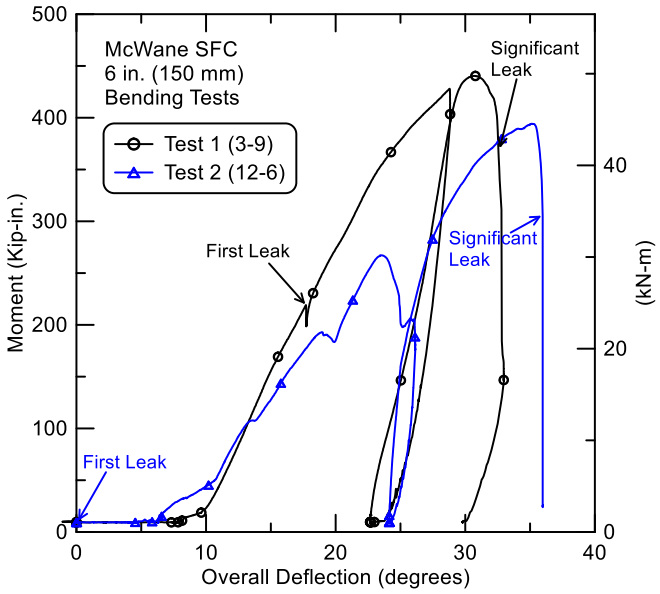


Figure 3.30. Moment vs. Deflection Comparisons for McWane SFC Bending Tests

### 3.6.4. Comparisons of McWane SFC Bending Tests

The moment vs. deflection comparisons for the McWane SFC bending tests are shown in Figure 3.30. Comparing results between Specimens 1 (3-9) and 2 (12-6) shows differences in moment vs. deflection relationships for the two locking segment orientations to applied loads. Under pipe and water weight, Specimen 1 (3-9) deflected 8.2 degrees while Specimen 2 (12-6) only deflected 4.5 degrees. Specimen 1 (3-9) produced larger deflection because of the lack of material at the slots at crown and invert. Specimen 1 (3-9) subsequently showed stiffer rotational responses than Specimen 2 (12-6).

Specimen 1 (3-9) first leaked at the X joint on the order of 10 drops/sec (25 ml/min) at an applied moment of 219 kip-in. (24.7 kN-m) with an associated overall deflection of 17.7 degrees. The leakage at the X joint was relatively constant throughout the test. Specimen 1 (3-9) achieved a maximum moment of 440 kip-in. (49.7 kN-m) at 30.6 degrees of deflection. The applied moment decreased to 372 kip-in. (42.0 kN-m), and the pipe leaked at the B joint with a significant rate on the order of 10 gals/min (38 l/min) at 32.5 degrees of overall deflection.

In Test 2 (12-6), first leakage of approximately 10 drops/sec (25 ml/min) was observed at the X joint at the beginning of the test. This leakage stopped afterward when the pipe reached a moment of 202 kip-in. (22.8 kN-m) at 20.5 degrees of pipe deflection. The invert locking segments of the P and B joint fell out at overall deflections of 25.6 and 32.2 degrees, respectively. A maximum applied moment of 393 kip-in. (44.4 kN-m) was achieved at 34.9 degrees of pipe deflection. The applied moment then rapidly decreased, and the pipe failed and leaked at the B joint with a significant rate greater than 10 gals/min (38 l/min) at 36.0 degrees of overall deflection.

### 3.7. Summary of Bending Tests

Results were presented for pressurized four-point bending tests of nominal 6-in. (150-mm)-diameter sections of two McWane SFCs and one separated TR Flex® joint provided by McWane Ductile. The purpose of the tests was to develop moment vs. rotation relationships to characterize pipe joint performance with respect to leakage and structural integrity. It should be noted that the term "rotation" in this report is equivalent to "deflection" as used commonly in commercial pipeline information.

Table 3.3 summarizes moment and rotation data for each test. In the TR Flex® bending test, the locking segments were installed at 12 and 6 o'clock positions. First leakage of approximately developed at a rotation of 11.9 degrees. The leakage was relatively constant during the test. At 17.5 degrees of joint rotation, the invert locking segment fell out of the joint. The pipe achieved a maximum 19.4 degrees of deflection. The pipe leaked at a significant rate at 21.3 degrees of joint rotation.

Two bending tests were performed on McWane SFC specimens. SFC Tests 1 and 2 had the locking segments located at 3-9 o'clock and 12-6 o'clock positions, respectively. The rotational response of SFC Specimens 1 (3-9) and 2 (12-6) varies. Under pipe and water weight, Specimen 1 (3-9) deflected 8.2 degrees while Specimen 2 (12-6) only deflected 4.5 degrees. Specimen 1 (3-9) produced larger deflection because of the lack of material at the slots at crown and invert. Specimen 1 (3-9) subsequently showed stiffer rotational responses than Specimen 2 (12-6).

Specimen 1 (3-9) first leaked at the X joint on the order of 10 drops/sec (25 ml/min) at an overall deflection of 17.7 degrees. The leakage at the X joint was relatively constant throughout the test. Specimen 1 (3-9) achieved a maximum moment of 440 kip-in. (49.7 kN-m) at 30.6 degrees of deflection. The applied moment then decreased, and the pipe leaked at a significant rate at the B joint with an overall deflection of 32.5 degrees.

Table 3.3. Results of Four-Point Bending Tests

| Bending Test | First Leakage | | Maximum Moment | | Maximum Deflection at Significant Leakage |
|---|---|---|---|---|---|
| | Deflection | Moment | Deflection | Moment | |
| TR Flex® (12-6 o'clock)[a] | 11.9° | 137 kip-in. (15.5 kN-m). | 19.4° | 387 kip-in. (44.0 kN-m). | 21.3° |
| SFC 1 (3-9 o'clock) | 17.7° | 219 kip-in (24.7 kN-m) | 30.6° | 440 kip-in. (49.7 kN-m) | 32.5° |
| SFC 2 (12-6 o'clock)[b] | ≈ 0° | Self-weight | 34.9° | 393 kip-in. (44.4 kN-m) | 36.0° |

[a] Invert locking segment fell out at 17.5°

[b] Invert locking segment fell out of P and B joints at 25.6° and 32.2°, respectively.

In Test 2 (12-6), first leakage of approximately 10 drops/sec (25 ml/min) was observed at the X joint at the beginning of the test. This leakage stopped when the pipe reached a deflection of 20.5 degrees. The invert locking segments of the P and B joint fell out at overall deflections of 25.6 and 32.2 degrees, respectively. A maximum applied moment of 393 kip-in. (44.4 kN-m) was achieved at 34.9 degrees of pipe deflection. The applied moment then rapidly decreased, and the pipe failed by significant leakage at the B joint at 36.0 degrees of overall deflection.

# Section 4
# Joint Axial Tension and Compression Tests

## 4.1. Introduction

This section summarizes three pressurized tension tests of two McWane Seismic Flex Couplings (SFCs) and one separated TR Flex® joint and one pressurized compression test of a McWane SFC. All joint axial tests were conducted on nominal 6-in. (150-mm)-diameter sections. The locking segments were positioned at the springline of the pipe, i.e., the 3-9 positions. The test results are used to determine the force vs. displacement relationships and limit states of TR- Flex® and McWane SFCs.

## 4.2. TR Flex® Tension Test

The TR Flex® tension test specimen was 15.4 ft. (4.68 m) long with an outside diameter of 6.9 in. (175 mm) and a wall thickness of 0.3 in. (7.6 mm.). The spigot was fully inserted inside the bell at the beginning of the test. Full insertion refers to the position when the end of the spigot is in contact with the base of the TR Flex® bell. Figure 4.1 shows the TR Flex® tension test setup.

### 4.2.1. Instrumentation

Four strain gages were mounted at the crown, invert, east springline, and west springline at 38.5 in. (978 mm) north of the bell face on the bell side and 38.0 in. (965 mm) south of the bell face on the spigot side. Four string pots were installed at crown, invert, east springline, and west springline to measure joint axial pullout from the bell. An actuator and load cell were installed on the load frame to apply and measure tensile force at the end of the pipe. An electronic pressure transducer, located at the north end cap, measured internal water pressure. The instrument locations and gage names are shown and listed in Figure 4.1 a) and Table 4.1, respectively.

### 4.2.2. Force vs. Displacement

The specimen was filled with water and pressurized. The pressurizing sequence is shown in Figure 4.2. As the pressure was increased to approximately 80 psi (550 kPa), the axial load on the pipe end caps was 2.4 kips (13 kN), and there was no movement the joints. Axial loading was subsequently applied while the pipe was under the initial thrust load.

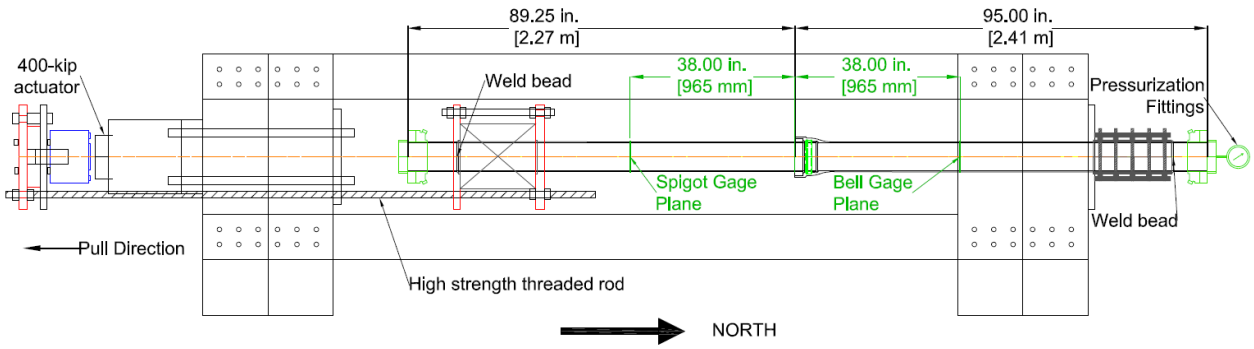


a) Schematic of Instrumentations

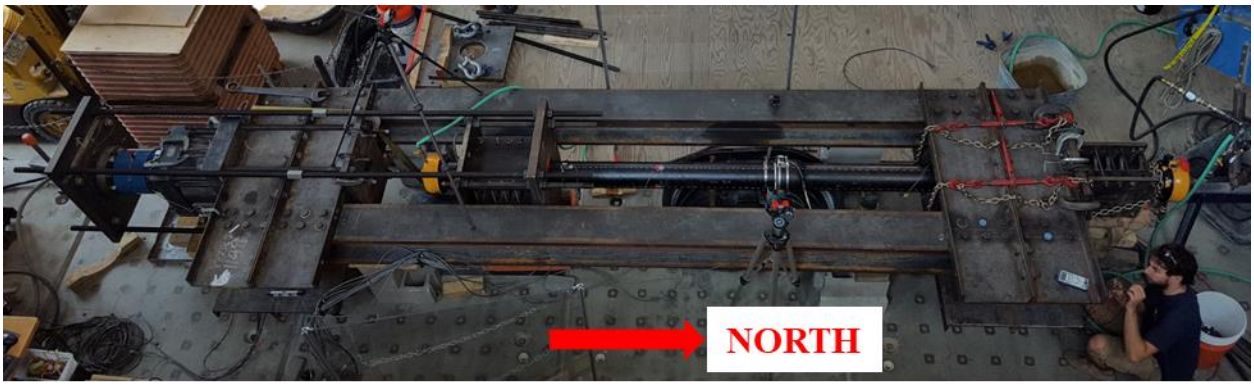


b) Photo of Test Setup

Figure 4.1. TR Flex® Tension Test Layout

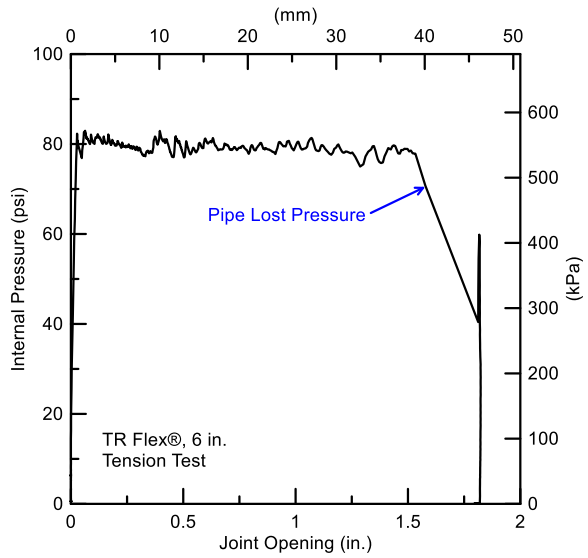


Figure 4.2. Internal Pressure vs. Joint Opening for TR Flex® Tension Test

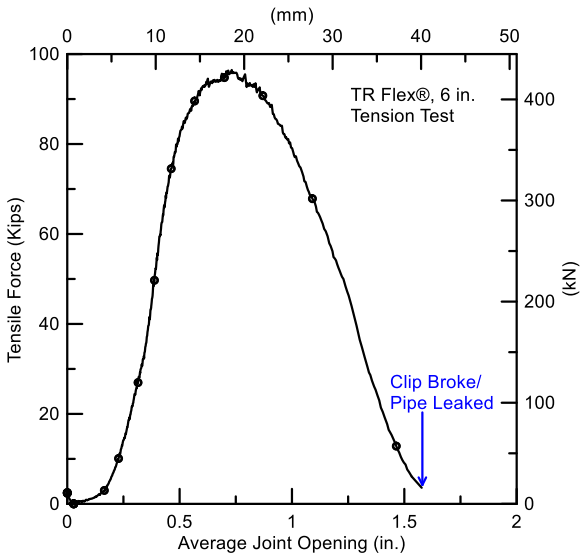


Figure 4.3. Tensile Force vs. Joint Opening for TR Flex® Tension Test

Table 4.1. Instrumentation for TR Flex® Tension Test

| Location | Instrument Description | Instrument Designation |
|---|---|---|
| 38 in. North of Bell Face | Crown, Axial Strain | BC |
| 38 in. North of Bell Face | Invert, Axial Strain | BI |
| 38 in. North of Bell Face | East Springline, Axial Strain | BE |
| 38 in. North of Bell Face | West Springline, Axial Strain | BW |
| 38 in. North of Bell Face | Crown, Circumferential Strain | BCC |
| 38 in. North of Bell Face | Invert, Circumferential Strain | BIC |
| 38 in. North of Bell Face | East Springline, Circumferential Strain | BEC |
| 38 in. North of Bell Face | West Springline, Circumferential Strain | BWC |
| 38 in. South of Bell Face | Crown, Axial Strain | SC |
| 38 in. South of Bell Face | Invert, Axial Strain | SI |
| 38 in. South of Bell Face | East Springline, Axial Strain | SE |
| 38 in. South of Bell Face | West Springline, Axial Strain | SW |
| 38 in. South of Bell Face | Crown, Circumferential Strain | SCC |
| 38 in. South of Bell Face | Invert, Circumferential Strain | SIC |
| 38 in. South of Bell Face | East Springline, Circumferential Strain | SEC |
| 38 in. South of Bell Face | West Springline, Circumferential Strain | SWC |
| Bell Face | Joint Crown String Pot | HSP_C |
| Bell Face | Joint Invert String Pot | HSP_I |
| Bell Face | Joint East Springline String Pot | HSP_E |
| Bell Face | Joint West Springline String Pot | HSP_W |
| Actuator | Load Cell | Atlas 400kip Load |
| Actuator | Displacement | Act_Disp |
| Internal Pressure | Pressure Transducer | Pressure |

1 in. = 25.4 mm

Loading began at a rate of 1 in. (25.4 mm) per minute. Figure 4.3 shows the relationships of tensile force vs. joint displacement for the TR Flex® joint. As tensile force was applied, the spigot was pulled from the bell and the spigot weld bead to bear against and transfer concentrated load onto the locking segments. The progressive movements of the joint and locking segments are provided in Figures 4.3 and 4.4. The peak load of 96.5 kips (429 kN) was achieved at 0.73 in. (18.5 mm) of joint opening. The tensile force subsequently declined, corresponding to cracking of the left-hand locking segment on the west springline. When the joint reached 1.57 in. (39.8 mm) of displacement at the load of 3.6 kips (16 kN), the left-hand locking segment broke, and the pipe began to leak.

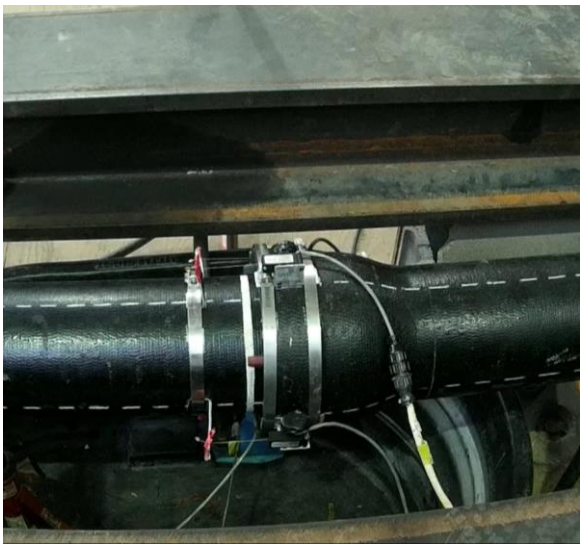

a) Joint Fully Inserted

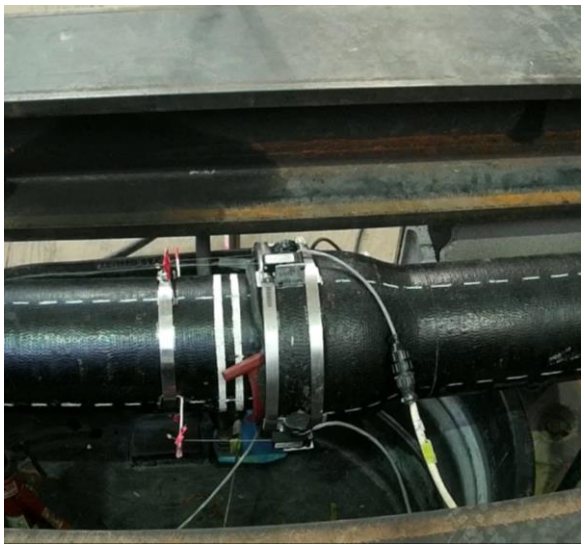

b) Joint Fully Extended and Locking Segments Rotated Inward

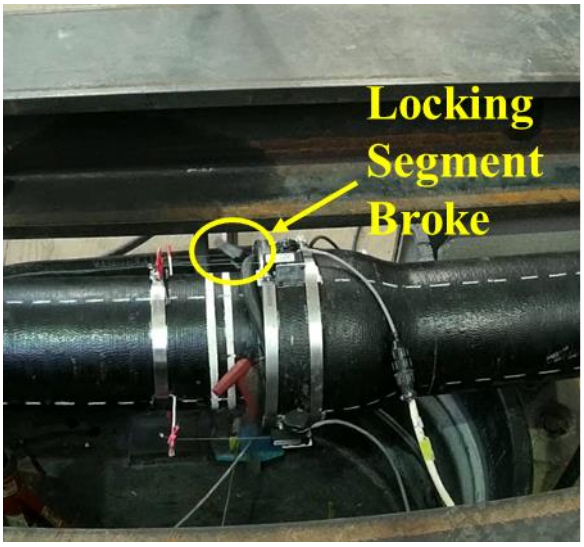


c) Left-Hand (Black) Locking Segment Broke

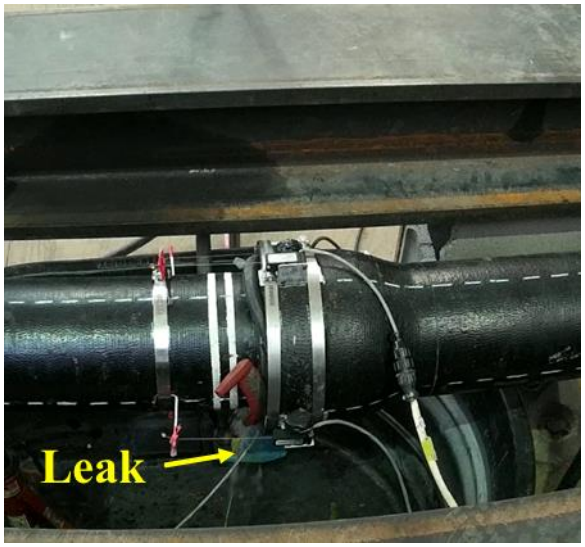


d) Pipe Leaked

Figure 4.4. Successive Photos of TR Flex® Joint

a) Joint Fully Inserted

b) Joint Fully Extended and Locking Segments Rotated Inward

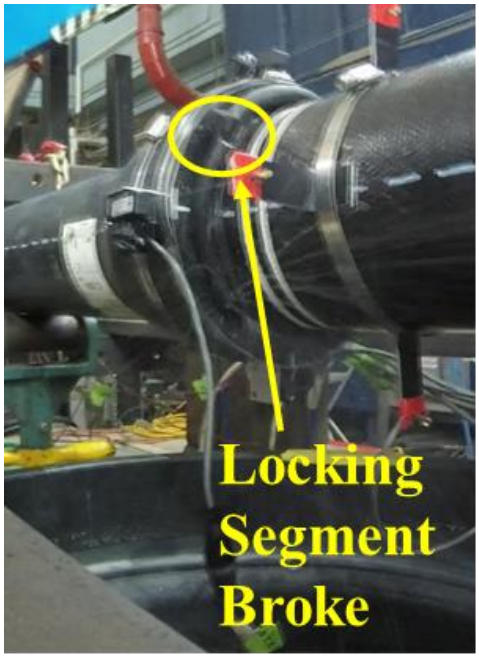


c) Left-Hand (Black) Locking Segment Broke

d) Pipe Leaked

Figure 4.5. Successive Photos of TR Flex® Looking at Left-Hand Locking Segment

### 4.3. McWane SFC Tension Tests

The second and third tension tests were performed on nominal 6-in. (150-mm)-diameter with McWane SFCs. The McWane SFC tension test specimens were 14.5 ft. (4.43 m) long. The purpose of conducting two tension tests was to provide a replicate test to confirm tensile capacity and axial pullout displacement. The pipe spigots were initially fully inserted into the bells and pressurized. Figure 4.6 provides the McWane SFC tension test setup.

#### 4.3.1. Instrumentation

Four strain gages were mounted at the crown, east springline, invert, west springline, and invert at 33.0 in. (838 mm) north of the P joint bell face on the bell side and 27.0 in. (686 mm) south of the B joint bell face on the spigot side. A total of nine string pots were used. Three string pots were installed for each joint at crown, east springline, and west springline to measure joint axial displacements. An actuator and load cell were installed on the load frame to apply and measure tensile force at the end of the pipe. An electronic pressure transducer, located at the north end cap, measured internal water pressure. The instrument locations and gage names are shown and listed in Table 4.2.

#### 4.3.2. Tension Test 1 Force vs. Displacement

The pipe was restrained at the end with a load cell and a retractable jack to measure axial load caused by internal pressure as the joints opened. The pressurizing sequence is shown in Figure 4.7. The specimen was filled with water and pressurized to approximately 80 psi (550 kPa) for the first 7 in. (178 mm) of total joint displacement, causing approximately 2.4 kips (13 kN) of axial load on the pipe end caps. The load cell and jack were then removed to allow the internal pressure to open the joints. The pressure of about 20 psi (140 kPa) was required to open the rest of the available stroke of the joints. The pipe reached the fully open position at 10.8 in. (274 mm) of total joint displacement.

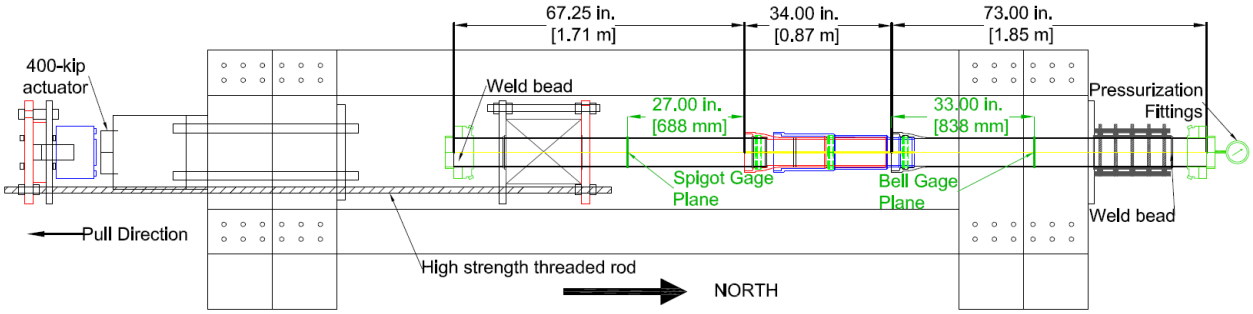


a) Schematic of Instrumentations

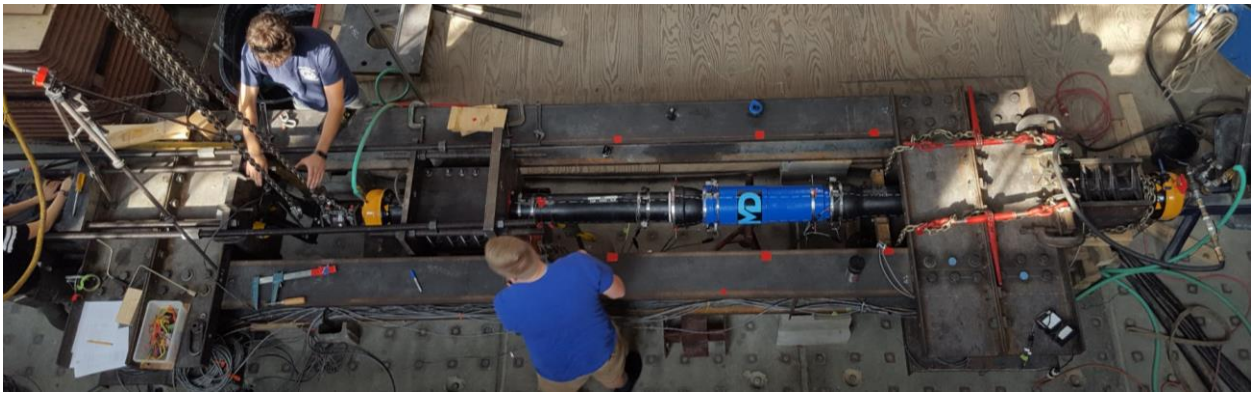

b) Photo of Test Setup

Figure 4.6. TR Flex® Tension Test Layout

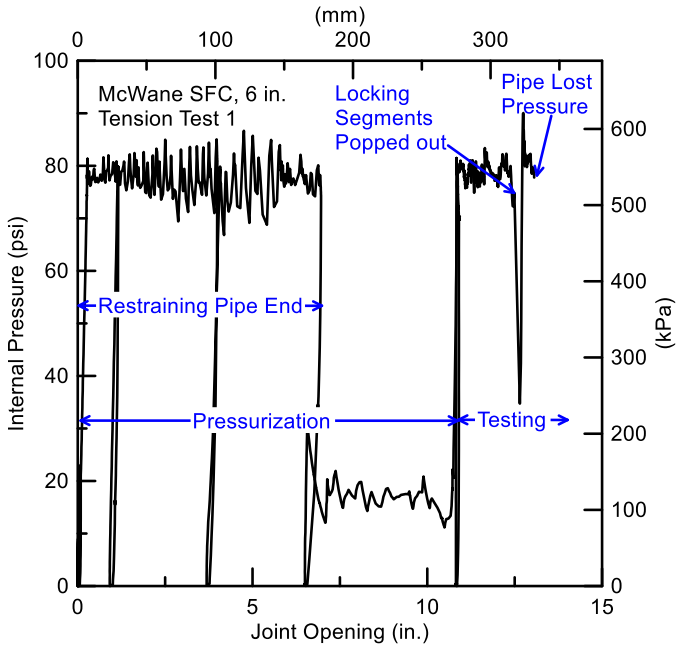


Figure 4.7. Internal Pressure vs. Total Joint Opening for McWane SFC Tension Test 1

Table 4.2. Instrumentation for McWane SFC Tension Tests

| Location | Instrument Description | Instrument Designation |
|---|---|---|
| 33 in. North of P Joint Bell Face | Crown, Axial Strain | BC |
| 33 in. North of P Joint Bell Face | Invert, Axial Strain | BI |
| 33 in. North of P Joint Bell Face | East Springline, Axial Strain | BE |
| 33 in. North of P Joint Bell Face | West Springline, Axial Strain | BW |
| 33 in. North of P Joint Bell Face | Crown, Hoop Strain | BCC |
| 33 in. North of P Joint Bell Face | Invert, Hoop Strain | BIC |
| 33 in. North of P Joint Bell Face | East Springline, Hoop Strain | BEC |
| 33 in. North of P Joint Bell Face | West Springline, Hoop Strain | BWC |
| 27 in. South of B Joint Bell Face | Crown, Axial Strain | SC |
| 27 in. South of B Joint Bell Face | Invert, Axial Strain | SI |
| 27 in. South of B Joint Bell Face | East Springline, Axial Strain | SE |
| 27 in. South of B Joint Bell Face | West Springline, Axial Strain | SW |
| 27 in. South of B Joint Bell Face | Crown, Hoop Strain | SCC |
| 27 in. South of B Joint Bell Face | Invert, Hoop Strain | SIC |
| 27 in. South of B Joint Bell Face | East Springline, Hoop Strain | SEC |
| 27 in. South of B Joint Bell Face | West Springline, Hoop Strain | SWC |
| B Joint Bell Face | Joint Crown String Pot | S_C |
| B Joint Bell Face | Joint East Springline String Pot | S_E |
| B Joint Bell Face | Joint West Springline String Pot | S_W |
| X Joint Bell Face | Joint Crown String Pot | X_C |
| X Joint Bell Face | Joint East Springline String Pot | X_E |
| X Joint Bell Face | Joint West Springline String Pot | X_W |
| P Joint Bell Face | Joint Crown String Pot | P_C |
| P Joint Bell Face | Joint East Springline String Pot | P_E |
| P Joint Bell Face | Joint West Springline String Pot | P_W |
| Actuator | Load Cell | Atlas 400kip Load |
| Actuator | Displacement | Act. Disp. |
| Internal Pressure | Pressure Transducer | Pressure |

1 in. = 25.4 mm

Axial loading by the actuator was subsequently applied at a rate of 1 in. (25.4 mm) per minute while the pipe was under the initial thrust load. The internal pressure was 82 psi (570 kPa). Figures 4.8 to 4.11 show the relationships of tensile force vs. displacement of the B, X, P, and total joints, respectively. The applied force caused the spigot weld beads to bear against the locking segments for all joints. The progressive movements of the joint and locking segments are provided in Figures 4.12 and 4.13. The peak load of 70.7 kips (314 kN) was achieved at 11.9 in. (302 mm) of total joint opening. The force subsequently declined. Load concentration caused by the locking segments at the springline of the pipe caused the spigot to deform inward from a circular to an oval shape. This inward deformation at the springline allowed the locking segments to slide past the weld bead so that the spigot pulled from the bell. At 18.2 kips (81.0 kN) of tensile force, the locking segments popped out of the X joint. At this point the X and total joint displacements were 11.6 in. (295 mm) and 12.5 (318 mm), respectively. The internal pressure suddenly dropped to 35 psi (240 kPa). The test was paused. The pressure was, however, able to recover to 82 psi (570 kPa). The test was resumed, and the force continued to decrease until it dropped to zero. The leakage was observed at the X joint at 13.0 in. (330 mm) of total joint displacement.

### 4.3.3. Tension Test 1 and 2 Comparison

The tensile force vs. total joint displacement relationship comparison between two McWane SFC tension tests is provided in Figure 4.14. Both tensile specimens show similar behaviors and limit states. Internal water pressure caused axial load in the pipes and fully opened the SFC joints to 10.8 in. (274 mm) and 11.1 in. (282 mm) for Tests 1 and 2, respectively. Test 1 reached the maximum tensile force of 70.7 kips (314 kN) at 11.9 in. (302 mm) of total joint opening. The peak load of 61.8 kips (275 kN) was measured at a corresponding total joint displacement of 12.1 in. (307 mm) in Test 2. The load then declined substantially. The locking segments popped out of the X joints in both tests at 12.5 in. (318 mm) of total joint displacement, but the pipes were still able to maintain full water pressure. The tests were continued until significant leakage at the X joint was observed at 13.0 in. (330 mm) and 13.4 in. (340 mm) of total joint displacement in Tests 1 and 2, respectively.

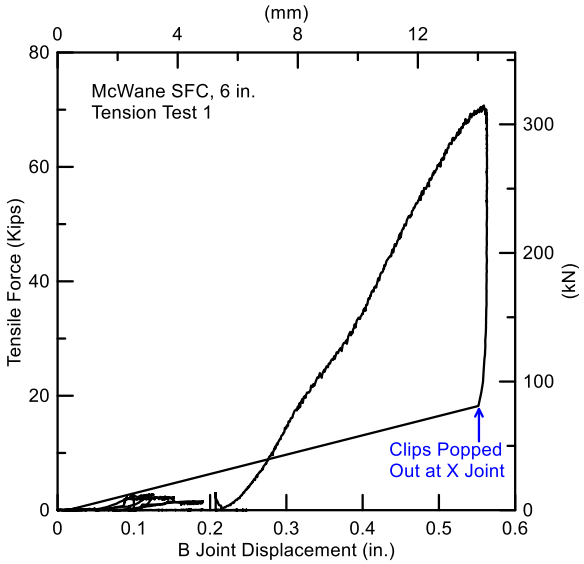


Figure 4.8. Tensile Force vs. B Joint Opening for SFC Tension Test 1

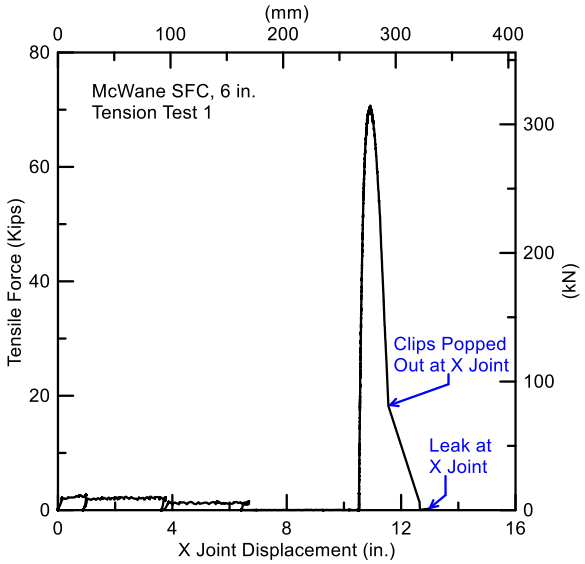


Figure 4.9. Tensile Force vs. X Joint Opening for SFC Tension Test 1

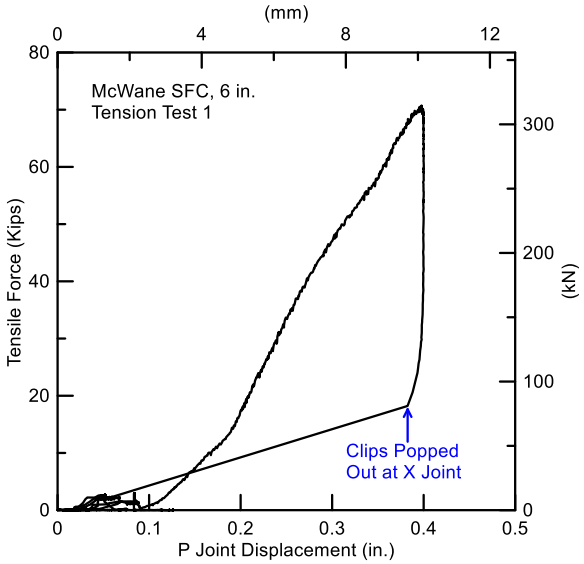


Figure 4.10. Tensile Force vs. P Joint Opening for SFC Tension Test 1

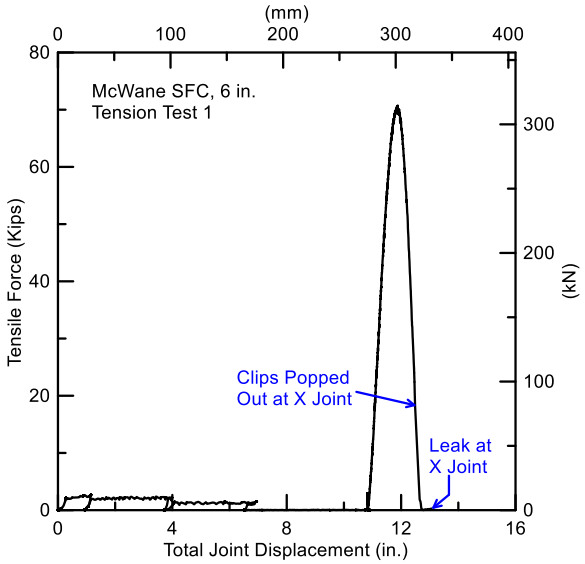


Figure 4.11. Tensile Force vs. Total Joint Opening for SFC Tension Test 1

a) Joint Fully Inserted

b) Joint Fully Extended and Locking Segments Rotated Inward

c) Locking Segments Popped out

d) Pipe Leaked

Figure 4.12. Successive Photos of McWane SFC Tension Test 1

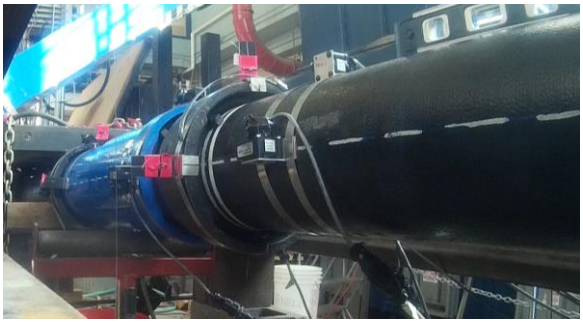

a) Joint Fully Inserted

b) Joint Fully Extended and Locking Segments Rotated Inward

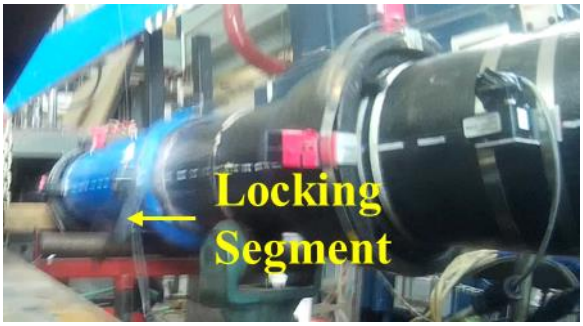


c) Locking Segments Poped Out

d) Pipe Leaked

Figure 4.13. Successive Photos of McWane SFC Tension Test 1 Looking at Left-Hand Locking Segment

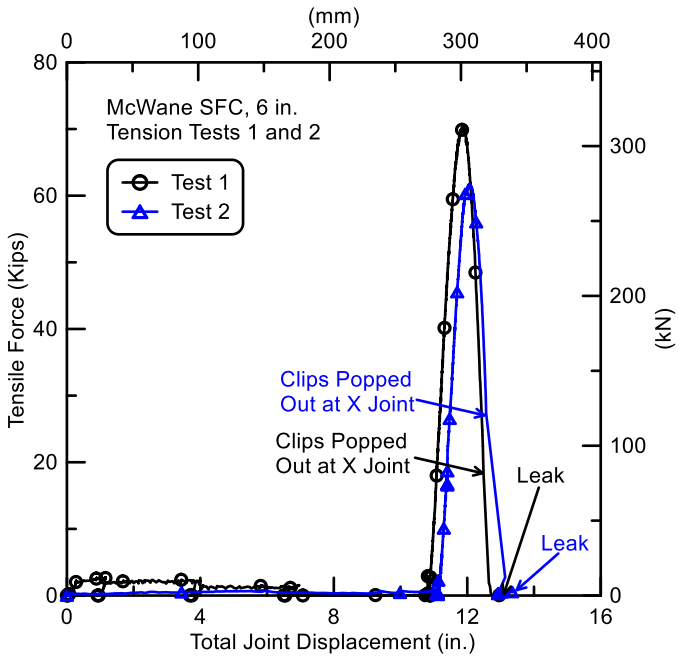


Figure 4.14. Tensile Force vs. Total Joint Opening Comparison between McWane SFC Tension Tests 1 and 2

## 4.4. McWane SFC Compression Tests

The compression test layout is shown in Figure 4.15. The test specimen was 12.5 ft. (3.8 m) long, and the joint was fully inserted at the beginning of the test. The pipe was pressurized to 80 psi (550 kPa)

### 4.4.1. Instrumentation and Test Procedures

Four strain gages were mounted on the bell 21.5 in. (546 mm) north of the P joint bell face at the crown, invert, and springlines. Four other strain gages were also installed on the spigot 10.25 in. (260 mm) south of the B joint bell face at the same positions. Three string pots were installed at the crown and springlines at each joint. An actuator and load cell were installed on the load frame to apply and measure compressive force at the end of the spigot. An electronic pressure transducer, located at the north end cap, measured internal water pressure. To support the self-weight of the pipe, the bell end adapter was suspended on an overhead crane, and the spigot was placed on a wheeled wooden dolly. The instrumentations are shown in Figure 4.15.

After the specimen was instrumented and centered in the test frame, the test was initiated by starting the data acquisition system and laboratory hydraulic systems. Figure 4.16 shows the test specimen mounted in the compression test frame. The specimen was secured to the actuator to prevent joint pullouts during pressurization and pressurized to approximately 80 psi (550 kPa). A pressure relief value was installed onto the pressurization fittings in order to bleed excessive pressure caused by compressive movement beyond 100 psi (689 kPa). The test was performed under displacement control using the servo-hydraulic actuator at a rate of 1 in. (25.4 mm) per minute. Figure 4.17 shows the internal pressure vs. joint closure.

### 4.4.2. Force vs. Displacement

Compressive force and joint displacements were measured by the load cell and string pots, respectively. Figures 4.18 to 4.21 show the compressive force vs. displacements of the B, X, P, and total joints, respectively. Also shown in Figures 3.22 to 3.25 is the force at the proportional limit. The proportional force, $P_{prop}$, is the product of the proportional stress of 32.8 ksi (226 MPa) based on the tensile coupon test data and the cross-sectional area of the specimen of 6.22 $in^2$ (4010 $mm^2$), giving the force at the proportional limit, $P_{prop}$, of 204 kips (907 kN).

Table 4.3. Instrumentation for McWane SFC Compression Test

| Location | Instrument | Instrument Name |
|---|---|---|
| 21.5 in. North of P Joint Bell Face | Crown, Axial Strain | BC |
| 21.5 in. North of P Joint Bell Face | Invert, Axial Strain | BI |
| 21.5 in. North of P Joint Bell Face | East Springline, Axial Strain | BE |
| 21.5 in. North of P Joint Bell Face | West Springline, Axial Strain | BW |
| 21.5 in. North of P Joint Bell Face | Crown, Hoop Strain | BCC |
| 21.5 in. North of P Joint Bell Face | Invert, Hoop Strain | BIC |
| 21.5 in. North of P Joint Bell Face | East Springline, Hoop Strain | BEC |
| 21.5 in. North of P Joint Bell Face | West Springline, Hoop Strain | BWC |
| 10.25 in. South of B Joint Bell Face | Crown, Axial Strain | SC |
| 10.25 in. South of B Joint Bell Face | Invert, Axial Strain | SI |
| 10.25 in. South of B Joint Bell Face | East Springline, Axial Strain | SE |
| 10.25 in. South of B Joint Bell Face | West Springline, Axial Strain | SW |
| 10.25 in. South of B Joint Bell Face | Crown, Hoop Strain | SCC |
| 10.25 in. South of B Joint Bell Face | Invert, Hoop Strain | SIC |
| 10.25 in. South of B Joint Bell Face | East Springline, Hoop Strain | SEC |
| 10.25 in. South of B Joint Bell Face | West Springline, Hoop Strain | SWC |
| P Joint Bell Face | P Joint Crown String Pot | P_C |
| P Joint Bell Face | P Joint East Springline String Pot | P_E |
| P Joint Bell Face | P Joint West Springline String Pot | P_W |
| X Joint Bell Face | X Joint Crown String Pot | X_C |
| X Joint Bell Face | X Joint Invert String Pot | X_E |
| X Joint Bell Face | X Joint East Springline String Pot | X_W |
| B Joint Bell Face | B Joint Crown String Pot | B_C |
| B Joint Bell Face | B Joint East Springline String Pot | B_E |
| B Joint Bell Face | B Joint West Springline String Pot | B_W |
| Actuator | Load Cell | Interface Load |
| Actuator | Displacement | Act. Disp. |
| Internal Pressure | Pressure Transducer | Pressure |

1 in. = 25.4 mm

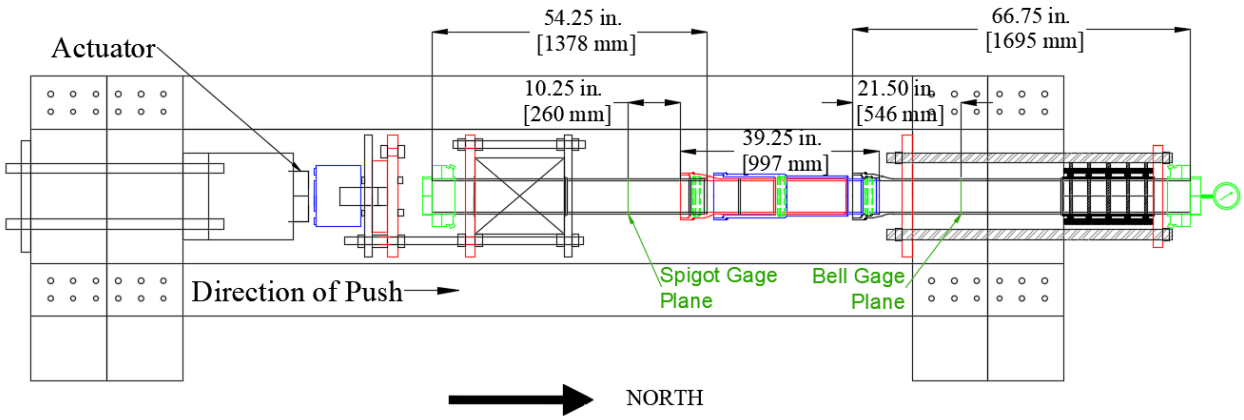


Figure 4.15. Compression Test Layout

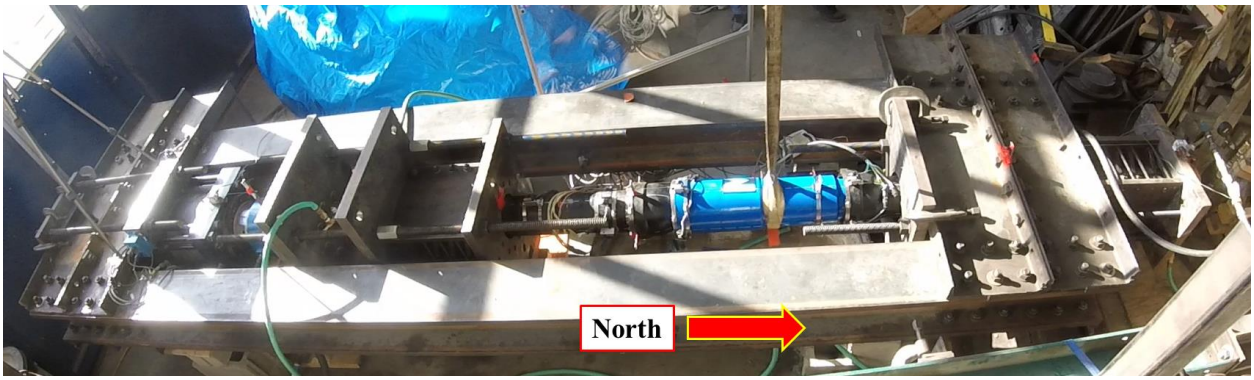


Figure 4.16. Test Specimen in Compression Frame

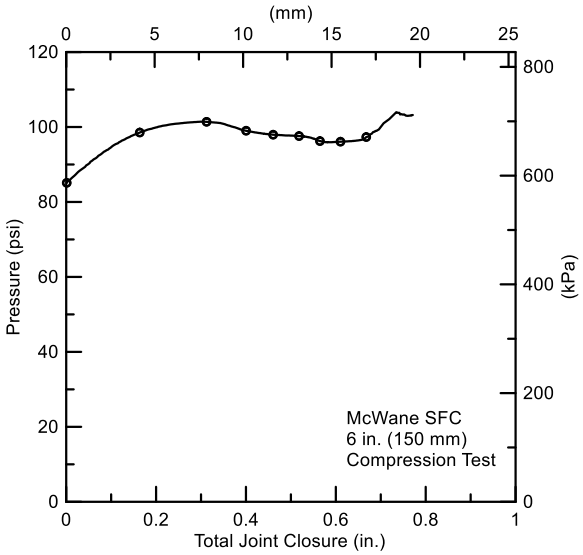


Figure 4.17. Internal Pressure vs. Joint Closure

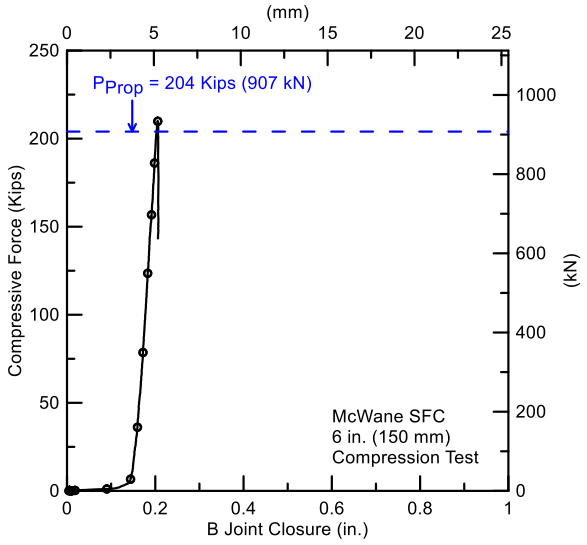


Figure 4.18. Compressive Force vs. P Joint Closure for SFC Compression Test

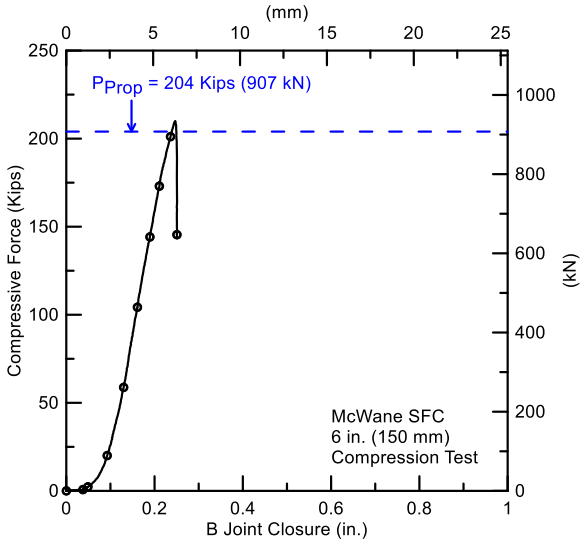


Figure 4.19. Compressive Force vs. X Joint Closure for SFC Compression Test

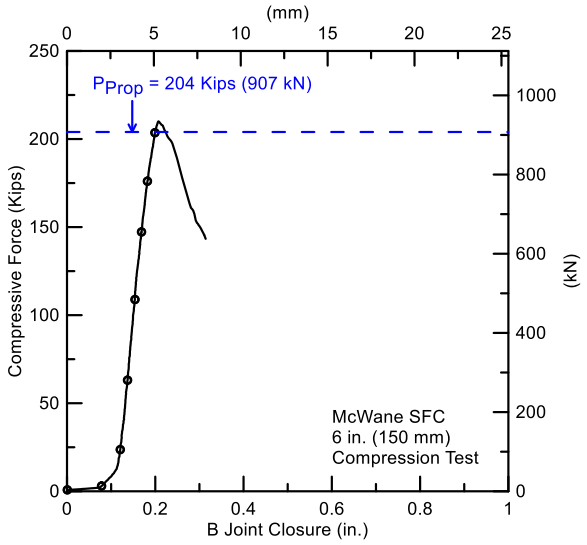


Figure 4.20. Compressive Force vs. B Joint Closure for SFC Compression Test

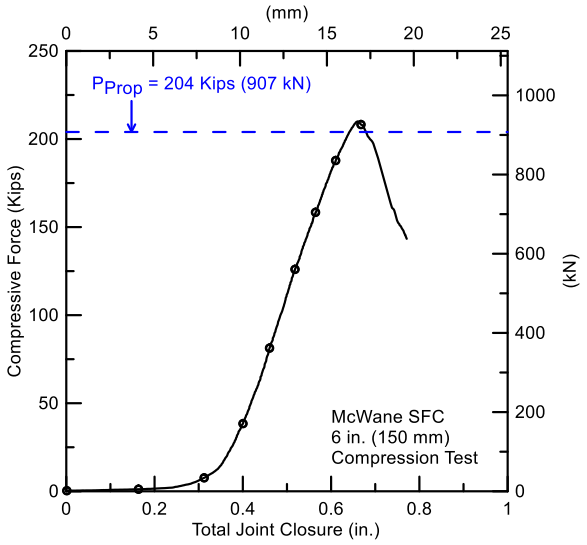


Figure 4.21. Compressive Force vs. Total Joint Closure for SFC Compression Test

Once the actuator began applying compressive movement to the pipe, each joint provided approximately 0.1 in. (2.5 mm) of displacement before becoming fully seated, and the compressive force then increased. At the total joint closure of 0.66 in. (16.7 mm), the pipe reached the maximum compressive force of 210 kips (934 kN), which is very close to the calculated proportional force of 204 kips (907 kN). After the maximum compressive force had been achieved, the load dropped rapidly, and the pipe was sagging at the B joint. The downward movement at the B joint caused the wheeled wooden dolly to break when the SFC reached a total displacement of 0.77 in. (19.6 mm) at a corresponding actuator force of 143 kips (636 kN). Attempts were made to straighten the pipe. However, the pipe already had significant irrecoverable deformation, and it could not return to the original position, as illustrated in Figure 4.22. No leakage was observed in this test.

### 4.4.3. Joint Rotation

The compressive force applied by the actuator caused the SFC joints to fully seat and begin to rotate. Joint rotations are more noticeable in the vertical direction than the horizontal direction. Therefore, joint vertical rotations are calculated by the joint string pots, as follows

$$\theta_{\text{Vertical}}\,(^\circ) = \tan^{-1}\left(\frac{\text{Crown Str. Pot disp.} - \text{Avg. Springline Str. Pot disp.}}{\text{distance between Crown Str. Pot and Springline}}\frac{180^\circ}{\pi}\right) \quad (4.1)$$

Figure 4.23 shows the relationship between each joint vertical rotation vs. total joint closure. Since the joint vertical rotation at the B joint is most dominant in the SFC, the compressive force and B joint vertical rotation are plotted against total joint displacement in Figure 4.24 to find the relationship between the compressive force and plastic deformation. The B joint had a relatively small vertical rotation during the first 0.3 in. (7.6 mm) of total joint closure. When all joints were fully seated, the compressive force started to increase as well as the B joint rotation. The B joint rotation during this part of the test was caused by slight differences in the alignment of the weld bead, which may occur during the fabrication process. After the pipe achieved the maximum compressive force past its proportional limit, the vertical rotation of the B joint increased rapidly from 1.4° to 4° at the end of the test. The change in rate of the B joint rotation after the proportional limit signifies the inflection point when the DI pipe material surpassed the elastic limit, and plastic deformations began.

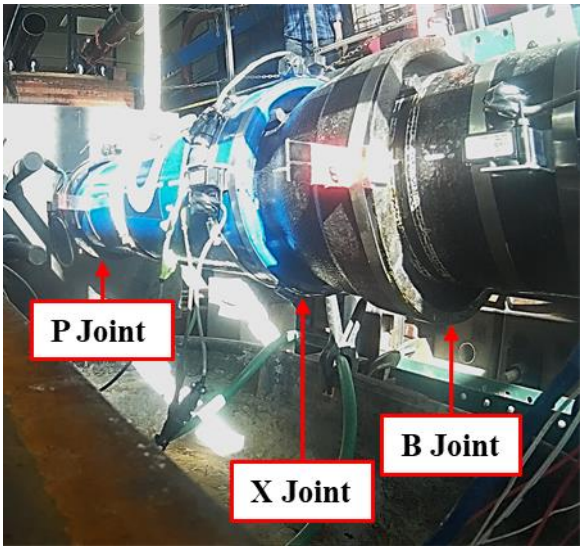


a) Side View Before Test

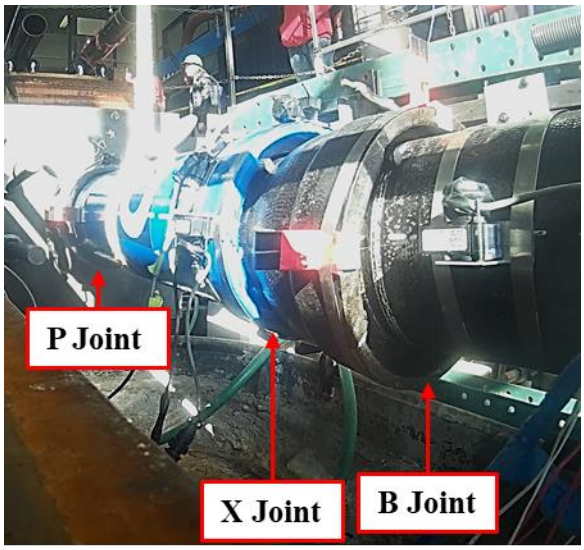


b) Side View After Test

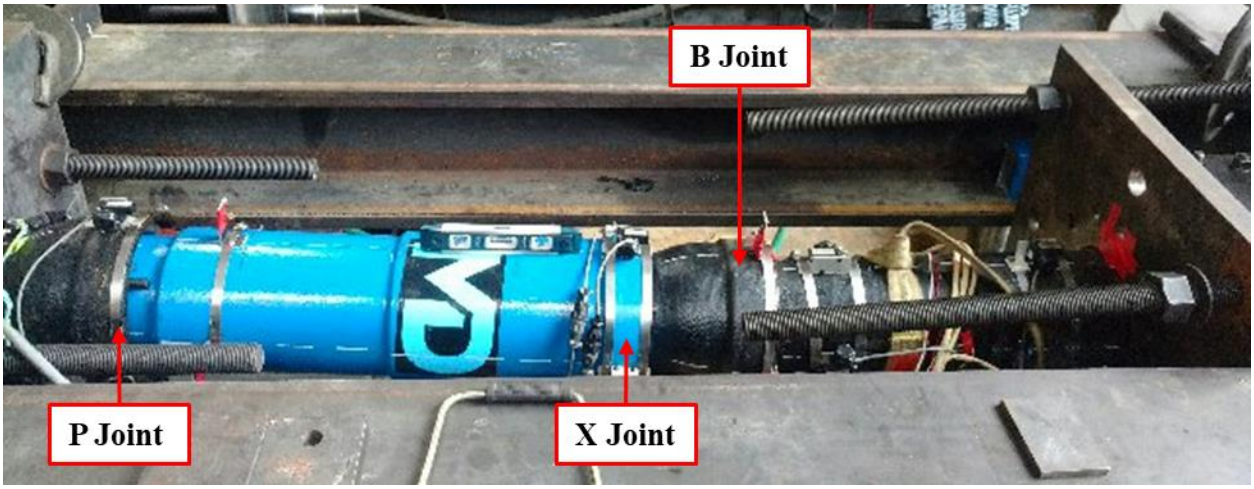


c) Overall View After Test

Figure 4.22. Irrecoverable Deformation at B Joint

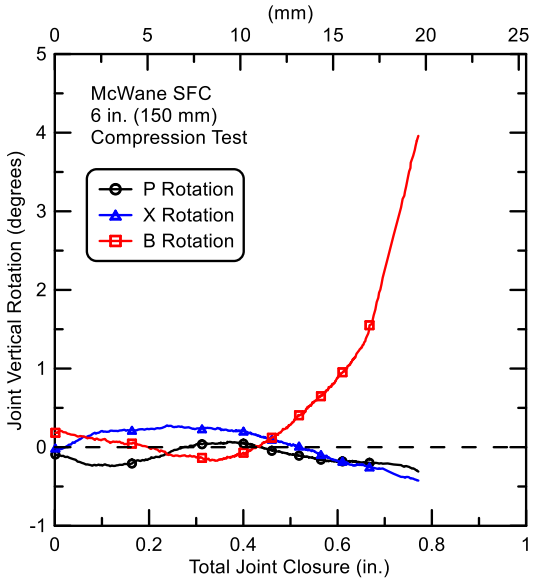


Figure 4.23. Joint Vertical Rotations vs. Total Joint Displacement

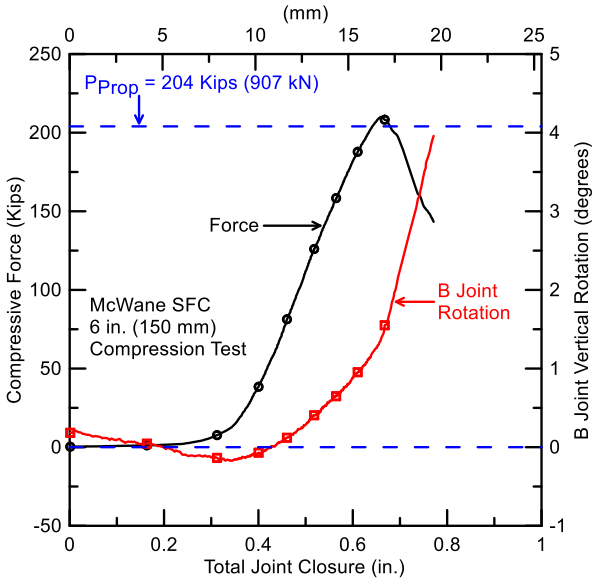


Figure 4.24. Compressive Force and B Joint Vertical Rotation vs. Total Joint Displacement

## 4.5. Summary from Joint Tension and Compression Tests

Three tension tests, two McWane SFCs and one separated TR Flex® joint, and one compression test on a McWane SFC were performed on the 6-in. (150-mm)-diameter DI specimens. All tests began at the fully inserted positions. In the TR Flex® joint tension test, the peak load of 96.5 kips (429 kN) was achieved at 0.73 in. (18.5 mm) of joint opening. Leakage during the test was observed at 1.57 in. (39.8 mm) of displacement when the left-hand locking segment broke.

Two McWane SFC tension tests resulted in an average SFC total displacement of 11.0 in. (279 mm). The average maximum tensile force of 66.3 kips (295 kN) was measured at the average displacement of 12.0 in. (305 mm). Both SFC specimens were able to carry additional displacement until significant leakage was observed at the X joint at 13.2 in. (335 mm) of average total joint displacement.

The compressive testing showed that the McWane SFC had a maximum compressive load capacity at about the DI proportional limit of 204 kips (907 kN). Once the proportional limit was achieved, the pipe started to behave plastically and have irrecoverable deformation such that a significant rotation was observed at the B joint. However, no leakage occurred during the compression test.

# Section 5
# Fault Rupture Test

## 5.1. Introduction

This section presents the results of the large-scale fault rupture test performed with a ductile iron pipeline equipped with McWane Seismic Flex Couplings (SFCs). The test was performed in the large-scale test basin at the Cornell University Large Scale Lifelines Testing Facility.

## 5.2. Experimental Setup

Figure 5.1 is a plan view of the test layout which shows the fault rupture plane and approximate locations of the four actuators generating basin movement. The pipeline consisted of three ductile iron pipe segments with two SFCs positioned at 5 ft. (1.5 m) on either side of the fault. The intersection angle between the pipe and fault was 50°. The objective of the test was to impose abrupt ground deformation on the pipeline, which was representative of left lateral strike slip fault rupture, and severe ground deformation that can occur along the margins of liquefaction-induced lateral spreads and landslides. The pipeline was constructed to evaluate its capacity to accommodate full-scale fault movement through the simultaneous axial pullout at two different SFCs. Measuring simultaneous performance of multiple joints allows for confirmation that the pipeline will respond to ground failure as intended, understand the complex interaction among the different joints, and determine the maximum ground deformation and axial pipeline load that can be sustained before joint leakage.

The pipeline was buried in the Cornell large-scale test basin in partially saturated sand that was compacted to have an average friction angle of $\phi' = 42^{o}$, equivalent in strength to that of a medium dense to dense granular backfill. The pipeline was assembled so that the X joint at each SFC could pull from the bells approximately 8.5 in. (216 mm) before the weld rings made contact with the locking segments. During the test, the south part of the basin remained stationary, while the north part was displaced to the north and west by large-stroke actuators to cause soil rupture and slip at the interface between the two parts of the test basin.

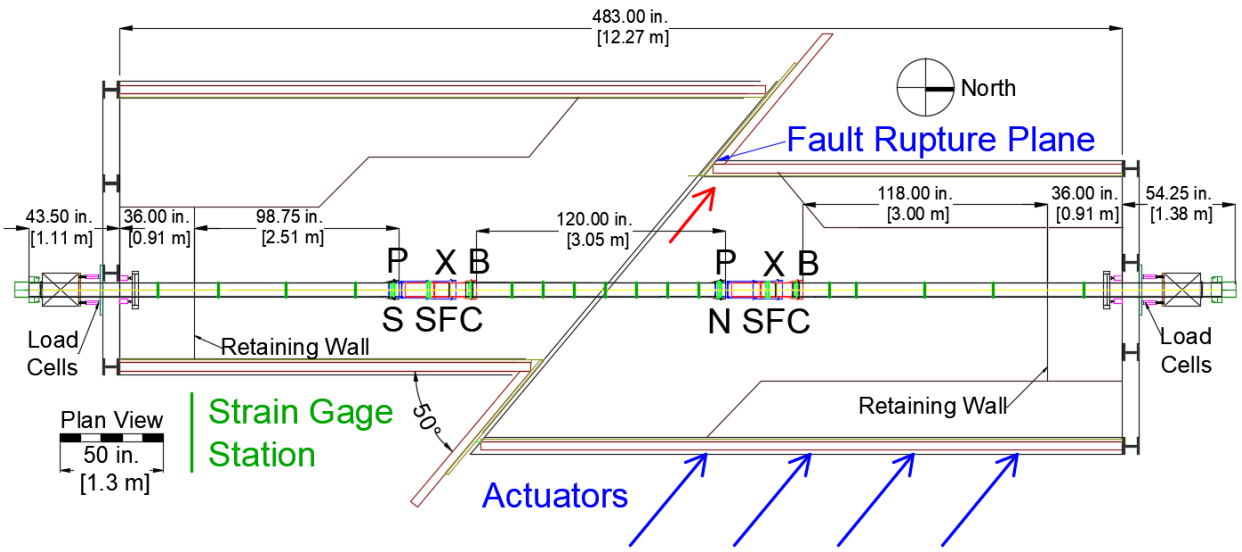


a) Overall Test Configurations

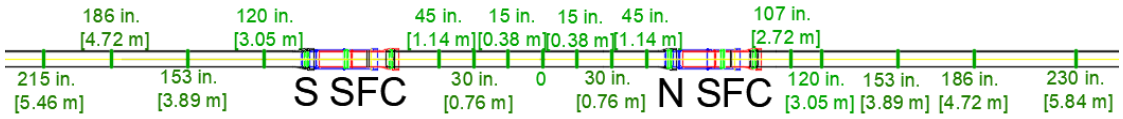


b) Strain Gage Layout

Figure 5.1. Plan View of Pipe Centered McWane SFC Specimen in Test Basin

A 125-in. (3.18 m)-long pipe section was placed directly over the fault, with an intersection angle of 50°. A 207-in. (5.26-m)-long pipe with an SFC was connected at the north end of the pipeline. Lastly, a 178-in. (4.52-m)-long pipe with an SFC was connected at the south end of the pipeline. The 6.9-in. (175-mm) outer-diameter pipe was placed on a bed of soil 10.6 in. (269 mm) in depth. The depth of burial to top of pipe was 33.5 in. (851 mm) resulting in 51.0 in. (1.30 m) of total soil depth within the test basin

The simulated fault rupture caused both tensile and bending strains in the pipeline. The length of the pipeline buried in soil, also described as “test portion,” was approximately 34 ft. (10 m) long. The pipe was pressurized with water to approximately 80 psi (550 kPa). The north (movable) portion of the test basin is connected to four MTS hydraulic actuators with load cells controlled by a MTS Flextest GT controller. All actuators were operated in synchronized displacement control.

### 5.2.1. Test Procedure

The general test procedure, after all instruments were installed, soil placed, and pipe filled with water, was:

a) Begin data acquisition and start the servo-controlled hydraulic system,
b) Introduce and verify internal water pressure,
c) Move the test basin at a rate of 1 ft./minute (305 mm/minute) until pipe failure (full pressure loss),
d) Stop basin movement but maintain hydraulic actuator pressure,
e) Verify data acquisition, and
f) Excavate.

At a fault displacement of 33.4 in. (848 mm), the pipeline lost its the internal pressure, indicating leakage. After verification of total pressure lost, the test was then stopped at 33.7 in. (856 mm) of fault displacement. This fault displacement corresponds to an axial movement of 21.7 in. (550 mm)

### 5.2.2. Instrumentation

Figure 5.1, a plan view of the test layout, shows the locations of the instruments along the test pipeline. The instrumentation consisted of strain gages at sixteen gage planes along the pipeline, load cells at the ends of the pipeline and string pots to measure joint displacements and rotations. Eighty-four strain gages were installed at the sixteen gage planes along the pipeline to evaluate axial forces and bending moments. Strain gages were positioned at the crown (C) and invert (I), and at the east (E) and west (W) springlines of the pipe. Table 5.1 provides the number of strain gage station locations with respect to the fault. Strain gage locations were chosen on the basis of the expected deformed shape and axial behavior of the pipeline as determined from direct tension and four-point bending tests performed at Cornell University as well as the results of finite element analyses of the test. Strain gage stations S215 and N230 were installed to provide redundant measurements of the end loads. Strain gage stations close to the joints, S120, S45, N45, and N107 were placed to assess strain concentration near the SFCs.

Table 5.1. Strain Gage Locations and Coding System for SFC Fault Rupture Test

| Gage Station | Gages | Distance from Fault |
|---|---|---|
| S215 | S215E-East Springline, Longitudinal<br>S215C-Crown, Longitudinal<br>S215W-West Springline, Longitudinal<br>S215I-Invert, Longitudinal | 215 in. (5.46 m) south |
| S186 | S186E-East Springline, Longitudinal<br>S186C-Crown, Longitudinal<br>S186W-West Springline, Longitudinal<br>S186I-Invert, Longitudinal | 186 in. (3.86 m) south |
| S153 | S153E-East Springline, Longitudinal<br>S153C-Crown, Longitudinal<br>S153W-West Springline, Longitudinal<br>S153I-Invert, Longitudinal | 153 in. (3.04 m) south |
| S120 | S120EA-East Springline, Longitudinal<br>S120CA-Crown, Longitudinal<br>S120WA-West Springline, Longitudinal<br>S120IA-Invert, Longitudinal<br>S120EC-East Springline, Circumferential<br>S120CC-Crown, Circumferential<br>S120WC-West Springline, Circumferential<br>S120IC-Invert, Circumferential | 120 in. (3.04 m) south |
| S45 | S45EA-East Springline, Longitudinal<br>S45CA-Crown, Longitudinal<br>S45WA-West Springline, Longitudinal<br>S45IA-Invert, Longitudinal<br>S45EC-East Springline, Circumferential<br>S45CC-Crown, Circumferential<br>S45WC-West Springline, Circumferential<br>S45IC-Invert, Circumferential | 45 in. (2.24 m) south |
| S30 | S30E-East Springline, Longitudinal<br>S30C-Crown, Longitudinal<br>S30W-West Springline, Longitudinal<br>S30I-Invert, Longitudinal | 30 in. (0.79 m) south |
| S15 | S15E-East Springline, Longitudinal<br>S15C-Crown, Longitudinal<br>S15W-West Springline, Longitudinal<br>S15I-Invert, Longitudinal | 15 in. (0.38 m) south |
| 0 | 0E-East Springline, Longitudinal<br>0C-Crown, Longitudinal<br>0W-West Springline, Longitudinal<br>0I-Invert, Longitudinal | 0 |
| N15 | N15E-East Springline, Longitudinal<br>N15C-Crown, Longitudinal<br>N15W-West Springline, Longitudinal<br>N15I-Invert, Longitudinal | 15 in. (0.38 m) north |

Table 5.1. Strain Gage Locations and Coding System for SFC Fault Rupture Test (completed)

| Gage Station | Gages | Distance from Fault |
|---|---|---|
| N30 | N30E-East Springline, Longitudinal<br>N30C-Crown, Longitudinal<br>N30W-West Springline, Longitudinal<br>N30I-Invert, Longitudinal | 30 in. (0.79 m) north |
| N45 | N45EA-East Springline, Longitudinal<br>N45CA-Crown, Longitudinal<br>N45WA-West Springline, Longitudinal<br>N45IA-Invert, Longitudinal<br>N45EC-East Springline, Circumferential<br>N45CC-Crown, Circumferential<br>N45WC-West Springline, Circumferential<br>N45IC-Invert, Circumferential | 45 in. (1.07 m) north |
| N107 | N107EA-East Springline, Longitudinal<br>N107CA-Crown, Longitudinal<br>N107WA-West Springline, Longitudinal<br>N107IA-Invert, Longitudinal<br>N107EC-East Springline, Circumferential<br>N107CC-Crown, Circumferential<br>N107WC-West Springline, Circumferential<br>N107IC-Invert, Circumferential | 107 in. (2.24 m) north |
| N120 | N120EA-East Springline, Longitudinal<br>N120CA-Crown, Longitudinal<br>N120WA-West Springline, Longitudinal<br>N120IA-Invert, Longitudinal<br>N120EC-East Springline, Circumferential<br>N120CC-Crown, Circumferential<br>N120WC-West Springline, Circumferential<br>N120IC-Invert, Circumferential | 120 in. (3.04 m) north |
| N153 | N153E-East Springline, Longitudinal<br>N153C-Crown, Longitudinal<br>N153W-West Springline, Longitudinal<br>N153I-Invert, Longitudinal | 153 in. (4.06 m) north |
| N186 | N186E-East Springline, Longitudinal<br>N186C-Crown, Longitudinal<br>N186W-West Springline, Longitudinal<br>N186I-Invert, Longitudinal | 186 in. (5.46 m) north |
| N230 | N230E-East Springline, Longitudinal<br>N230C-Crown, Longitudinal<br>N230W-West Springline, Longitudinal<br>N230I-Invert, Longitudinal | 230 in. (6.68 m) north |

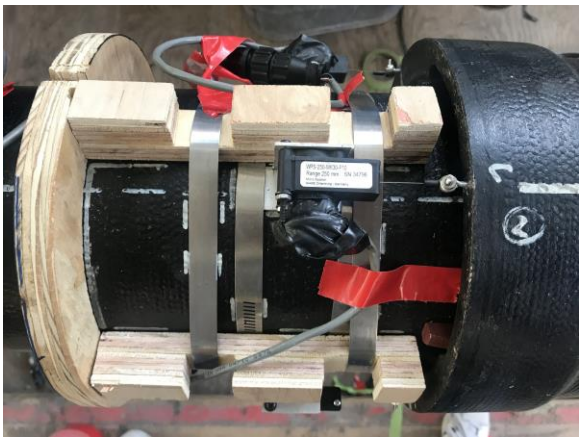

a) B Joint

b) X Joint

c) P Joint

Figure 5.2. String Pot Setups

Figure 5.3. Pipe Joints with Protective Shielding

Table 5.2. String Pot Locations and Labeling for McWane SFC Fault Rupture Test

| Location | Displacement Measurement Device | Type and Stroke |
|---|---|---|
| South P Joint | SPE – East Springline | String pot ± 1.5 in. |
| | SPC – Crown | String pot ± 1.5 in. |
| | SPW – West Springline | String pot ± 1.5 in. |
| South X Joint | SXE – East Springline | String pot ± 20 in. |
| | SXC – Crown | String pot ± 20 in. |
| | SXW – West Springline | String pot ± 20 in. |
| South B Joint | SBE – East Springline | String pot ± 10 in. |
| | SBC – Crown | String pot ± 10 in. |
| | SBW – West Springline | String pot ± 10 in. |
| North P Joint | NPE – East Springline | String pot ± 1.5 in. |
| | NPC – Crown | String pot ± 1.5 in. |
| | NPW – West Springline | String pot ± 1.5 in. |
| North X Joint | NXE – East Springline | String pot ± 20 in. |
| | NXC – Crown | String pot ± 20 in. |
| | NXW – West Springline | String pot ± 20 in. |
| North B Joint | NBE – East Springline | String pot ± 10 in. |
| | NBC – Crown | String pot ± 10 in. |
| | NBW – West Springline | String pot ± 10 in. |

1 in. = 25.4 mm

Figure 5.2 shows the setup of the string potentiometers (pots). Three string pots were placed at each joint to measure the joint pullout and rotation. Table 5.2 provides the locations and the labeling of the joint string pots. Two string pots were mounted at the east and west springlines of the bell. The other string pot was installed at the crown of the bell. The spigots and bell end adapters were inserted approximately 0.5 in. (12.7 mm) into the plain end adapters and bells, respectively. The X joint was positioned at 1.5 in. (38 mm) from the fully inserted position in order to provide adequate space for string pot installation. After the instrumentation was installed, protective shielding was wrapped around the joint. Figure 5.3 is an overview of the pipe joint with the protective shielding.

Four calibrated load cells were positioned at each end of the test basin. Table 5.3 provides the locations and the labeling of the load cells. Forty survey marks were scribed along the crown of the specimen. The pipe was surveyed with a total station instrument prior to burial to determine its initial position, and again after the test, to provide a measure of global pipeline deformation.

Table 5.3. Load Cell Locations and Labeling for McWane SFC Fault Rupture Test

| Location | Load Cell |
|---|---|
| South End | SW Top Ld –West, Top<br>SE Top Ld –East, Top<br>SW Bot Ld –West, Bottom<br>SE Bot Ld –East, Bottom |
| North End | NW Top Ld – West, Top<br>NE Top Ld – Outer, East, Top<br>NW Bot Ld – West, Bottom<br>NE Bot Ld – East, Bottom |

### 5.2.3. Soil Preparation

The soil used during the test was crushed, washed, glacio-fluvial sand obtained from RMS Gravel, Dryden, NY, consisting of particles mostly passing the ¼ in. (6.35 mm) sieve. Figure 5.4 shows the grain size distribution of the RMS graded sand. Approximately 6-in. (152-mm)-thick lifts of soil were placed and compacted until there was 33.5 in. (851 mm) cover of compacted sand above the pipe crown. Every layer was compacted to the same extent and moistened with water in a similar way to achieve uniformity. Dry density measurements were taken for each layer using a Troxler Model 3440 densitometer. Moisture content measurements were obtained using both soil samples and the densitometer at the same locations.

The target value of dry density was $\gamma_{dry}$ = 106 lb/ft$^3$ (16.7 kN/m$^3$), and the target value of moisture content was w = 4.0 %. These conditions for the RMS graded sand correspond to an angle of shearing resistance (friction angle) of the sand of approximately 42º. Eight measurements of dry unit weight and moisture content were made for each soil lift. The average and standard deviation of all dry unit weight measurements were 106.7 lb/ft$^3$ (16.8 kN/m$^3$) and 1.7 lb/ft$^3$ (0.3 kN/m$^3$), respectively. Moisture content measurement had an average of 4.9% and standard deviation of 0.5%. The soil strength properties are representative of a well-compacted dense sand.

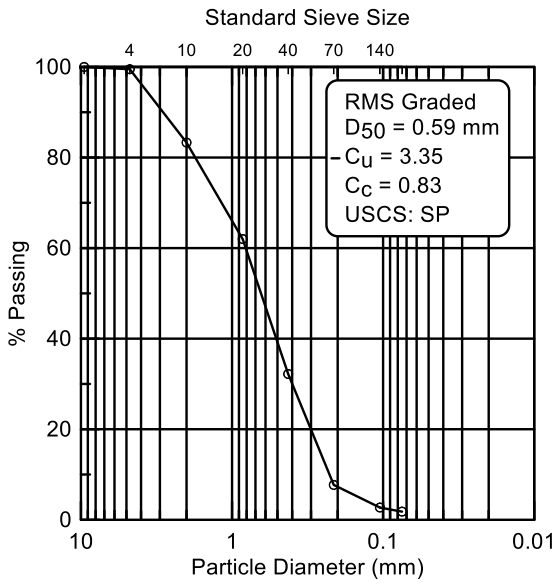


Figure 5.4. Particle Size Distribution of RMS Graded Sand

## 5.3. Experimental Results of Split Basin Test

### 5.3.1. Test Basin Movements

Two short-stroke actuators (SSAs) and two long-stoke actuators (LSAs) are connected between the movable portion of the test basin and the modular reaction wall in the laboratory. Each SSA has a displacement range of ± 2 ft (± 0.61 m) for a total stroke of 4 ft (1.22 m) and load capacity of 100 kips (445 kN) tension and 145 kips (645 kN) compression. Each LSA has a displacement range of ± 3 ft (0.91 m) for a total stroke of 6 ft (1.83 m) and load capacity of 63 kips (280 kN) tension and 110 kips (489 kN) compression.

Figure 5.5 shows the average displacement of the four actuators, which is equivalent to the fault displacement, with respect to time.

### 5.3.2. Internal Water Pressure

The pipe was pressurized to 80 psi (550 kPa) before any basin movement, and remained constant pressure during the test. The basin movement caused the pipe to increase in overall length, causing fluctuations in pressure. Figure 5.6 shows the pipe internal pressure vs. fault displacement. At a fault displacement of 33.4 in. (848 mm), there was a large loss of pressure in the pipe. This fault displacement corresponds to 21.5 in. (546 mm) of axial pipeline displacement. After verification of total pressure loss, the test was then stopped at 33.7 in. (856 mm) of fault displacement. This fault displacement corresponds to a basin axial movement of 21.7 in. (550 mm).

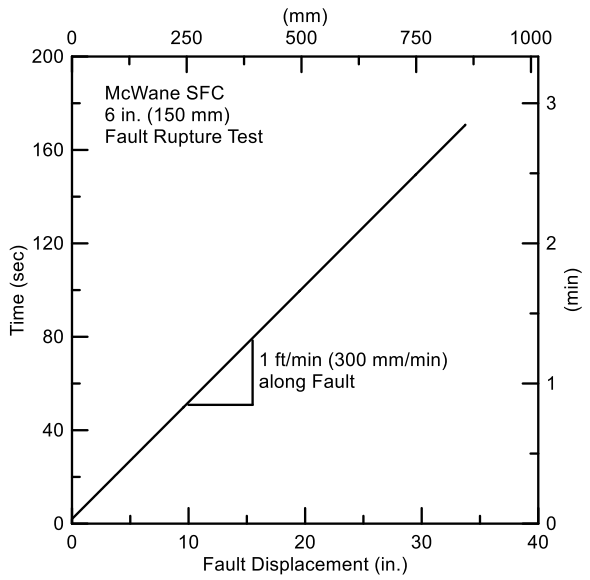


Figure 5.5. Fault Displacement vs. Time

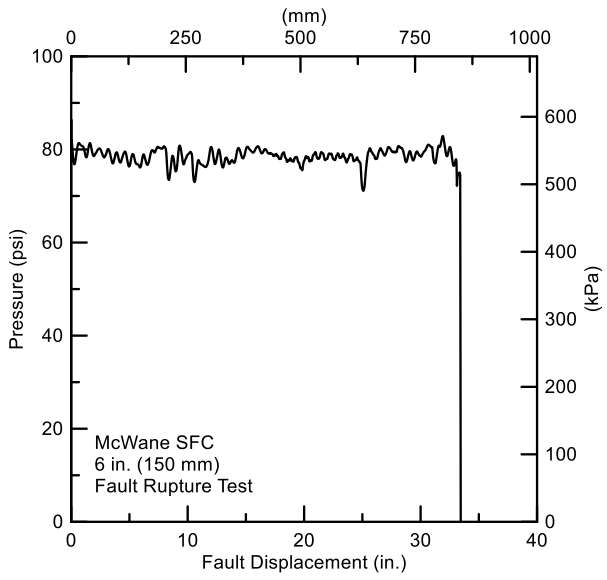


Figure 5.6. Internal Water Pressure vs. Fault Displacement

### 5.3.3. Survey Results

The Bovay Laboratory uses a general coordinate system established in 2012 as part of Cornell's participation in the George E. Brown, Jr. Network for Earthquake Engineering Simulation (NEES). The coordinate system was developed using a Leica Flexline TS02 reflectorless total station to identify baseline positions within the laboratory. When the DI pipeline with the McWane SFCs was placed in the basin and backfilled to approximately the springline depth, survey measurements were taken at 40 marked locations along the pipe crown. These data provide a baseline of the initial pipe position. Following careful pipe excavation with minimal disturbance, these pipes was re-surveyed for a final position at 33.7 in. (856 mm) of fault displacement. These data provide very close locations of the maximum pipe displacement at the maximum basin displacement. The test hydraulics remained on during pipe exposure to prevent the entire system from relaxing.

Figure 5.7 shows, on a greatly exaggerated scale, the Leica data for the initial and final pipe positions. The data shown in Figure 5.7 were used to estimate the overall SFC displacements and deflections. The survey data suggested the total axial movement and lateral offset of the pipeline are 21.1 in. (536 mm) and 26.9 in. (683 mm), respectively. The axial movement consists of 11.6

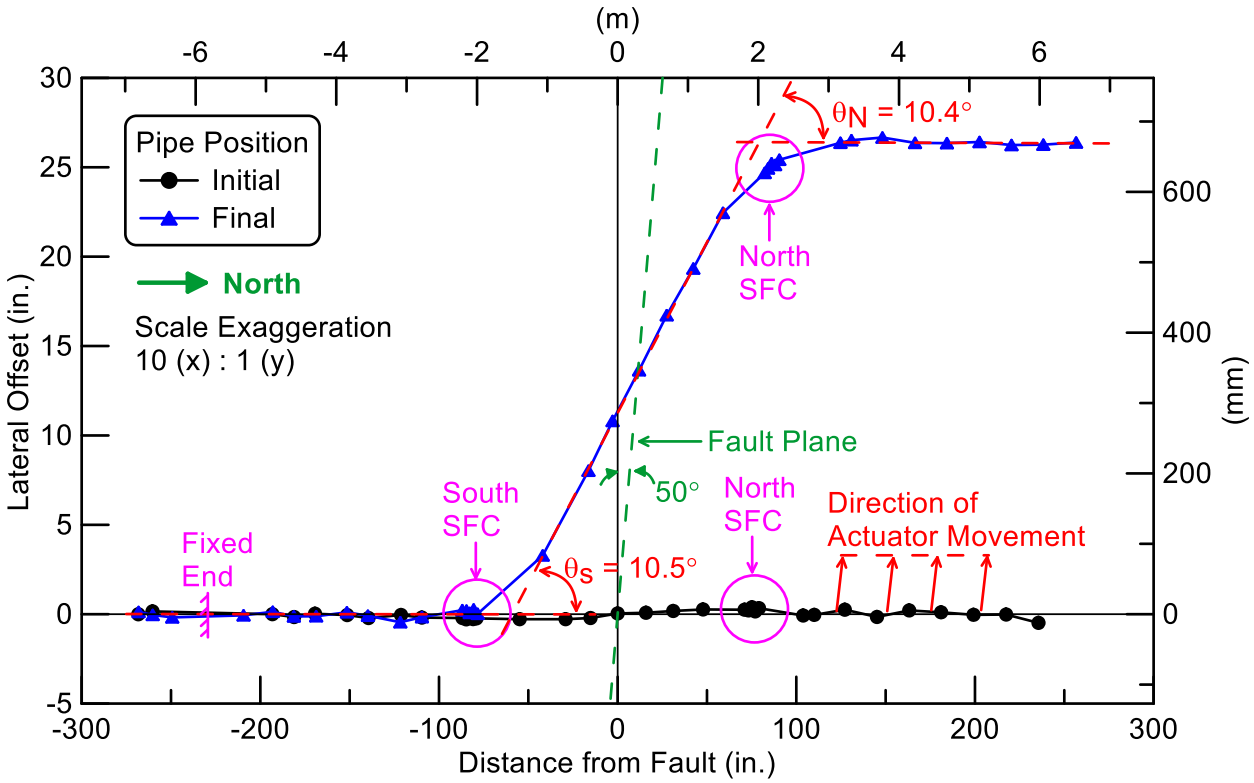


Figure 5.7. Initial and Final Pipeline Positions from Surveying Measurements

in. (295 mm) at the south SFC and 9.5 in. (241 mm) at the north SFC. The slope of each pipe section was found and used to calculate the south and north SFC overall deflection. In this report "deflection" is used to describe the angular deflection of the pipe, consistent with industry usage. The north and south SFC deflection obtained from the survey data are 10.5 and 10.4 degrees, respectively.

### 5.3.4. Joint Displacements

The development of the joint displacement/rotations systems and the required protection was a challenging task. The system had to be non-intrusive to the mechanical performance of the SFC, yet robust enough to withstand the experimental environment. The joint pullout movements were measured using string pots and confirmed by survey measurements. The string pot locations are given in Section 5.2.2 and shown in Table 5.2. Each joint has a total of three string pots. The positioning and protection of these pots required great attention to detail and anticipated rough treatment during the tests. However, these measurements are critical in evaluating the overall

behavior of the SFC. Figure 5.3 shows the joint with thin metal protective shields to prevent soil from interfering with the joint instrumentation. Again, maintain the overall joint flexibility while providing instrumentation protection was critical.

Figures 5.8 and 5.9 show the displacement at each joint of the south and north SFCs, respectively. The total SFC displacement is a sum of P, X, and B joint openings, and is shown in Figure 5.10. The test basin movement was accommodated by the SFC displacements. The south SFC, however, displaced faster such that the south and north SFCs were fully extended at 17.4 in. (442 mm) and 28.0 in. (711 mm), respectively. At a fault displacement of 33.4 in. (848 mm), the south B joint was pulled out and leaked, corresponding to an additional 3.5 in. (89 mm) of axial displacement after all SFCs were fully extended.

Table 5.4 summarizes the movements of each portion of the SFCs at a fault displacement of 33.4 in. (848 mm) as well as a comparison to SFC displacements obtained from the survey data at 33.7 in. (856 mm) of fault displacement. In Table 5.4, the openings of each of the joints are given, along with the cumulative opening of two SFCs. Small displacements on the order of 0.5 in, to 1.0 in. (13 mm to 25 mm) were observed at the B and P joints. These values are closely related to the maximum B and P joint opening of 0.6 in. (15 mm) from the two Cornell direct tension tests. However, the south B joint opening was higher than the other three joints because it was the location where the spigot dislodged and caused the pressure loss. The average displacement of the two X joint was 9.3 in. (236 mm). It must be noted that the X joint was installed at 1.5 in. (38 mm) from fully inserted position for string pot instrumentation. Had the X joints been set at the fully inserted positions, each X joint in the fault rupture test would have been able to accommodate a total displacement of 9.3 in. (236 mm) + 1.5 in. (38 mm) = 10.8 in. (274 mm), which is close to the X joint opening at the fully extended position of 10.5 in. (267 mm) from the Cornell joint direct tension tests discussed in Section 4.3. Furthermore, had the two X joints been fully inserted with the same pipeline configuration, 3.0 in. (78 mm) of axial displacement would have been available in the pipeline for additional fault movement. Therefore, the pipeline would have been able to accommodate a total [3 in. (78 mm) + 21.5 in. (546 mm)]/ cos 50° = 38.1 in. (968 mm) of fault displacement.

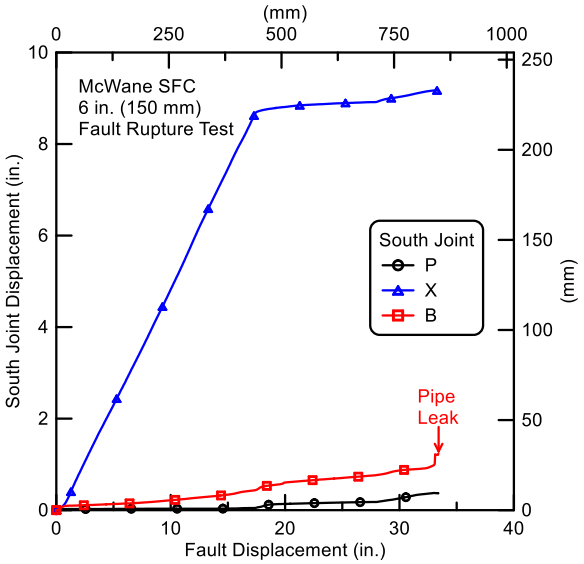


Figure 5.8. South Joint Openings vs. Fault Displacement

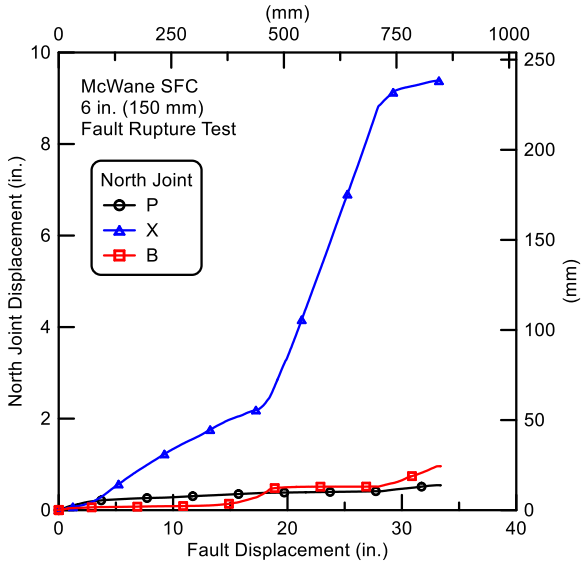


Figure 5.9. North Joint Openings vs. Fault Displacement

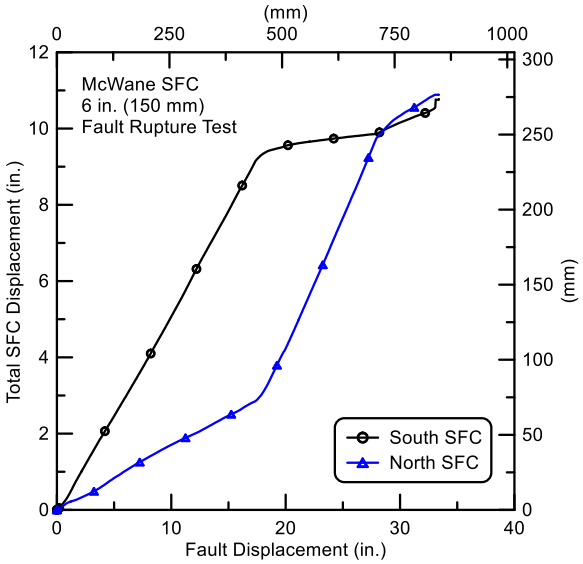


Figure 5.10. Total SFC Displacement vs. Fault Displacement

Table 5.4. Joint Openings of McWane SFCs

| Direction from Fault | Joints | | | | Survey Data |
|---|---|---|---|---|---|
| | B (in.) | X[a] (in.) | P (in.) | ∑ = SFC (in.) | SFC (in.) |
| South | 1.2 | 9.2 | 0.4 | 10.8 | 11.6 |
| North | 1.0 | 9.4 | 0.5 | 10.9 | 9.5 |
| Average | 1.1 | 9.3 | 0.5 | 10.9 | 10.6 |
| Two SFC joints | 2.2 | 18.6 | 0.9 | 21.7 | 21.1 |
| Axial Basin Extension (in.) | (33.4 in.) cos 50° | | | | 21.5 |
| Cornell Tension Tests | One fully extended SFC = 11.0 in. -1.5 in. = 9.5 in.<br>One leaked SFC = 13.2 in. -1.5 in. = 11.7 in. | | | | 21.2 |

1 in. = 25.4 mm

[a] X joint was set at 1.5 in. (38 mm) from fully inserted position for string pot instrumentation

### 5.3.5. Joint Rotations (Deflections)

Joint rotations (deflections) were determined using the string pots at each joint and confirmed by survey measurements. It is critical to note that the observed failure during this test was due to the south B joint pullout. Joint rotation is calculated from the string pot measurements at each joint as:

$$\text{Rotation}\left(\text{deg}\right) = \tan^{-1}\left(\frac{\text{East String Pot Displacement} - \text{West String Pot Displacement}}{\text{Separation Distance between the String Pots}}\frac{180}{\pi}\right) \quad (5.1)$$

Figures 5.11 and 5.12 show the rotation at each joint of the south and north SFCs, respectively. The total SFC deflection is a sum of P, X, and B joint rotations, and is shown in Figure 5.13.

As the test basin was displaced, the south SFC moved closer to the fault and accommodated most of the fault offset with a maximum deflection of 13.7° while the north deflection was 11.6° at the end of the test. The highest rotation of 11.6° was detected at the south B joint, which was the closest joint the fault and where the failure occurred. Table 5.5 presents a comparison between the joint deflections determined using the string pot measurements and the survey data.

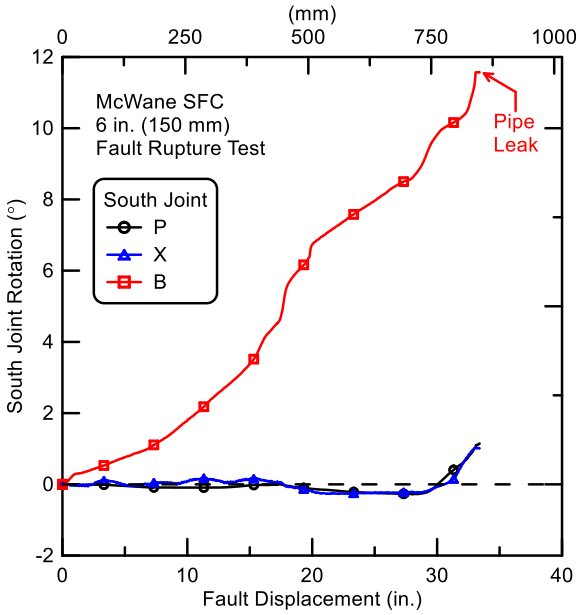


Figure 5.11. South SFC Joint Rotations vs. Fault Displacement

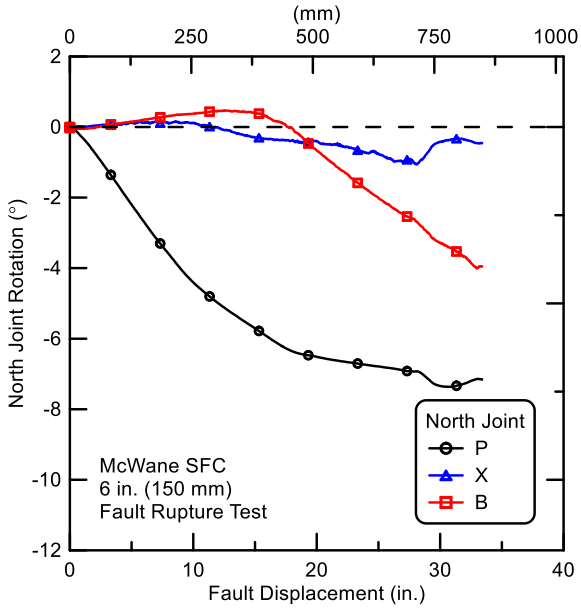


Figure 5.12. North SFC Joint Rotations vs. Fault Displacement

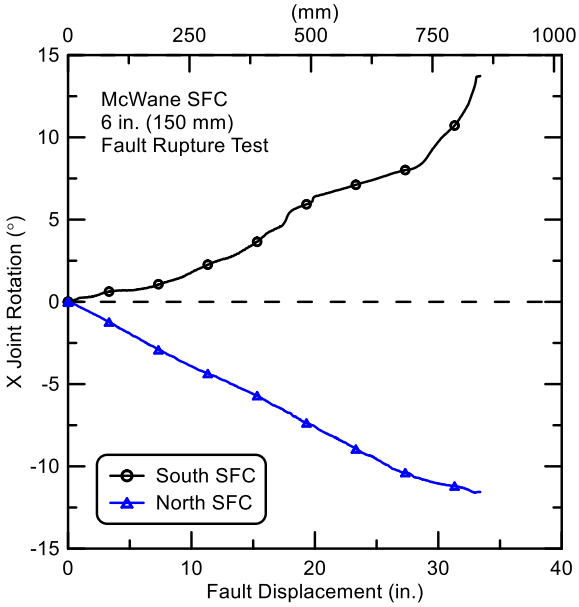


Figure 5.13. Total SFC Deflections vs. Fault Displacement

Table 5.5. Joint Deflections of McWane SFCs

| SFC | String Potentiometers Data | | | | Survey Data |
|---|---|---|---|---|---|
| | P Joint (degrees) | X Joint (degrees) | B Joint (degrees) | SFC Deflection (degrees) | SFC Deflection (degrees) |
| South | 1.1 | 1.0 | 11.6 | 13.7 | 10.5 |
| North | -7.2 | -0.5 | -3.9 | -11.6 | -10.4 |

Positive refers to rotation in counter-clockwise direction

### 5.3.6. End Loads and Pipe Axial Forces

The axial tensile loads were measured with four load cells at the south end of the test basin and four load cells at the north end. The sum of the four load cells at each end of the test basin gives the total axial end load. Figure 5.14 shows the total load at the south and north ends of the test basin vs. fault displacement. At a fault displacement of approximately 28.0 in. (711 mm), both SFCs were fully extended, causing sharp increases in the end loads. This fault displacement corresponds to an axial basin displacement of 18.0 in. (457 mm).

Also included in Figure 5.14 are axial loads calculated from axial strain gages at planes close to the end of the test specimen. The axial force from average strain gage measurements was calculated as $F = \varepsilon AE$. The outside diameter of the pipe was OD = 6.9 in. (175 mm) and the average measured wall thickness was $t_W$ = 0.3 in. (7.6 mm). This gives a pipe wall cross-sectional area, A = 6.22 in.$^2$ (4013 mm$^2$). The Young's modulus of the ductile iron was E = 24,100 ksi (166 GPa), which was determined from tensile coupon tests. The axial forces in the pipe near the load cell locations were consistent with forces measured by the load cells.

The calculated axial loads at each gage plane along the pipeline are presented in Figure 5.15 for various levels of fault displacement. The SFC locations are shown in blue shaded areas. Figure 5.15 a) shows the tensile forces up to 20 in. (508 mm) of fault movement. Relatively low tensile forces were measured along the pipeline during these initial increments of displacement. The highest axial force was detected in the vicinity of the fault, and the loads were lower at locations further away from the fault.

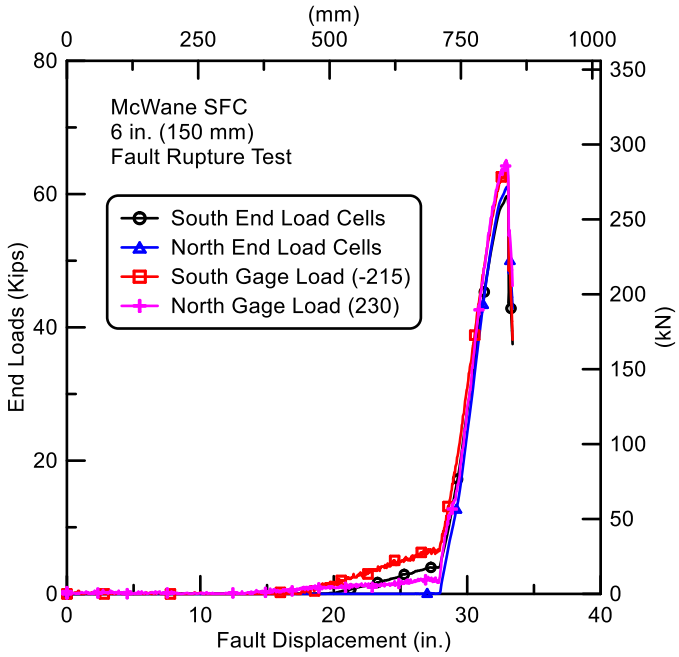


Figure 5.14. Comparison of Average End Force from Load Cells and Strain Gages

Figure 5.15 b) (note change in scale for load) shows that tensile forces were generally higher with increasing fault displacement. The highest axial force was detected at the fault location. The forces increased rapidly after 28 in. (711 mm) of fault displacement, indicating that all joint had been fully extended. Figure 5.15 c) shows the evolutions of the pipe axial loads from 30 in. (762 mm) to the end of test at 33.4 in. (848 mm) of fault displacement. At 33.0 in. (838 mm) of fault movement, the peak force of 88.9 kips (395 kN) was detected at the fault location. The axial forces then decreased, yielding similar behaviors as the joint axial tension tests. The highest force of 58.8 kips (262 kN) was also found at the fault before the pipe lost pressure at 33.4 in. (848 mm) of fault displacement.

### 5.3.7. Bending Moments

Bending moments, M, were calculated at each strain gage station along the pipeline as:

$$M = \frac{\varepsilon_{bend} EI}{c} \tag{5.2}$$

where bending strains, $\varepsilon_{bend,}$ is one half the difference between the springline strains; E is Young's modulus of the ductile iron of 24,100 ksi (166 GPa); I is moment of inertia of 33.9 $in^4$ (1410 $cm^4$); and c is distance to outer fiber of 3.45 in (87.6 mm).

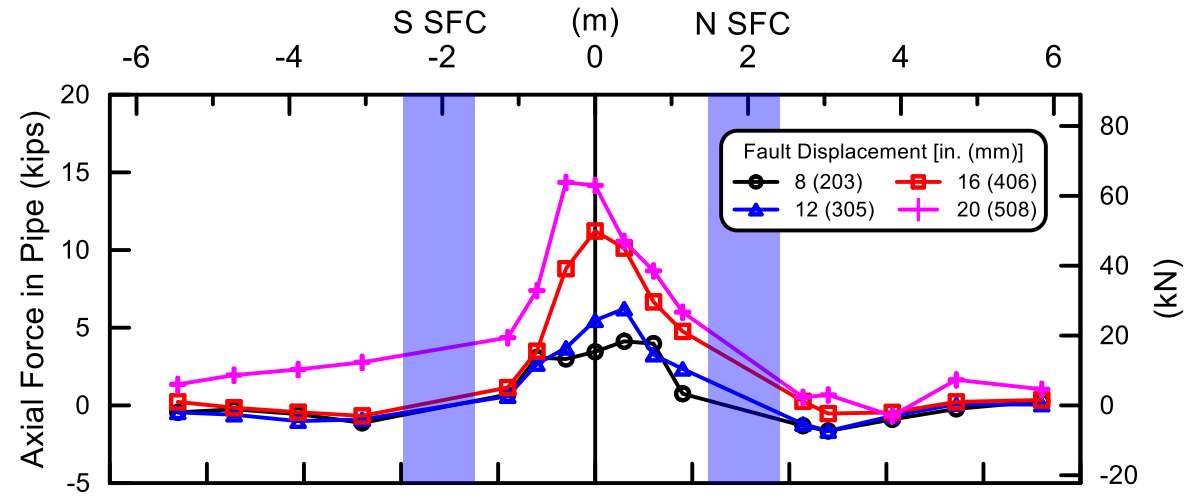


(a) 8 to 20 in. (203 to 508 mm) of Fault Displacement

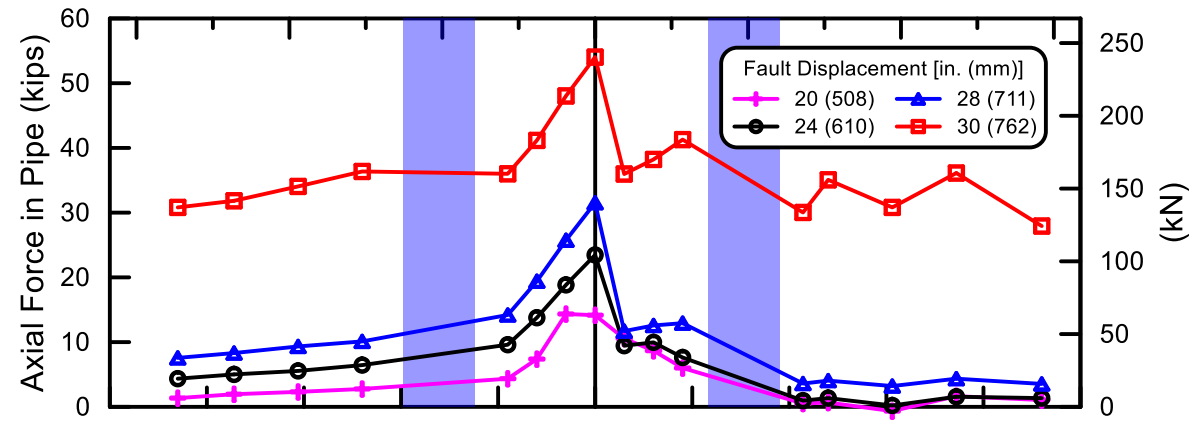


(b) 20 to 30 in. (508 to 762 mm) of Fault Displacement

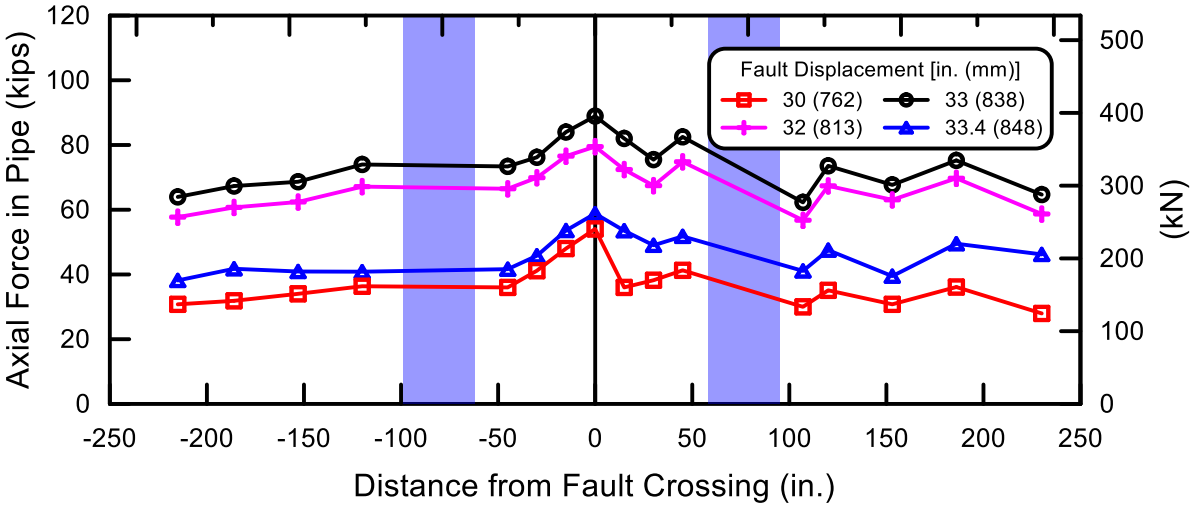


(c) 30 to 33.4 in. (762 to 848 mm) of Fault Displacement

Figure 5.15. Axial Forces in Pipe vs. Distance from Fault

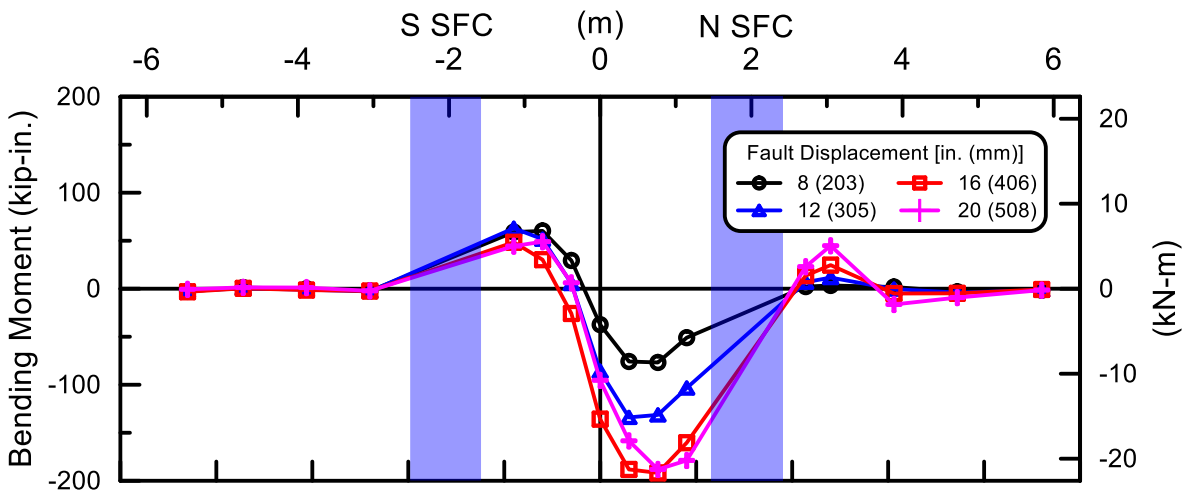


(a) 8 to 20 in. (203 to 508 mm) of Fault Displacement

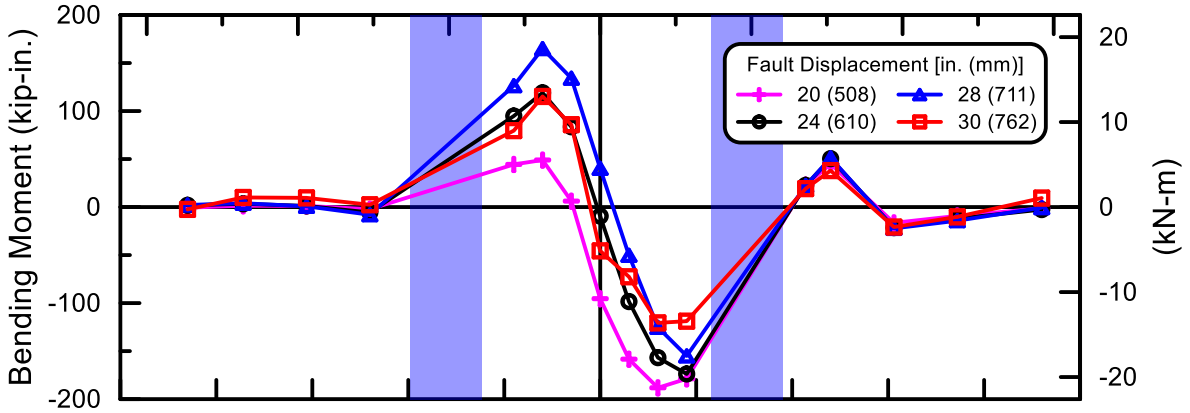


(b) 20 to 30 in. (508 to 762 mm) of Fault Displacement

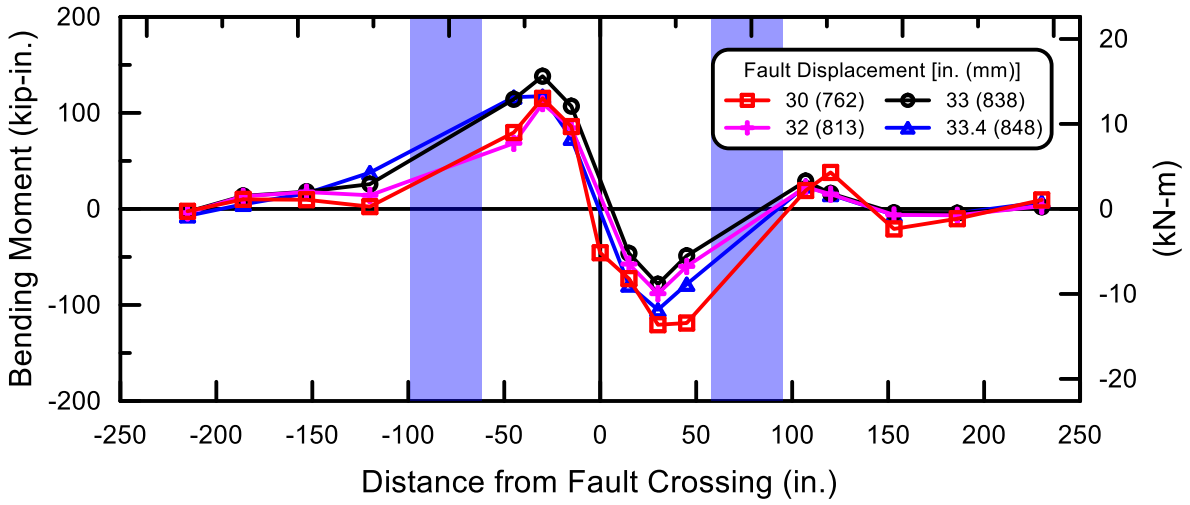


(c) 30 to 33.4 in. (762 to 848 mm) of Fault Displacement

Figure 5.16. Bending Moments in Pipe vs. Distance from Fault

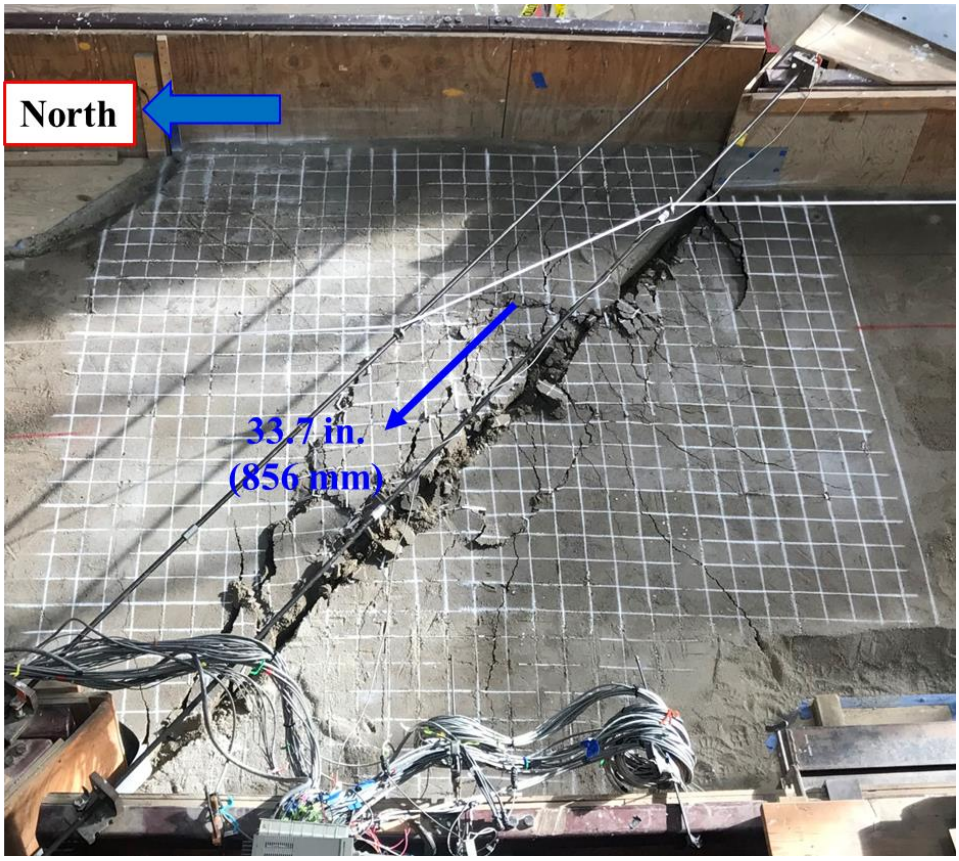


Figure 5.17. Fault Rupture at Test End

Figure 5.16 presents the bending moments measured along the pipeline corresponding to various levels of fault displacement. The SFC locations are shown in blue shaded areas. Figure 5.16 a) shows during the first 20 in. (508 mm) of fault displacement, bending moments along the pipeline were relatively low, except the area between the fault and the north SFC. Figure 5.16 b) shows that the moments were higher as the fault movement increased. The measurements disclose an anti-symmetric pattern of moment distribution centered on the fault. The peak moments were detected at 30 in. (762 mm) away on both sides of the fault. Figure 5.16 c) shows a consistent bending moment distribution for fault movements of 30 in. (762 mm) to 33.4 in. (848 mm). Noticeable bending moments occurred between the north and south SFCs with the highest moments on the order of 110 kip-in. (12.4 kN-m) detected at 30 in. (762 mm) away on both sides from the fault. Moments near the fault location were generally low, indicating that it is near the inflection point of the pipeline.

a) Before Burial

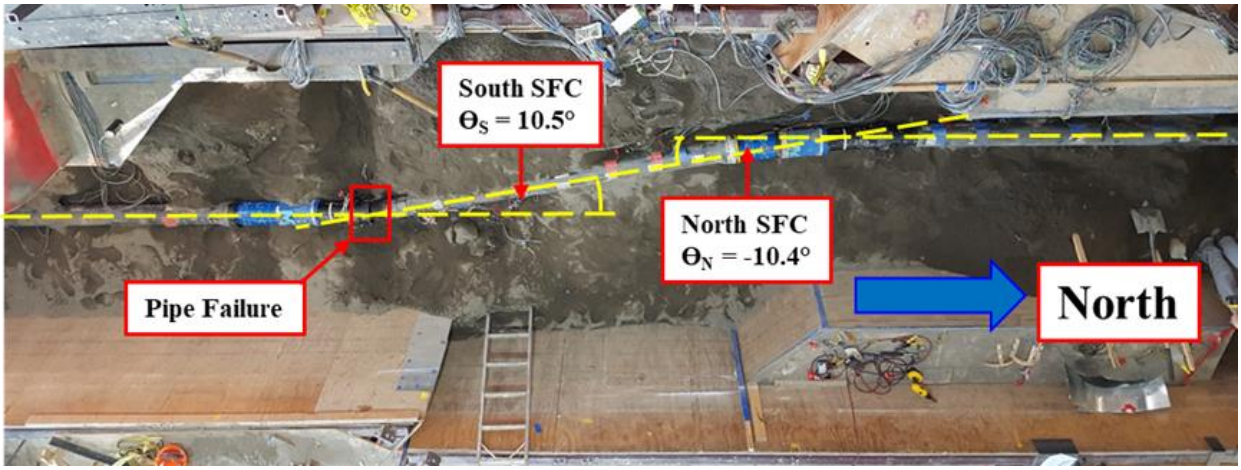


b) After Excavation

Figure 5.18. Overhead View of Pipeline (a) before burial and (b) after excavation (angles shown from total station surveying measurements)

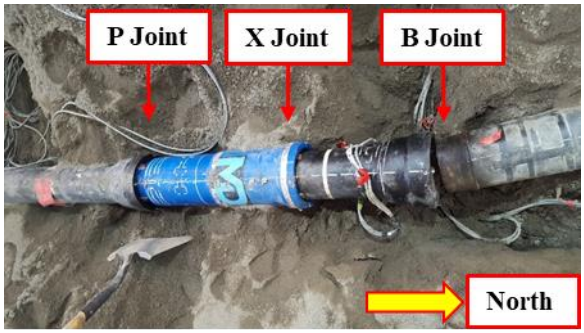


a) Plan View of South SFC

b) Close-up View of South SFC B Joint

Figure 5.19. B Joint Pullout at South SFC following Test without Protective Shield

### 5.3.8. Deformed Shape and Pipe Failure

Figure 5.17 shows the surface of the fault rupture at the end of the test. Figure 5.18 a) shows a photo of the pipeline before backfilling and burial of the pipe. Failure of the B joint pullout at the south SFC was the overall failure mode. After fault rupture, the pipeline was excavated carefully in a manner that preserved its deformed shape as shown in Figure 5.18 b). Angles of S5 and N5 SFC deflection are also illustrated in Figure 5.18 b). These deflection angles were obtained from the Leica data as discussed in Section 5.3.3. Figure 5.19 presents the B joint pullout at the south SFC without the protective shield after excavation. The plan views of the south SFC and its B joint following the excavation are illustrated in Figure 5.19 a) and b) respectively.

## 5.4. Summary of Fault Rupture Test

A 34-ft (10-m)-long, three-piece section of a ductile pipeline was tested at the Cornell Large-Scale Lifelines Facility. The pipeline had two McWane SFCs located 5 ft. (1.5 m) north and south of the 50º fault. The pipe was instrumented with eighty-four strain gages installed at sixteen locations along the pipeline to measure strains and to evaluate axial forces and bending moments. Strain gages were positioned at the crown (C), invert (I) east (E) springline, and west (W) springline of the pipe. There were three string pots at each sub-joint to measure joint movements and to evaluate joint rotation. Four load cells were placed outside the test basin at each end, reacting between the test basin structural frame and pipe end restraint to measure axial force. The pipe was pressurized to approximately 80 psi (550 kPa).

The pipeline was buried in the Cornell large-scale test basin in partially saturated sand that was compacted to have an average friction angle of $\phi = 42^{o}$, equivalent in strength to that of a medium dense to dense granular backfill. The depth of burial to top of pipe was 33.5 in. (851 mm). During the test, the south part of the basin remained stationary, while the north part was displaced to the north and west by large-stroke actuators to cause soil rupture and slip at the interface between the two parts of the test basin. The north section of the test basin was displaced along a $50^{o}$ fault at a rate of 1 ft (300 mm) per minute. The basin was displaced until the pipe lost water pressure at 33.4 in. (848 mm) fault displacement, which corresponds to 21.5 in. (546 mm) of axial extension of the test basin and pipe. Following excavation, a spigot pullout was observed at the south B joint.

The forces at the south and north end of the test basin were about 60 and 90 kips (267 kN). The largest axial force in the pipe, as determined from the strain gage readings, of 88.9 kips (395 kN) was achieved at the fault location at 33.0 in. (838 mm) of fault movement. The axial force at the fault then decreased to 58.8 kips (262 kN) when the pipe lost pressure at 33.4 in. (848 mm) of fault displacement.

The test measurements confirm that the pipeline was able to accommodate fault rupture through axial displacements and deflections at two SFCs. They also provide a comprehensive and detailed understanding of how the movement was accommodated at each joint, the sequence of movements, and combined axial pullout and rotation at each joint. The DI pipeline with two SFCs accommodated the total axial movement of 21.5 in. (546 mm). It must be noted that the X joint was installed at 1.5 in. (38 mm) from fully inserted position to allow for the joint instrumentation. Had the X joints been set at the fully inserted positions, the pipeline would have accommodated 24.5 in. (622 mm) of total axial displacement. On average, each SFC would have displaced on the order of 12.3 in. (274 mm). This displacement was close to the movement measured in the previous joint direct tension testing of the McWane SFC. Had more McWane SFCs been added to the DI pipeline in a similar setup as the fault rupture test, the pipeline would have accommodated more fault movement. For example, if the DI pipeline was installed with four fully collapsed McWane SFCs for the fault rupture test, the amount of a 50-degree fault displacement sustained by the pipeline would have been on the order of 76.2 in. (1.94 m). This displacement is equivalent to 49 in. (1.24 m) of axial movement.

The maximum deflection measured at the south SFC was about 10.5 degrees, thus demonstrating the ability of the joints to sustain significant levels of combined axial pullout and deflection. The maximum stresses sustained by the pipeline, corresponding to the largest pipeline deformation, were well within the elastic range of pipeline behavior.

The ductile iron pipeline equipped with McWane Seismic Flex Couplings (SFCs) was able to accommodate significant fault movement through axial pullout and rotation of the joints. Fault rupture simulated in the large-scale test is also representative of the most severe ground deformation that occurs along the margins of liquefaction-induced lateral spreads and landslides. The amount of tensile strain that can be accommodated with the ductile iron pipeline will depend on the number and spacing of the McWane SFCs and the positioning of the spigot within the bell at the pipeline joints. The pipeline used in the fault rupture test was able to accommodate a minimum of 21.5 in. (546 mm) of axial extension, corresponding to an average tensile strain of 4.5% along the pipeline. Such extension is large enough to accommodate the great majority (over 99%) of liquefaction-induced lateral ground strains measured by high resolution LiDAR after each of four major earthquakes during the recent Canterbury Earthquake Sequence (CES) in Christchurch, NZ (O'Rourke, et al., 2014). These high resolution LiDAR measurements for the first time provide a comprehensive basis for quantifying the ground strains caused by liquefaction on a regional basis. To put the CES ground strains in perspective, the levels of liquefaction-induced ground deformation measured in Christchurch exceed those documented in San Francisco during the 1989 Loma Prieta earthquake and in the San Fernando Valley during the 1994 Northridge earthquake. They are comparable to the levels of most severe liquefaction-induced ground deformation documented for the 1906 San Francisco earthquake, which caused extensive damage to the San Francisco water distribution system. The test confirms that the ductile iron pipes equipped with the McWane SFCs are able to sustain large levels of ground deformation through axial displacement and deflection under full-scale conditions of abrupt ground rupture.

# Section 6
# Summary

McWane Ductile has developed a Seismic Flex Coupling (SFC) to connect to TR Flex® bell and spigot ductile iron (DI) pipes. Sections of 6-in. (150-mm)-diameter DI pipes with the McWane SFCs were tested at Cornell University to 1) evaluate the stress-strain-strength characteristics of the DI, 2) determine the capacity of the joint in direct tension and compression, 3) evaluate the bending resistance and moment vs. rotation relationship of McWane SFCs and one separated TR Flex® joint, and 4) evaluate the capacity of a 6-in. (150-mm) DI pipeline with McWane SFCs to accommodate fault rupture using the Cornell full-scale split-basin testing facility.

Test results are summarized for tensile stress-strain-strength characteristics, direct joint tension and compression, bending test results, pipeline response to fault rupture. The significance of test results is given under the headings that follow.

## Tensile Stress-Strain-Strength Characteristics

The uniaxial tension testing of ductile iron (DI) from McWane specimens was completed in accordance with ASTM – E8 2016 standards (ASTM, 2016). The yield stress and ultimate stress exceeded the ANSI/AWWA C151/A21.51-17 60-42 standard (AWWA, 2017) by 25% and 27%, respectively. The strains at failure measured with bondable strain gages and a laser extensometer were 4.1%. The elastic modulus is E = 24,100 ksi (166 GPa), and Poisson's ratio is 0.27, consistent with typical DI.

## Bending Test Results

Four-point bending tests were performed on pressurized nominal 6-in. (150-mm)-sections of two McWane SFCs and one separated TR Flex® joint. The purpose of these tests was to develop moment vs. rotation relationships for these types of joints.

In the TR Flex® bending test, first leakage of approximately 10 drops/sec (25 ml/min) developed at a deflection of joint less than 12 degrees and an applied moment of 137 kip-in. (15.5 kN-m). The pipe leaked at a significant rate on the order of 10 gal/min (38 l/min) at 21.3 degrees of joint deflection. Significant leakage is defined as flow exceeding 10 gal/min (38 l/min).

Two tests were performed on SFCs. Specimen 1 showed stiffer rotational responses than Specimen 2, and first leaked at the X joint on the order of 10 drops/sec (25 ml/min) with an

associated overall deflection of 17.7 degrees. Later in the test, Specimen 1 leaked at the B joint with a significant rate on the order of 10 gals/min (38 l/min) at 32.5 degrees of overall deflection. Specimen 2 first leaked about 10 drops/sec (25 ml/min) at the X joint at the beginning of the test. The pipe failed and leaked at the B joint with a significant rate greater than 10 gals/min (38 l/min) at 36.0 degrees of overall deflection.

**Direct Joint Tension and Compression**

Three tension tests, two McWane SFCs and one separated TR Flex® joint, and one compression test were performed on the 6-in. (150-mm)-diameter DI specimens. All tests began at the fully inserted positions. In the TR Flex® joint tension test, the peak load of 96.5 kips (429 kN) was achieved at 0.73 in. (18.5 mm) of joint opening. Leakage was observed at 1.57 in. (39.8 mm) of displacement when the left-hand locking segment broke.

McWane SFC tension test specimens provided the average SFC total displacement of 11.0 in. (279 mm) under internal water pressure of 80 psi (550 kPa). The average maximum tensile force of 66.3 kips (295 kN) was measured at the average displacement of 12.0 in. (305 mm). Both SFC specimens were able to carry additional displacement until significant leakage was observed at the X joint at 13.2 in. (335 mm) of average total joint displacement.

The compressive testing showed that the McWane SFC had a maximum compressive load capacity at about the DI proportional limit of 204 kips (907 kN). Once the proportional limit was achieved, the pipe started to behave plastically and have irrecoverable deformation such that a significant rotation was observed at the B joint. However, no leakage was found during the compression test.

**Pipeline Response to Fault Rupture**

A 34-ft (10-m)-long, three-piece section of a ductile pipeline was tested at the Cornell Large-Scale Lifelines Facility. The pipeline had two McWane SFCs located 5 ft (1.5 m) north and south of the 50º fault. The pipe was pressurized to approximately 80 psi (550 kPa). The pipe was placed on a bed of compacted partially saturated sand, aligned, instruments checked, and then backfilled with compacted sand to a depth of cover of 33.5 in. (851 mm) above the pipe crown. The north section of the test basin was displaced along a 50º fault at a rate of 12 in. (300 mm) per minute. At a fault displacement of roughly 33.4 in. (848 mm), the pipe lost pressure. An additional 0.3 in. (76 mm) of test basin movement was applied to ensure a complete pressure loss in the system, and the test

was then stopped. Following excavation, a spigot pullout was observed at the south B joint.

The test measurements confirm that the pipeline was able to accommodate fault rupture through axial displacements and deflections at two SFCs. The data also provide a comprehensive and detailed understanding of how the movement was accommodated at each joint, the sequence of movements, and the combined axial pullout and rotation at each joint. The DI pipeline with two SFCs accommodated the total axial movement of 21.5 in. (546 mm). In the experiments, the X joint was installed at 1.5 in. (38 mm) from fully inserted position to accommodate joint instrumentation. Had the X joints been set at the fully inserted positions, the pipeline would have accommodated 24.5 in. (622 mm) of total axial displacement. On average, each SFC would have displaced on the order of 12.3 in. (274 mm). This displacement was nearly identical to the movement measured in the previous joint direct tension testing of the McWane SFC. The maximum deflection measured at the south SFC was about 10.5 degrees, thus demonstrating the ability of the joints to sustain significant levels of combined axial pullout and deflection. The maximum stresses sustained by the pipeline, corresponding to the largest pipeline deformation, were well within the elastic range of pipeline behavior.

The ductile iron pipeline equipped with McWane Seismic Flex Couplings (SFCs) was able to accommodate significant fault movement through axial pullout and joint deflection (rotation). Fault rupture simulated in the large-scale test was representative of the most severe ground deformation that occurs along the margins of liquefaction-induced lateral spreads and landslides.

**Significance of Test Results**

The amount of tensile strain that can be accommodated with the ductile iron pipeline will depend on the number and spacing of the McWane SFCs and the positioning of the spigot within the bell at the pipeline joints. The four-joint pipeline used in the large-scale split-basin test was able to accommodate at least 21.5 in. (461 mm) of axial extension, corresponding to an average tensile strain of 4.5% along the pipeline. Such extension is large enough to accommodate the great majority (over 99%) of liquefaction-induced lateral ground strains measured by high resolution LiDAR after each of four major earthquakes during the recent Canterbury Earthquake Sequence (CES) in Christchurch, NZ. These high resolution LiDAR measurements for the first time provide a comprehensive basis for quantifying the ground strains caused by liquefaction on a regional basis. To put the CES ground strains in perspective, the levels of liquefaction-induced ground

deformation measured in Christchurch exceed those documented in San Francisco during the 1989 Loma Prieta earthquake and in the San Fernando Valley during the 1994 Northridge earthquake. They are comparable to the levels of most severe liquefaction-induced ground deformation documented for the 1906 San Francisco earthquake, which caused extensive damage to the San Francisco water distribution system. The fault rupture test confirms that the DI pipes equipped with the McWane SFCs are able to sustain without leakage large levels of ground deformation through axial displacement and deflection under full-scale conditions of abrupt ground rupture.

## References


ASTM International (2016). "Standard Test Methods for Tension Testing of Metallic Materials", *ASTM Standards*. E8/E8M - 13a, 1 – 28.

AWWA (2017). "Ductile Iron Pipe, Centrifugally Cast for Water", *AWWA Standard*. ANSI/AWWA C151/A21.51-17.

O'Rourke, TD (1998). "An Overview of Geotechnical and Lifeline Earthquake Engineering", Geotechnical Special Publication No. 75, ASCE, Reston, VA, Proceedings of Geotechnical Earthquake Engineering and Soil Dynamics Conference, Seattle, WA, Aug. 1998, Vol. 2, pp.1392-1426.

O'Rourke, TD and JW Pease (1997). "Mapping Liquefiable Layer Thickness for Seismic Hazard Assessment", Journal of Geotechnical Engineering, ASCE, New York, NY, Vol. 123, No.1, January, pp. 46-56.

O'Rourke, TD., A Bonneau, JW. Pease, P Shi, and Y Wang (2006). "Liquefaction Ground Failures in San Francisco" Earthquake Spectra, EERI, Oakland, CA, Special 1906 San Francisco Earthquake Vol. 22, No. 52, Apr., pp. 691-6112.

O'Rourke, TD, Jeon, S-S, Toprak, S, Cubrinovski, M, Hughes, M, van Ballegooy, S, and Bouziou, D (2014) "Earthquake Response of Underground Pipeline Networks in Christchurch, NZ", Earthquake Spectra, EERI, Vol. 30, No.1, pp. 183-204**.**

Pease, JW and TD O'Rourke (1997), "Seismic Response of Liquefaction Sites", Journal of Geotechnical Engineering, ASCE, New York, NY, Vol. 123, No. 1, January, pp. 37-45.